

5-2010

## Host-pathogen interactions of secreted and surface Staphylococcus aureus factors

Vanessa Vazquez

Follow this and additional works at: [https://digitalcommons.library.tmc.edu/utgsbs\\_dissertations](https://digitalcommons.library.tmc.edu/utgsbs_dissertations)



Part of the [Biochemistry Commons](#), and the [Microbiology Commons](#)

---

### Recommended Citation

Vazquez, Vanessa, "Host-pathogen interactions of secreted and surface Staphylococcus aureus factors" (2010). *The University of Texas MD Anderson Cancer Center UTHealth Graduate School of Biomedical Sciences Dissertations and Theses (Open Access)*. 25.

[https://digitalcommons.library.tmc.edu/utgsbs\\_dissertations/25](https://digitalcommons.library.tmc.edu/utgsbs_dissertations/25)

This Dissertation (PhD) is brought to you for free and open access by the The University of Texas MD Anderson Cancer Center UTHealth Graduate School of Biomedical Sciences at DigitalCommons@TMC. It has been accepted for inclusion in The University of Texas MD Anderson Cancer Center UTHealth Graduate School of Biomedical Sciences Dissertations and Theses (Open Access) by an authorized administrator of DigitalCommons@TMC. For more information, please contact [digitalcommons@library.tmc.edu](mailto:digitalcommons@library.tmc.edu).

**Host-pathogen interactions of secreted and surface *Staphylococcus aureus* factors**

by

Vanessa Vazquez, B.S.

APPROVED:

---

Supervisory Professor  
Magnus Höök, Ph.D.

---

Burton Dickey, M.D.

---

Theresa Koehler, Ph.D.

---

C. Wayne Smith, M.D.

---

Yi Xu, Ph.D.

APPROVED:

---

Dean, The University of Texas  
Health Science Center at Houston  
Graduate School of Biomedical Sciences

**HOST-PATHOGEN INTERACTIONS OF SECRETED AND SURFACE  
*STAPHYLOCOCCUS AUREUS* FACTORS**

A

Dissertation

Presented to the Faculty of  
The University of Texas  
Health Science Center at Houston  
and  
The University of Texas  
M.D. Anderson Cancer Center  
Graduate School of Biomedical Sciences  
in Partial Fulfillment  
of the Requirements  
for the Degree of  
DOCTOR OF PHILOSOPHY

by

Vanessa Vazquez, B.S.  
Houston, TX

May 2010

## ACKNOWLEDGEMENTS

The scientific support and training that I received during my undergraduate years established the foundation necessary to embark on this journey. Riaz Ahmad, Armando Cruz-Rodz, and Jerry Nielsen challenged me to understand basic scientific principles. Walt Seideman, rest in peace, offered me my first laboratory position and taught me 'old-school' techniques - complete with mouth pipetting!

Many individuals helped me throughout my graduate studies. First, I acknowledge my supervisory professor, Magnus Höök for his advising me during my graduate studies. Next, are the professors who served on my advisory, examination, and supervisory committees: Richard Cook, David Haviland, Steven Norris, Duen Yan, Gabriela Bowden, Theresa Koehler, Eric Brown, Burton Dickey, Yi Xu, and Wayne Smith, with a special recognition to Theresa Koehler for serving on all three committees!

During my graduate career, I had the opportunity to communicate and collaborate with several scientists. Timothy Foster, Ed Feil, Francois Vandenesch, Jerrilyn Howell, and Kristina Hulten all provided reagents that were used in this study. Additionally, Wayne Smith and his laboratory members Fong Lam, Jie Li, and Michele Mariscalco are acknowledged for providing technical training. Alan Prejusa is also recognized for his technical expertise. Members of the Center for Infectious and Inflammatory Diseases helped me on a daily basis by providing reagents and technical skills. I thank Allison Bartlett, Janeu Houston, and Xiaowen Liang for invaluable experimental assistance. I also thank Brooke Russell for her comments and critique.

Lastly, I acknowledge former peers, Maria Labadeira-Rey and Magda Barbu. These two individuals helped me with every aspect of being a graduate student. They taught me how to use software and laboratory equipment, design experiments, evaluate data, and technical jargon, such as 'eyeball-o-metrics.'

## ABSTRACT

Host-pathogen interactions of secreted and surface *Staphylococcus aureus* factors

Publication No. \_\_\_\_\_

Vanessa Vazquez

Supervisory Professor: Magnus Höök, Ph.D.

*Staphylococcus aureus* is an opportunistic bacterial pathogen that can infect humans and other species. It utilizes an arsenal of virulence factors to cause disease, including secreted and cell wall anchored factors. Secreted toxins attack host cells, and pore-forming toxins destroy target cells by causing cell lysis. *S. aureus* uses cell-surface adhesins to attach to host molecules thereby facilitating host colonization. The Microbial Surface Components Recognizing Adhesive Matrix Molecules (MSCRAMMs) are a family of cell-wall anchored proteins that target molecules like fibronectin and fibrinogen. The Serine-aspartate repeat (Sdr) proteins are a subset of staphylococcal MSCRAMMs that share similar domain organization. Interestingly, the amino-terminus, is composed of three immunoglobulin-folded subdomains (N1, N2, and N3) that contain ligand-binding activity. Clumping factors A and B (ClfA and ClfB) and SdrG are Sdr proteins that bind to fibrinogen (Fg), a large, plasma glycoprotein that is activated during the clotting cascade to form fibrin. In addition to recognizing fibrinogen, ClfA and ClfB can bind to other host ligands.

Analysis of *S. aureus* strains that cause osteomyelitis led to the discovery of the bone-sialoprotein-binding protein (Bbp), an Sdr protein. Because several MSCRAMMs target more than one molecule, I hypothesized that Bbp may recognize other host proteins. A ligand screen revealed that the recombinant construct Bbp<sub>N2N3</sub> specifically recognizes human Fg. Surface plasmon resonance was used to determine the affinity of Bbp<sub>N2N3</sub> for Fg, and a dissociation constant of 540 nM was determined. Binding experiments performed with recombinant Fg chains were used to map the binding of Bbp<sub>N2N3</sub> to the Fg A $\alpha$  chain.

Additionally, Bbp expressed on the surface of *Lactococcus lactis* and *S. aureus* Newman mediated attachment of these bacteria to Fg A $\alpha$ . To further characterize the interaction between the two proteins, isothermal titration calorimetry and inhibition assays were conducted with synthetic Fg A $\alpha$  peptides. To determine the physiological implications of Bbp binding to Fg, the effect of Bbp on fibrinogen clotting was studied. Results show that Bbp binding to Fg inhibits the formation of fibrin. The consequences of this interaction are currently under investigation.

Together, these data demonstrate that human Fg is a novel ligand for Bbp. This study indicates that the MSCRAMM Bbp may aid in staphylococcal attachment by targeting both an extracellular matrix and a blood plasma protein. The implications of these novel findings are discussed.

## TABLE OF CONTENTS

Acknowledgements .....	iii
Abstract .....	iv
Table of Contents .....	vi
List of Illustrations .....	vii
List of Tables .....	ix
Abbreviations .....	x
<b>Chapter I: Introduction .....</b>	<b>1</b>
<b>Chapter II: Pantan-Valentine Leukocidin causes necrotizing pneumonia</b>	
Introduction .....	28
Materials and Methods .....	30
Results .....	32
Discussion .....	39
<b>Chapter III: The MSCRAMM Bbp targets the fibrinogen A<math>\alpha</math> chain</b>	
Introduction .....	42
Materials and Methods .....	47
Results .....	58
Discussion .....	79
<b>Chapter IV: Binding mechanism of Bbp to fibrinogen</b>	
Introduction .....	83
Materials and Methods .....	86
Results .....	89
Discussion .....	95
<b>Chapter V: Discussion .....</b>	<b>98</b>
Bibliography .....	106
Vita .....	124

## LIST OF ILLUSTRATIONS

1-1	Domain organization of MSCRAMMs .....	8
1-2	Cartoon representation of the collagen hug model .....	11
1-3	Domain organization of the Sdr proteins .....	12
1-4	Structural representation of dock, lock, and latch model .....	14
1-5	Cartoon representation of the binding between SdrG and fibrinogen.....	15
1-6	Structure of fibrinogen .....	17
1-7	<i>Staphylococcus aureus</i> platelet activation .....	20
2-1	The purified Pantan-Valentine Leukocidin subunits are active .....	33
2-2	PVL-induced inflammatory cytokine secretion .....	34
2-3	PVL expression enhances the virulence of isogenic <i>S. aureus</i> strains .....	36
2-4	Percent survival following intranasal inoculation with <i>S. aureus</i> .....	37
3-1	MSCRAMMs target different sites in the fibrinogen chains .....	46
3-2	<i>In vitro</i> expression of Bbp .....	59
3-3	Bbp <sub>N2N3</sub> construct .....	60
3-4	Purified Bbp <sub>N2N3</sub> .....	61
3-5	Bbp <sub>N2N3</sub> binding to Fg .....	63
3-6	Fg species screen.....	64
3-7	Bbp <sub>N2N3</sub> Surface Plasmon Resonance .....	65
3-8	Reduced Fg Far Western .....	67
3-9	Purified individual Fg chains .....	68
3-10	A $\alpha$ truncation mutants.....	69
3-11	Full-length and Bbp <sub>N2N3</sub> binding to A $\alpha$ truncation mutants .....	71
3-12	Isothermal titration calorimetry of Fg A $\alpha$ peptides and Bbp <sub>N2N3</sub> .....	72
3-13	Peptide inhibition .....	74



3-14	Alignment of sequences from several species .....	75
3-15	Inhibition of fibrin formation.....	78
4-1	Alignment of the N2N3 domains of SdrG, ClfA, and Bbp .....	90
4-2	Delta lock and latch Bbp <sub>N2N3</sub> mutants.....	91
4-3	BbpCys-Cys .....	93
4-4	Rescue of BbpCys-Cys binding .....	94
5-1	Alignment of full-length SdrE and Bbp .....	101
5-2	Structural comparison of SdrE and Bbp .....	102
5-3	Comparison of SdrE <sub>N2N3</sub> and Bbp <sub>N2N3</sub> activities.....	104

## LIST OF TABLES

1-1	<i>Staphylococcus aureus</i> vaccines in clinical trials .....	24
3-1	<i>Staphylococcus aureus</i> MSCRAMMs with multiple ligands.....	43
3-2	Oligonucleotides used in this study .....	48
3-3	Constructs used in this study .....	53
3-4	Peptides synthesized for this study .....	56
3-5	Isothermal Titration Calorimetry data.....	73
4-1	Oligonucleotides used in this study .....	87

## ABBREVIATIONS

$\alpha$ -HL: Alpha-hemolysin

AP: Alkaline-phosphatase

Bbp: Bone-sialoprotein-binding protein

BHIB: Brain-heart infusion broth

BSA: Bovine serum albumin

BCIP: 5-Bromo-4-Chloro-3'-Indolylphosphate p-Toluidine Salt

BSP: Bone-sialoprotein

C3: Complement factor 3

CA-MRSA: Community-associated methicillin resistant *Staphylococcus aureus*

CHIPS: Chemotaxis inhibitory protein of staphylococci

ClfA, B: Clumping factor A, B

Cna: Collagen adhesin

DLL: Dock, lock, and latch

DTT: Dithiothreitol

Eap: Extracellular adherence protein

Efb: Extracellular fibrinogen-binding protein

ELISA: Enzyme-linked immunosorbent assay

Fc $\gamma$ RIIa: Fc gamma receptor IIa

Fc: Fragment crystallizable (of immunoglobulins)

Fg: Fibrinogen

FnbpA, B: Fibronectin-binding protein A, B

GAPDH: Glyceraldehyde-3-phosphate dehydrogenase

HA-MRSA: Hospital-associated methicillin resistant *Staphylococcus aureus*

Hlb: Hemolysin beta

HlgA, B, C: Hemolysin gamma A, B, C

HRP: Horseradish peroxidase

ICAM-1: Intercellular adhesion molecule 1

IgA, E, G, M: Immunoglobulin A, E, G, M

IL-1, -3, -4, -6, -8, -10, -12: Interleukin-1, -3, -4, -6, -8, 1-0, -12

IP-10: Interferon-inducible protein 10

IPTG: Isopropyl- $\beta$ -D-thiogalactosidase

IsdA, B, C, D, E, F, H: Iron-responsive surface determinant A, B, C, D, E, F, H

ITC: Isothermal titration calorimetry

LD<sub>50</sub>: Lethal dose of 50%

LFA-1: Lymphocyte function associated antigen-1

LPS: Lipopolysaccharide

Luk: Leukocidin

MAP: MHC class II analogue protein

MHCII: Major histocompatibility complex class II

MIP-1, -5: Macrophage inflammatory protein-1, -5

MRSA: methicillin resistant *Staphylococcus aureus*

MSCRAMM: Microbial surface component recognizing adhesive matrix molecules

NBT: Nitroblue tetrazolium chloride

PBS: Phosphate buffered saline

PCR: Polymerase chain reaction

PE: Phycoerythrin

PFT: Pore-forming toxin

PTSAgs: Pyrogenic toxin superantigens

PVL: Panton-Valentine Leukocidin

RGD (motif): Arginine-glycine-aspartate sequential residues that bind to integrins

rpm: Revolutions per minute

RT-PCR: Reverse transcriptase polymerase chain reaction

SAK: Staphylokinase

SCIN: Staphylococcus complement inhibitor

SdrC, D, E, G: Serine-aspartate repeat protein C, D, E, G

SDS-PAGE: Sodium-dodecyl-sulfate polyacrylamide gel electrophoresis

SE: Staphylococcal enterotoxins

SPR: Surface Plasmon resonance

SSSS: Staphylococcal scalded skin syndrome

SSTI: Skin and soft tissue infection

TBS: Tris-buffered saline

TCR: T cell receptor

Th1, 2: T helper 1, 2

TNFR1: Tumor necrosis factor receptor 1

TSS: Toxic shock syndrome

TSST-1: Toxic shock syndrome toxin-1

vWF: von Willebrand factor

WST-1: 2-(4-iodophenyl)-3-(4-nitrophenyl)-5-(2,4-disulfophenyl)-2H-tetrazolium

## **CHAPTER I**

### **Introduction**

## CHAPTER I

### Introduction

*Staphylococcus aureus* is an opportunistic pathogen that causes a multitude of diseases in humans and other species. It was discovered in the 1880s by Sir Alexander Ogston as a cause of abscess infections, and its name originates from the Greek “*staphyle*” and “*kokkos*” for “bunch of grapes” and the Latin “*aureus*” for “golden” because the organism exists in clusters, and its colonies are yellow in color (1). *S. aureus* is a gram-positive organism that contains a cell wall composed of peptidoglycan and lipoteichoic acid. The bacterium is catalase-positive, ferments mannitol, produces coagulase, and is not motile. Although *S. aureus* is aerobic and grows best at 30-37°C, it tolerates growth at low oxygen, under high osmotic pressure and at a wide temperature range (82) (12).

#### **Types of *S. aureus* infections**

Approximately 30-50% of healthy humans are colonized on the skin or nares with *S. aureus*, and 20% of the population is considered to be persistent carriers. Persistent carriage of the bacterium increases the risk of developing infections. Additionally, individuals with acquired immune deficiency syndrome, diabetes, or post-surgery are at increased risk of developing infections. Nosocomial infections are obtained by patients who are currently undergoing treatment for another complication, especially by post-operative patients (82).

*S. aureus* has the ability to cause different diseases. Infections range from mild skin diseases like boils and pimples to more invasive illnesses. Uncomplicated skin and soft tissue infections (SSTIs) include cellulitis, impetigo, and furuncles (82). Fortunately, these infections can be successfully treated by surgical drainage and antibiotics (92).

Contrastingly, patients with complicated SSTIs may present with tissue necrosis and sepsis. They require admission into the hospital because they are at high risk of mortality or limb-loss (92). Prolonged uncomplicated SSTIs can also lead to development of osteomyelitis or necrotizing fasciitis (31). Furthermore, individuals may suffer from recurrent SSTIs, which may be remedied by decolonization (31).

Bacteremia is the presence of bacteria in the blood. The source of the systemic bacteria may be a localized focus of infection (72). Consequences of bacteremia arise as the bacteria leave the bloodstream and colonize other tissues like the kidney or endocardium. Bacteremia may also lead to life-threatening sepsis. *S. aureus* sepsis involves systemic inflammation, and severe sepsis includes acute organ failure. Sepsis is usually associated with bacteremia, and can be secondary to bacterial infection of the urinary tract, bone, kidney, or lungs (49) (53). Patients can be admitted into the intensive care unit for treatment, which can last for a few weeks.

*S. aureus* is the leading cause of osteomyelitis, characterized as an acute or a chronic bone infection. Pediatric patients often suffer from the hematogenous form of osteomyelitis, which is accompanied by a fever. Hematogenous osteomyelitis usually develops in long bones, like the femur and tibia, after colonization from the blood (115) (117). In adults, osteomyelitis is usually developed due to spread of a soft tissue infection or by introduction of *S. aureus* bacteria after trauma to the bone (115).

The second leading cause of food-borne illness is *S. aureus*. Gastroenteritis is characterized by nausea, abdominal cramps, diarrhea, and vomiting (7). Disease develops approximately 30 minutes to 8 hours after ingestion of contaminated food (7) (73). In addition to its fast onset, non-life-threatening *S. aureus* gastroenteritis can subside within 24 hours of illness (73). Although rare, gastroenteritis can lead to death, and elderly individuals have a higher incidence of mortality (7).



*S. aureus* is a causative agent of toxic shock syndrome (TSS), a severe disease characterized by high fever, capillary leakage, hypotension, and often involves rash, diarrhea and vomiting, and disseminated intravascular coagulation. *S. aureus* is considered the sole etiology of TSS associated with tampon use in women, where there is also a presence of ulcerative vaginitis (27). TSS is a major problem in pediatric burns, and it is the most frequent cause of unexpected deaths in these patients (141). Currently, pediatric burn cases have surpassed the amount of menstruation-related TSS (141).

*S. aureus* infections can cause pneumonia, an infection of the lungs. Necrotizing pneumonia, which is characterized by inflammation, vascular leakage, and tissue destruction in the lungs is severe (23). *S. aureus* is the most frequently isolated pathogen from patients suffering from ventilator-associated pneumonia due to colonization of the lower airways after mechanical ventilation (4).

Infective endocarditis is a complication of *S. aureus* disease with a mortality rate of 20-30%. Symptoms of disease are fever and fatigue. It involves infection of the endovasculature and, commonly, implanted materials like prosthetic heart valves (136). Pediatric endocarditis is associated with children suffering from congenital heart disease (2). A recent report found that *S. aureus* was the etiologic agent of infective endocarditis in 40% of the study group (2).

### ***S. aureus* antibiotic resistance and therapy**

*S. aureus* has acquired the ability to resist the action of antibiotics (29). Methicillin-resistant *S. aureus* (MRSA) has become predominant in hospital settings, accounting for the majority of nosocomial infections worldwide (82). These strains are referred to as hospital associated-MRSA (HA-MRSA). Patients with HA-MRSA have established risk factors such as prolonged hospitalization, prolonged antimicrobial therapy, surgical procedures, dialysis, indwelling vascular devices, and proximity to patients in the hospital

who are infected or colonized with MRSA (82). However, MRSA cases have been recently reported in healthy individuals with no established risk factors. Because these infections are apparently acquired in the community and are not related to the hospital environment, they are referred to as community-associated MRSA (CA-MRSA) (59) (51). CA-MRSA cases are now being reported all over the world, and their numbers are climbing. Infections due to CA-MRSA seem to primarily affect children and young adults with no predisposing factors. Contrary to HA-MRSA, CA-MRSA strains are susceptible to most antimicrobials except for  $\beta$ -lactams (32), but due to the rapid onset of complications, treatment is often ineffective.

Antibiotic resistance may arise by three mechanisms. The first is acquired resistance via a horizontal transfer, from other bacteria, of genes that encode for a resistance-conferring molecule, commonly, the *mecA* gene product, which is a penicillin-binding protein. Secondly, chromosomal mutations can give rise to resistance. The third mechanism is antibiotic selection (18).

Antibiotics may select for resistant organisms by killing the susceptible population and leaving only the resistant bacteria, which then multiply causing an antibiotic-resistant infection (122). Studies suggest that some antibiotics may be better at selecting for resistance than others due to the ability of a particular compound to possess higher diffusion capabilities, as is the case of fluoroquinolones (122). Additionally secretion of the antibiotic into the individual's sweat could eradicate susceptible bacteria on the skin, which has been shown for ciprofloxacin (61). It has been postulated that vancomycin resistance may be associated with selection on strains colonizing the intestines. It is generally believed that vancomycin resistance frequency decreases as use of vancomycin decreases (122).

The standard therapies for *S. aureus* infections are antibiotics. Nafcillin and oxacillin are the common therapeutics for susceptible *S. aureus* strains. Due to increased

development of resistance, rifampin, is not used alone but in combination with other antibiotics, like nafcillin or vancomycin (37). SSTIs and CA-MRSA are treated with clindamycin, trimethoprim-sulfamethoxazole, or doxycycline (52). Vancomycin is the preferred treatment for other MRSA infections and for endocarditis (93). However, pneumonia and bone infections are treated with linezolid and clindamycin, respectively, due to their abilities to penetrate tissues (52). New studies suggest the use of daptomycin instead of standard therapy for endocarditis (64), possibly due to its lowered toxicity (41).

### **S. aureus pathogenesis**

*S. aureus* causes disease by attaching to host tissues, which it will subsequently colonize. Following these events, *S. aureus* establishes infection by killing host cells, interfering with host pathways, evading the immune response, and spreading to other sites (82). Furthermore, bacteria can form biofilms, which are difficult to treat with antibiotics. In order to accomplish infection, *S. aureus* has an arsenal of virulence factors.

### **Adhesins**

Adhesins are surface proteins used by the bacteria to attach to host molecules (39). After protein expression, they are secreted. Following transport, adhesins are anchored to the cell wall peptidoglycan by a sortase enzyme via a motif at the carboxy terminus (94). The LPXTG motif is used by sortase A to covalently link adhesins to the peptidoglycan via a transpeptidase reaction (94). Specifically, the sortase cleaves the bond between the threonine and the glycine, and the protein is anchored to the wall at the pentaglycine crossbridges. Sortase B uses the NPQTN motif (85). Using sequence analysis to identify staphylococcal proteins containing the LPXTG or NPQTN motif, 22 cell-wall anchored proteins have been identified, and a function has been attributed to half of these putative adhesins.

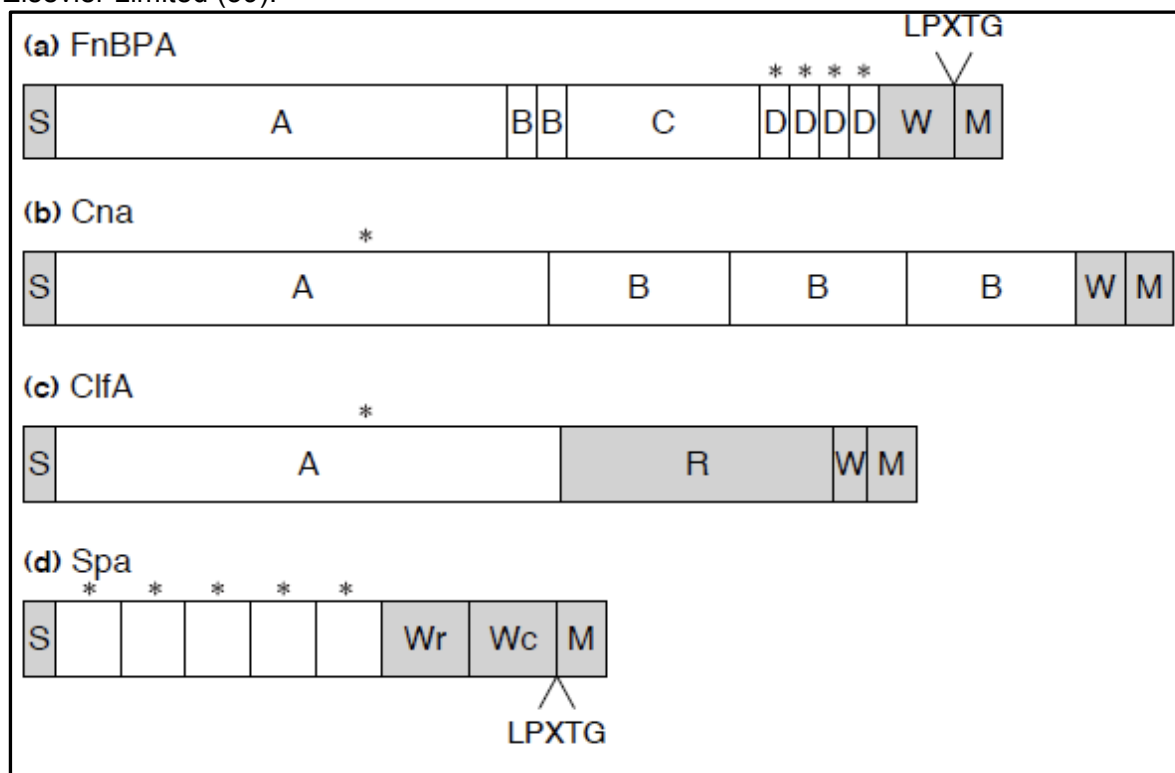
Microbial surface components recognizing adhesive matrix molecules (MSCRAMMs) are cell-wall anchored proteins that adhere to the host extracellular matrix or serum proteins (99). All of the characterized adhesins are MSCRAMMs. They target collagen, fibronectin, elastin, fibrinogen, and other molecules. They are redundant in their specificity, as *S. aureus* expresses at least two MSCRAMMs that recognize fibronectin, two that bind to heme, and at least four proteins that target fibrinogen. While the reason for this redundancy is unknown, our laboratory and others are working to elucidate the reason for this phenomenon and speculate the following reasons. First, some of the host proteins, like fibrinogen and fibronectin, are larger than 300,000 daltons and are composed of different polypeptide chains or different motifs that are involved in many reactions with other host cells, plasma proteins, or extracellular matrix. Secondly, the MSCRAMMs for which a ligand-binding site has been characterized appear to target many different sites within the same protein. This is the case for fibrinogen-binding MSCRAMMs (43) (22) (131).

MSCRAMMs share secondary structure similarities, although their linear sequence may contain little identity. The domain organization of many MSCRAMMs can be described from amino to carboxy terminus (Figure 1-1). Approximately the first 30 residues encode a signal sequence that targets the protein for transport to the cell surface (94). Next, the A domain has been characterized as the ligand-binding domain. C-terminal to the A domain, MSCRAMMs possess one or two repeat regions. Some of these repeated domains are believed to act as stalks that help the adhesin extend away from the cell surface. At the carboxy terminus, there is a wall-spanning region, followed by a membrane-spanning region. Between the latter two domains is the LPXTG anchoring motif (39).

### Protein A

Protein A may be the most characterized surface protein of *S. aureus*. Protein A binds to the plasma protein, von Willebrand factor (vWF) (57). This interaction can mediate

Figure 1-1. Domain organization of MSCRAMMs. Fibronectin binding protein A (FnbpA) (A), Collagen adhesin (Cna) (B), Clumping factor A (ClfA) (C), Protein A (Spa) (D). S: signal sequence; A: amino terminal A domain; B: B repeats; R: Serine-Aspartate repeats; W: wall spanning region; M: membrane spanning region; Wr: octapeptide repeat; Wc: non-repeated domain. Reprinted from Trends in Microbiology, 6 (12), TJ Foster and M Hook, Surface protein adhesins of *Staphylococcus aureus*, 484-488, 1998, with permission from Elsevier Limited (39).



attachment of *S. aureus* bacteria to vWF coated materials under shear flow forces (57). Protein A has also been characterized as a tumor necrosis factor receptor protein 1 (TNFR1)-binding protein (48). This interaction triggers airway inflammation in a murine pneumonia model (47). The most studied function of Protein A is its binding to the Fc region of immunoglobulin heavy chain (38). The structure of the binding domain in complex with the Fc fragment has been solved (24). In humans, Protein A can bind to IgM, IgA, and IgE but not as readily as it binds to IgG. Typically, antibodies recognize bacterial determinants with the variable region and bind to their cell-surface receptors via the Fc region. Because antibodies bind to Protein A via their Fc region, they are not available to ligate Fc receptors to stimulate immune clearance. Via its interaction with IgG, Protein A mediates an inhibition of phagocytosis. Furthermore, Protein A mutants are phagocytosed more readily than wild-type (50).

### Fnbps

*S. aureus* encodes two fibronectin binding proteins, FnbpA and FnbpB that also share similar domain organization (see Figure 1-1). They have been shown to confer binding of bacteria to fibronectin type I modules. *S. aureus* has long been considered to be an extracellular pathogen; however, FnbpA and FnbpB can mediate cell invasion by a mechanism that involves forming a fibronectin bridge with host cell  $\alpha_5\beta_1$  integrins (40). Additionally, the Fnbps are capable of binding to fibrinogen, and FnbpA also binds to elastin. Interestingly, FnbpA binds to fibrinogen and elastin via the same site (66).

### Cna

Collagen is targeted by the collagen binding adhesin, Cna. This protein has been shown to increase the virulence of *S. aureus* in a murine septic arthritis model, and it may also play a role in endocarditis (26) (60). Moreover, Cna was shown to be important for

hematogeneous spread in a murine osteomyelitis study (28). The structures of both the apo-form and Cna in complex with a synthetic collagen peptide have been solved, and the collagen-hug model has been proposed based on experimental data (142).

Cna binds to collagen via the N1 and N2 domains, which are connected by a linker region. The pocket between the N1 and N2 domains accommodates the binding of the triplex helix. Upon ligand binding, Cna and Ace wrap around or “hug” the collagen peptide, resulting in a tunnel formed by the linker and the N1 and N2 domains where the peptide can be held (Figure 1-2) (142).

### Isds

Iron-responsive surface determinants (Isd) proteins are another family of cell-wall anchored proteins. In order to survive in host systems, *S. aureus* must acquire iron, which is usually in complex with other molecules in the form of porphyrins or transferrin. IsdA and IsdC (86) can bind to heme; whereas IsdB recognizes heme and hemoglobin (83). A recent report determined the ability of IsdB to bind to the platelet integrin  $\alpha_{IIb}\beta_3$  which leads to platelet adhesion and aggregation (21). IsdH can bind to haptoglobin in order to sequester the iron. Interestingly, the Isd proteins are found in an operon that also encodes for the sortase B and transporter proteins IsdDEF (86).

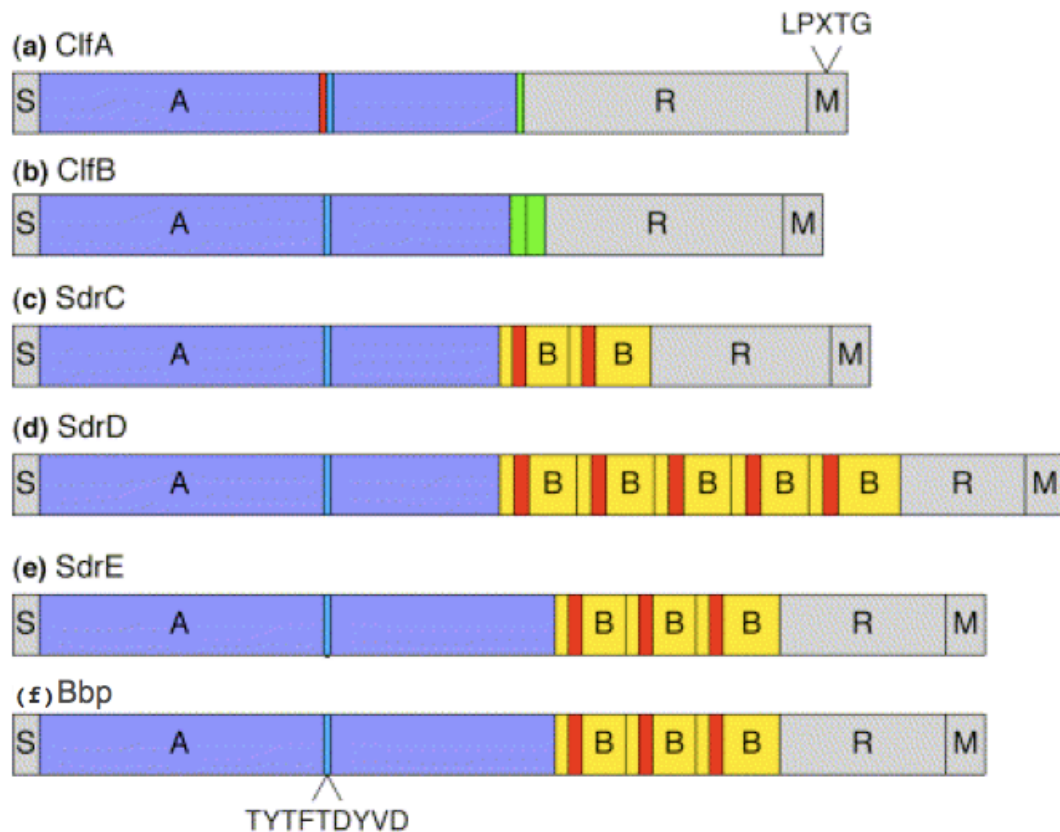
### Clfs

The clumping factors A and B (ClfA, ClfB) also target many ligands. Their basic domain organization is very similar: an amino-terminal ligand-binding domain and a carboxy terminal serine-aspartate repeat (SD) region. Thus, ClfA and ClfB are part of the Sdr subfamily of MSCRAMMs (Figure 1-3). The ligand-binding subdomain constructs of both proteins have been crystallized and the structure of ClfA in complex with a fibrinogen





Figure 1-3. Domain organization of the Sdr proteins. (A) ClfA: Clumping factor A; (B) Clumping factor B; (C) SdrC: SD repeat protein C; (D) SdrD: SD repeat protein D; (E) SdrE: SD repeat protein E; (F) Bbp: Bone sialoprotein-binding protein. S: signal sequence; A: amino terminal A domain; B: B-repeats; R: SD repeat region; M: membrane spanning region. Green: proline-rich region; Red: EF-hands; Blue: TYTFTDYVD. Adapted from Trends in Microbiology, 6 (12), TJ Foster and M Hook, Surface protein adhesins of *Staphylococcus aureus*, 484-488, 1998, with permission from Elsevier Limited (39).



peptide has been solved (43) (25). ClfA and ClfB recognize different Fg chains:  $\gamma$  and  $\alpha$ , respectively (43) (131) .

ClfA is considered to be the principal protein contributing to clumping by binding to fibrin clots. Moreover, it has been shown to play a role in a rat endocarditis model of infection (30), and enriched pooled immunoglobulins against ClfA had therapeutic effects against a catheter-induced aortic valve infective endocarditis rabbit model. (130). ClfA can interfere with Factor XIII mediated fibrin formation (79). In addition, ClfA binds to complement regulator factor I, which increases cleavage of the complement protein C3b (54). ClfB also binds to cytokeratin 10 and plays a role in binding to nasal epithelial cells (134) (132).

### SdrG

SdrG is a Fg-binding MSCRAMM of *S. epidermidis*. SdrG is discussed here because its structure and binding mechanism may closely mimic that of *S. aureus* MSCRAMMs discussed in detail throughout these studies. It targets the thrombin cleavage site of the B $\beta$  chain, and inhibits the release of fibrinopeptides B, which, in turn, inhibits the formation of fibrin (22). Its ligand-binding trench lies between the N2 and N3 domains.

The structures of apo-SdrG<sub>N2N3</sub> and of the complex formed by SdrG<sub>N2N3</sub> with a peptide corresponding to the B $\beta$  chain residues 6-20 were solved to determine the binding mechanism. The co-crystal structure shows that the peptide binds to a trench between the two immunoglobulin-like N2 and N3 domains (Figure 1-4) (102). In the dock, lock, and latch (DLL) mechanism, the Fg peptide docks into the ligand-binding trench formed between the N2 and N3 domains of SdrG<sub>N2N3</sub>. Next, the peptide is locked by a redirection of residues in the C-terminus of N3, which ultimately form a latch that holds the peptide in the ligand-binding trench by forming a  $\beta$ -strand by complementation (102) (10).

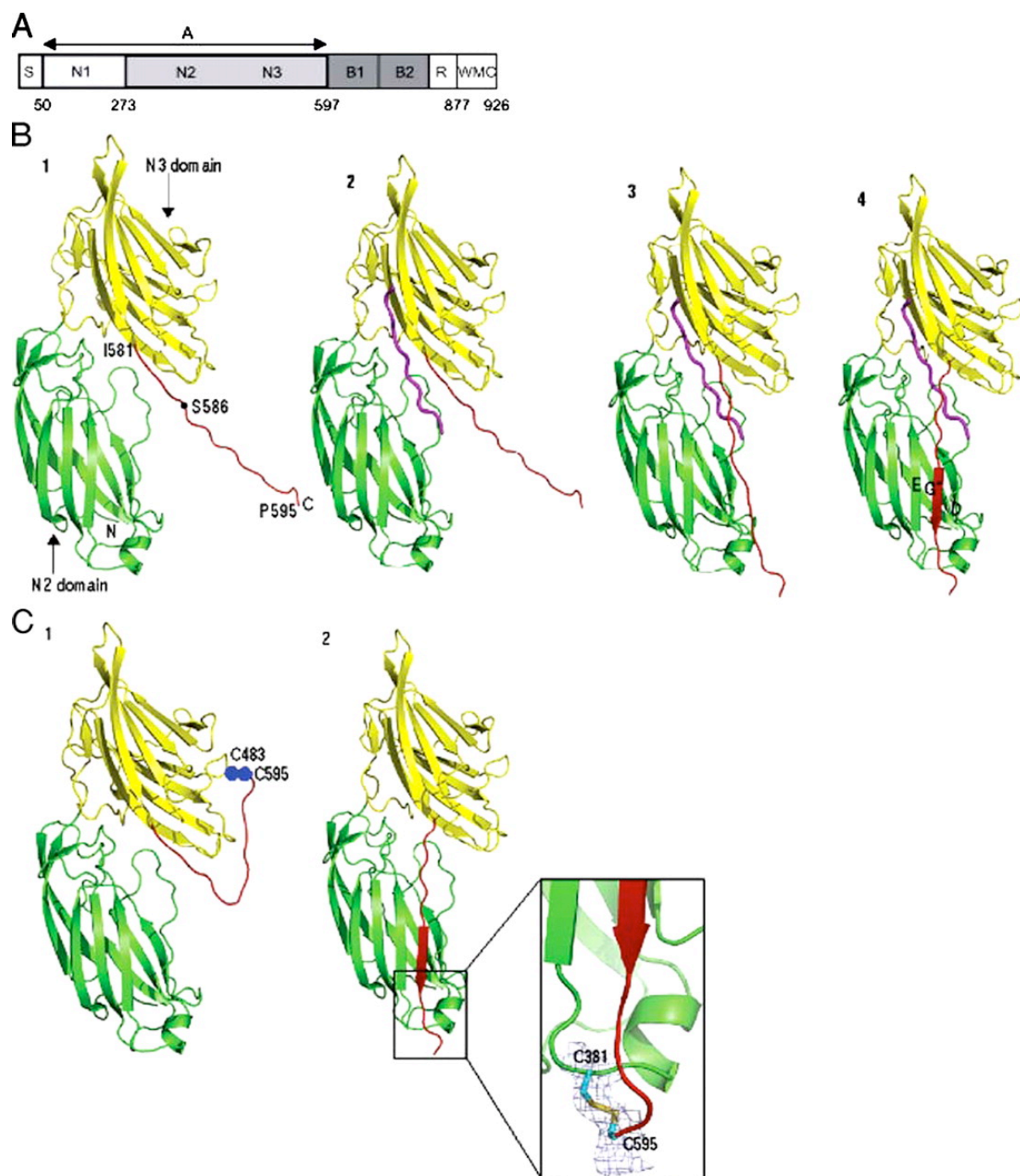
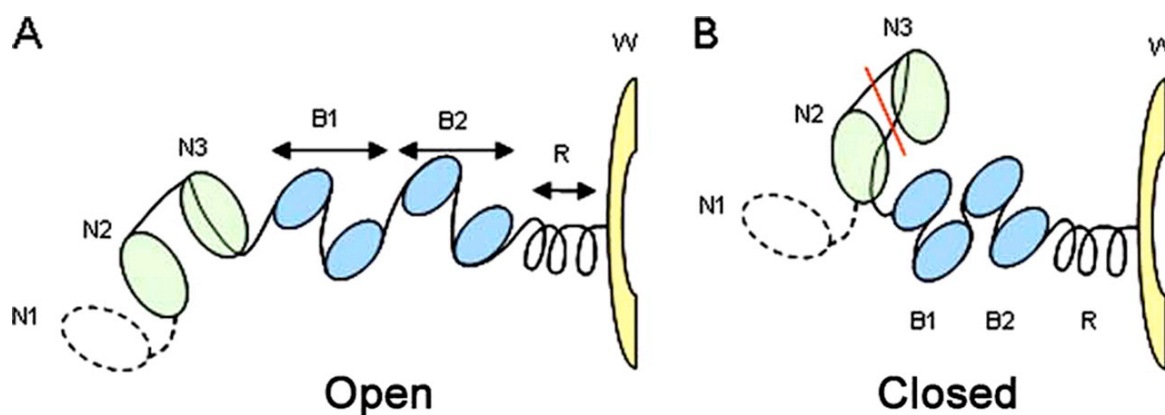


Figure 1-4. See next page for legend.

Figure 1-4. Previous page. Structural representation of the dock, lock, and latch model (A) Domain organization of SdrG. (B) Structure of SdrG<sub>N2N3</sub>. Yellow: N2, green: N3, red wavy line: lock and latch residues. 1) Open, unbound protein; 2) Ligand (purple) docks into the ligand binding trench; 3) The lock residues are redirected by ligand; 4) The latch forms a  $\beta$ -strand with the N2 domain holding the ligand in place. (C) Models for 1) permanently open SdrG(S483C,P595C) and 2) permanently closed SdrG(E381C, P595C). Inset: zoom view of the disulfide bond that covalently closes N2N3. Printed with permission from Journal of Biological Chemistry for nonprofit/noncommercial use : MG Bowden, AP Heuck, K Ponnuraj, E Kolosova, D Choe, S Gurusiddappa, SVL Narayana AE Johnson, and M Hook, Evidence for the “Dock, Lock, and Latch” Ligand Binding Mechanism of the Staphylococcal Microbial Surface Component Recognizing Adhesive Matrix Molecules (MSCRAMM) SdrG, 283, 638-647, 2008 (10).

Figure 1-5. Below. Cartoon representation of the binding between SdrG and fibrinogen. (A) The N2 and N3 regions are in open conformation without ligand and the B-repeats are extended. (B) The Fg peptide (red) is bound and the N2N3 domains are closed; the B repeats are compact due to the redirection of the latching residues. Printed with permission from Journal of Biological Chemistry for nonprofit/noncommercial use : MG Bowden, AP Heuck, K Ponnuraj, E Kolosova, D Choe, S Gurusiddappa, SVL Narayana AE Johnson, and M Hook, Evidence for the “Dock, Lock, and Latch” Ligand Binding Mechanism of the Staphylococcal Microbial Surface Component Recognizing Adhesive Matrix Molecules (MSCRAMM) SdrG, 283, 638-647, 2008 (10).



To biochemically support the findings, further experiments were performed using SdrG<sub>N2N3</sub> mutants (10). The apo form of SdrG<sub>N2N3</sub> has an available ligand trench, and a flexible N3 extension, or latch, this form is referred to as “open.” However, in the protein-peptide complex the N3 extending residues have been redirected to cover the ligand pocket; this form of the protein is referred to as “closed.” Therefore, mutations were introduced to force the protein to exist in either the open or closed conformations (Figure 1-5). Binding and Forster resonance energy transfer experiments confirmed that the peptide can only bind to an open conformation that closes after ligand binding (Figure 1-5) (10). Because the Sdr proteins are similar in domain organization and folding, the dock, lock, and latch mechanism of binding has been proposed for the Sdr family of MSCRAMMs

### Bbp

Studies with *S. aureus* strains that cause osteomyelitis led to the discovery that the bacteria bind to bone-sialoprotein (BSP) (110). Biochemical studies were used to attribute BSP binding to the determinant, bone-sialoprotein-binding protein (Bbp) (138). The binding residues were mapped to the amino-terminus of BSP. Bbp is an MSCRAMM in the Sdr sub-family; therefore, it shares similarities with the clumping factors and SdrG. Bbp has the conserved TYTFTDYVD motif in the A domain and three B-repeats. Antibody titers to Bbp are high in diabetic osteomyelitis patients. Clinically, anti-Bbp sera may be used to differentiate cases of osteomyelitis from soft tissue infections (101).

### Fg - a common MSCRAMM target

Fibrinogen (Fg) is a 340 kDa dimeric glycoprotein composed of two sets of three polypeptides, A $\alpha$ , B $\beta$ , and  $\gamma$  that are covalently linked by disulfide bonds (Figure 1-6). The central region of the dimer contains the amino-termini of the chains. Following the central domain is a coiled-coil region. The ends of the dimer are globular, and the A $\alpha$  chain forms

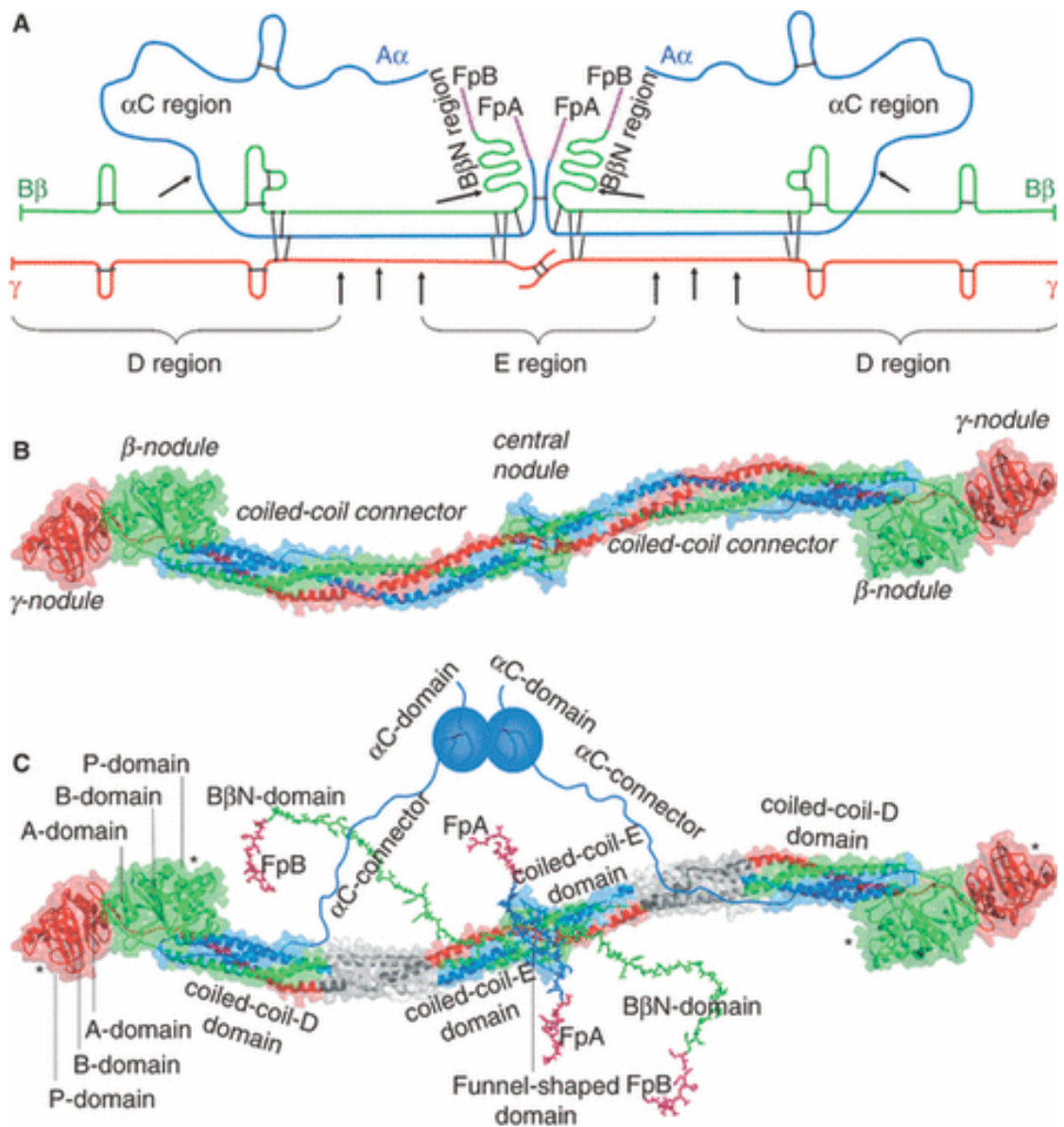


Figure 1-6. Structure of fibrinogen. (A) Individual Fg chains,  $\alpha$  (blue)  $\beta$  (green) and  $\gamma$  (red), FpA and FpB: fibrinopeptides A and B; black bars: disulfide bonds; triple arrows: plasmin cleavage sites for D and E fragments; single arrows: cleavage sites for removal of  $\alpha$ C and  $\beta$ N regions. (B) Crystal structure of fibrinogen. (C) Fibrinogen structure and other regions not crystallized: the  $\alpha$ C-domains;  $\alpha$ C-connectors; the amino-terminus of  $\beta$  ( $\beta$ N) displayed with random conformations; the A, B, and P domains of the D region; the holes and nodules are asterisked. Reprinted from Journal of Thrombosis and Haemostasis 7, 355-359, L Medved and JW Weisel, Recommendations for nomenclature on fibrinogen and fibrin, 2009 with permission from John Wiley and Sons (88).

a hairpin that directs its carboxy-terminus away from the ends of the dimer towards the central region (Figure 1-6). Crystallographic studies have elucidated the structure of Fg; however the carboxy-terminus of the A $\alpha$  chain ( $\alpha$ C) has not been crystallized with the rest of the molecule (67) (139). Instead, part of the  $\alpha$ C structure has been solved with nuclear magnetic resonance using smaller constructs (17) (128).

Hepatocytes synthesize 1.7-5 grams of Fg per day. Approximately 75% of the Fg is found in the plasma, while the rest is in the interstitium and lymph (123). Evidence of non-hepatocyte synthesis also exists (76). In addition, platelets may endocytose Fg, as it has been found in the  $\alpha$  granules (56) (55).

The major role of Fg is to form fibrin clots. During the clotting cascade, prothrombin is activated, and thrombin cleaves fibrinopeptide A from the amino-terminus of the A $\alpha$  chain, which exposes the 'a' knobs. The result is a fibrin monomer that binds to other fibrin monomers to form fibrin protofibrils (91). Next, thrombin cleaves fibrinopeptide B from the amino-terminus of the B $\beta$  chain, exposing the 'b' knobs (140). The protofibrils associate with each other to form fibrin fibers. Factor XIIIa is a transglutaminase that catalyzes the formation of covalent bonds between the  $\alpha$  and  $\gamma$  chains, this crosslinks the fibrin fibrils (116), forming an insoluble meshwork. Plasmin cleavage can degrade fibrin into one E and two D fragments (88).

Fg possesses a multitude of biological functions involving interactions with other proteins and cells in addition to its coagulation function. The  $\beta$  chain mediates the interaction between fibrin and heparin (97). Moreover, it can bind to endothelial cells via vascular endothelial-cadherin (5). Fibrinogen contains three arginine-glycine-aspartate (RGD) sites: two in the A $\alpha$  chain and one in the  $\gamma$  chain, that interact with  $\alpha_5\beta_1$ ,  $\alpha_v\beta_3$ , and  $\alpha_{IIb}\beta_3$  integrins on endothelial cells, fibroblasts, and platelets (119) (42) (3). In addition,

fibrinogen can bind to leukocytes via  $\alpha_M\beta_2$  (36). The A $\alpha$  chain can also bind to fibronectin (84).

#### MSCRAMM-mediated platelet activation

MSCRAMMs bind to platelets leading to activation and aggregation. In the presence of fibrinogen, platelet binding is enhanced (34) (Figure 1-7). The Fnbps use fibrinogen and fibronectin bridges with the platelet integrin  $\alpha_{IIb}\beta_3$  to activate platelets. Furthermore, the activation may occur via bridging Fc $\gamma$ RIIa on platelets with antibodies specific for Fnbps (35). Also, Protein A, ClfA, ClfB, and SdrE all bind to platelets causing their aggregation (96). Although no ligand has been reported for SdrE, its ability to bind to platelets was dependent upon the presence of an unknown plasma protein. Protein A can activate platelets via a direct interaction or through an immunoglobulin bridge to surface Fc receptors (96).

Surface anchored proteins contribute to the pathogenesis and survival of *S. aureus* in host tissues and blood. By binding to extracellular proteins, MSCRAMMs may mediate a stealth form and help the bacterium hide from host defense mechanisms, which they accomplish by coating the bacterial surface with host proteins or by invasion into host cells.

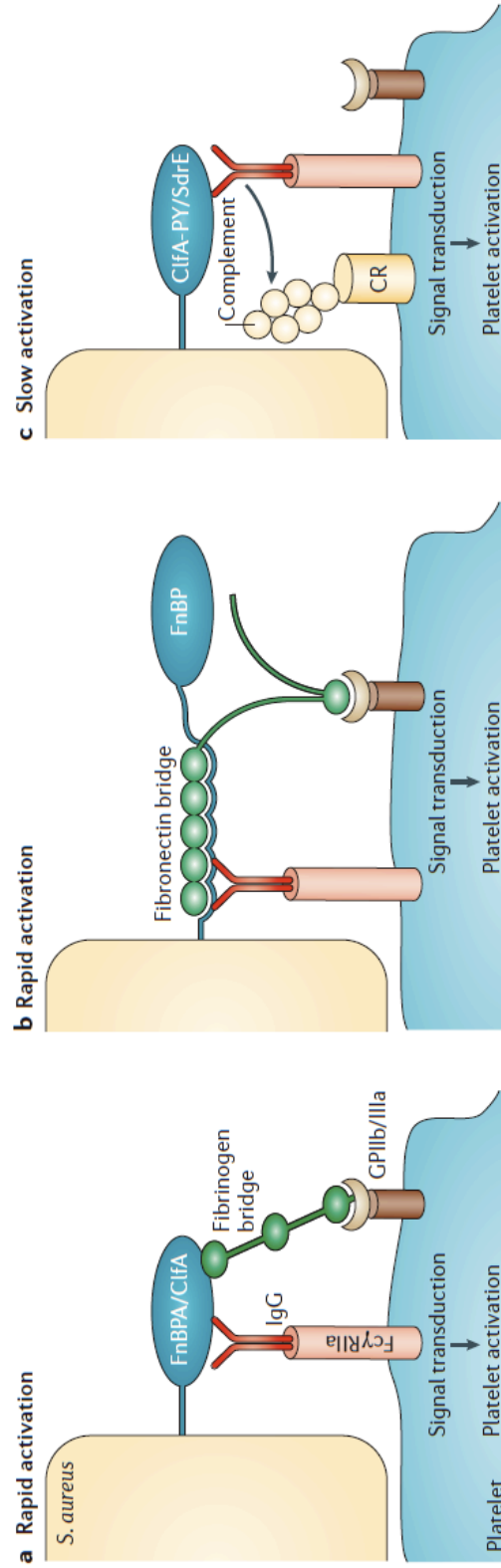
#### **Toxins**

Toxins are secreted bacterial proteins whose activities lead to host cell death. Targets have been identified for many staphylococcal toxins, and some are associated with a specific disease manifestation.

The  $\alpha$ -,  $\beta$ -,  $\gamma$ -, and  $\delta$ -hemolysins, leukocidin, and Panton-Valentine leukocidin (PVL) may all be encoded by a particular *S. aureus* strain. The  $\alpha$ - and  $\gamma$ -hemolysins, leukocidin and PVL are part of the pore-forming toxin family. The  $\alpha$ -toxin, or  $\alpha$ -hemolysin ( $\alpha$ -HL), has



Figure 1-7. *Staphylococcus aureus* platelet activation. (A) Rapid platelet activation occurs via a fibrinogen bridge of FnbpA or ClfA and the platelet integrin  $\alpha_{IIb}\beta_3$  with a protein-specific Immunoglobulin G (IgG) which binds to the Fc $\gamma$ RIIa. (B) Rapid platelet activation occurs via a fibronectin bridge of FnbpA and the platelet integrin GPIIb/IIIa with a protein-specific IgG which binds to the Fc $\gamma$ RIIa. (C) Slow platelet activation occurs when protein specific IgG binds to both the protein and to Fc $\gamma$ RIIa, leading to the classical pathway of complement activation. Reprinted by permission from Macmillan Publishers Ltd: Nature Reviews Microbiology, JR Fitzgerald, TJ Foster, D Cox, The interaction of bacterial pathogens with platelets, 4(6), 445-457, 2006 (34).



been widely studied. It inserts into the host cell membrane as a heptamer, and forms  $\beta$ -barrel pores on the surface. Multiple pores on the cell surface can lead to cell death. Virulence conferred by  $\alpha$ -HL has been implicated in many models of staphylococcal disease including mastitis, pneumonia, and subcutaneous lesions (11) (98) (16). In addition to red-blood cells, the toxin also targets immune and epithelial cells. Additionally,  $\beta$ -toxin is a sphingomyelinase that has been implicated in a mammary gland infection model (11). The  $\delta$ -hemolysin is a small cytotoxin and phenol-soluble modulins that can insert into the membrane of host cells (33). PVL,  $\gamma$ -hemolysin and leukocidin are bi-component toxins that require both subunits to bind to their target cells. The *S. aureus* *hlg* locus encodes three proteins: HlgA, HlgB, and HlgC. The HlgA-HlgB combination forms the hemolysin; whereas, the HlgB-HlgC combination forms leukocidin. The  $\gamma$ -hemolysin has been implicated in a rabbit endophthalmitis model of infection (121). PVL is specific for polymorphonuclear cells, monocytes, and macrophages, and its two components are LukS-PV and LukF-PV. CA-MRSA strains including the predominant clone, USA300, produce this toxin (125). These cytotoxins can target many cell types and have been implicated in various *S. aureus* diseases.

The staphylococcal enterotoxins (SE) and toxic shock syndrome toxin (TSST-1) are pyrogenic toxin superantigens (PTSAgs) and have been directly implicated in virulence. They bind to human major histocompatibility complex class II (MHCII) and T cell receptors (TCR) forming a crosslink between the two proteins. This interaction leads to T cell proliferation and release of cytokines causing an overwhelming inflammatory response in the host (90) (62). PTSAgs induce expansion of T cells specific for the TCR $\beta$ -chain variable region (109). TSST-1 and some SEs also cause vomiting. Staphylococcal food poisoning is attributed to the SEs, and it has been hypothesized that this is due to inflammation in the gastrointestinal tract caused by localized SE emetic reflex (63). TSST-1

is considered as the cause of all menstruation-related TSS. TSST-1 permeates and crosses the vaginal mucosa, explaining why patients do not appear bacteremic when suffering from menstruation-related TSS. Crystallographic data has been used to determine the interacting residues between PTSAGs and their targets. Depending on their exact location within the molecule, mutations in the TCR or MHCII binding residues may diminish or enhance activity of the PTSAGs (77).

### **Other virulence factors used for immune evasion**

Phagocytosis is a major mechanism of host defense against bacteria. *S. aureus* strains possess a capsule composed of polysaccharide. Strains with serotypes 5 and 8 show increased virulence in bacteremia, septicemia, and endocarditis (126), (95), (6). The enhanced virulence conferred by the capsule is due to its ability to decrease the uptake of bacteria by opsonophagocytosis (126). Also, pretreatment with antibodies against the capsule is protective in endocarditis (74).

Some staphylococcal proteins target the host complement pathway. The complement system is composed of proteins that are cleaved and activated to coat the bacteria and form a membrane attack complex. The extracellular fibrinogen-binding protein (Efb), the *Staphylococcus* complement inhibitor (SCIN), and staphylokinase (SAK) aid *S. aureus* in evasion by interfering with the action of serum complement proteins (108). Efb is able to bind to complement factor 3 (C3), thereby inhibiting the ability of C3 to coat the bacteria (75). SCIN inhibits C3b formation by binding to the C3 convertases, C4bC2a of the classical pathway and C3bBb of the alternative pathway, (108), thereby inhibiting bacterial phagocytosis and neutrophil killing. SAK activates plasminogen, which leads to its cleavage of the C3b and IgG that may coat the surfaces of bacteria and inhibit opsonophagocytosis (108).

Neutrophil recruitment is targeted by the chemotaxis inhibitory protein of staphylococci (CHIPS) and the extracellular adherence protein (Eap; also known as MHCII analogue protein, MAP). These are secreted proteins that can bind to two targets leading to immune evasion. First, the ability of neutrophils to migrate to the site of infection is inhibited by CHIPS binding to the formyl peptide receptor via the amino terminus of CHIPS (103). Also, by binding to the complement factor 5a receptor, CHIPS inhibits the chemoattractant C5a from binding to its receptor. Eap can bind to intercellular adhesion molecule-1 (ICAM-1), a ligand for the integrin lymphocyte-function-associated antigen (LFA-1), which is needed for neutrophil adhesion and, ultimately, extravasation (19).

### **Staphylococcal vaccine efforts**

Undoubtedly, the need for a vaccine for *S. aureus* is dire due to the increased number of infections caused by antibiotic resistant strains. Clinical and basic science research on *S. aureus* has provided the biomedical community with vast amounts of knowledge to understand the pathogenesis of *S. aureus* infections, but generating a vaccine for *S. aureus* is complicated. First, the bacterium has many virulence factors with redundant activities. Second, the diseases caused by *S. aureus* are varied. Furthermore, a significant proportion of the population is composed of asymptomatic carriers that may not develop disease. Due to their impaired immune status, immunocompromised individuals and those at elevated risk for infection, would be optimal candidates for passive immunization therapy. Active immunization would be ideal for individuals with the ability to mount an immune response, like healthcare workers. These factors pose a major challenge in deciphering how to best construct a vaccine.

Recently, pharmaceutical companies have conducted active and passive immunization programs (Summarized in Table 1-1). Nabi developed StaphVAX, which contains capsular antigens, and tested its efficacy in dialysis patients. Although, StaphVAX

Table 1 <i>Staphylococcus aureus</i> vaccines in clinical trials			
Product	Corporate Sponsor	Composition	Status
<i>Active immunization</i>			
StaphVAX	Nabi	CP5 and CP8	Phase 3 failed
V710 (0657 nl)	Merck	IsdB	Phase 2 in progress
<i>Passive immunization</i>			
INH-A21 (Veronate)	Inhibitex	Clumping factor A (ClfA, selected IVIG)	Phase 3 failed
Tefibazumab (Aurexis)	Inhibitex	ClfA (mAb)	Phase 2 completed
Altastaph	Nabi	Antibodies to CP5 and CP8	Phase 2 completed
Aurograb	NeuTec	Antibodies to ATP-binding cassette transporter	Phase 3 completed
Pagibaximab (BSYX-A110)	Biosynexus	Lipoteichoic acid (mAb)	Phase 2 completed

Table 1-1. *Staphylococcus aureus* vaccines in clinical trials. Reprinted from Infectious Disease Clinics of North America, 23 (1), AC Schaffer and JC Lee, Staphylococcal vaccines and immunotherapies, 153-171, 2009, with permission from Elsevier Limited (112).

failed phase III trials, it did show protection for a brief period of 3-40 weeks post-vaccination (114). Additionally, the antibodies in Nabi's AltaStaph vaccine were generated in subjects who had been immunized with StaphVax, and these were termed AltaStaph. AltaStaph failed phase II trials on bacteremic patients. Merck's V710 vaccine is composed of IsdB and has successfully undergone phase I testing (112). Inhibitex had two anti-ClfA preparations; Veronate was an IVIg that failed a phase III trial in neonates, and Aurexis was a humanized monoclonal with a successful phase II trial of bacteremic patients. Pagibaximab (BSYX-A110) by Biosynexus is a chimeric monoclonal against lipoteichoic acid that reduced the rate of developing bacteremia in neonates (133). Despite these efforts, a vaccine has not been approved by the FDA.

Preclinical studies have shown promise in developing vaccines against *S. aureus* infections targeted at toxins and surface components. A tetravalent vaccine composed of SdrD, SdrE, IsdA, and IsdB was tested in a murine kidney abscess model, and mice immunized with the four components survived challenge with clinical isolates (118). This approach is promising, as a vaccine against *S. aureus* may need to target multiple epitopes or proteins. Efforts to target the  $\alpha$ -HL have also shown success preclinically. Antibodies generated to an inactive  $\alpha$ -HL mutant (89) protected mice challenged with a lethal dose of clinical isolates in a pneumonia model (15). Furthermore, the mice had less inflammation, decreased bacterial burden, and less tissue destruction (15) (14). These animal studies have helped to elucidate potential vaccine candidates by discerning the benefit of antibodies against particular virulence factors.

## Summary

Antibiotics are the current treatment for *S. aureus* infections. With every wave of antibiotic resistance, the medical community has to adapt by using last line of defense antibiotics or by combining multiple antibiotics in order to clear the infections. With CA-

MRSA infections on the rise, there is a need to abrogate the spread of infections. Although the search for vaccine candidates has resulted in mixed successes, past attempts at *S. aureus* vaccines have indicated that staphylococcal virulence factors can elicit a protective response. By identifying and characterizing the events that occur between the bacteria and the infected host, valuable information can be gained about pathogenesis. This knowledge can then be used to develop disease models where the specific virulence factor's contribution can be analyzed. Also, these types of experiments have helped us to identify redundant functions of bacterial proteins. Conducting epidemiological studies may identify correlations between a particular disease and a virulence factor. These studies may serve as guides to identify functions. Ultimately, the virulence factors can be examined to link the epidemiologically associated factor with specific disease models.

In this study, a surface and a secreted factor of *S. aureus* were examined. First, I examined function of a secreted leukotoxin whose presence was associated with strains that cause necrotizing pneumonia. *In vitro* and *in vivo* analyses were performed to determine its role in disease. Secondly, an MSCRAMM that is implicated in hematogeneous osteomyelitis was studied. Through biochemical and biophysical assays, I identified a novel ligand for the adhesin. By dissecting the interaction with its ligand, I discovered its potential ability to abrogate host coagulation.

## **CHAPTER II**

**Panton-Valentine Leukocidin causes necrotizing pneumonia**



## CHAPTER II

### Panton-Valentine Leukocidin causes necrotizing pneumonia

#### Introduction

Analysis of CA-MRSA strains has revealed the presence of the Panton-Valentine leukocidin (PVL) (78) (46). PVL is a secreted toxin that is composed of two protein subunits, LukS-PV and LukF-PV, that act synergistically to form pores in the membranes of host monocytes, macrophages, and polymorphonuclear cells (20). PVL belongs to the pore-forming toxin (PFT) family that includes  $\alpha$ - and  $\gamma$ -hemolysin. With the exception of  $\alpha$ -hemolysin, the staphylococcal PFTs contain an S subunit (HlgA, HlgC, LukE, LukS-I, LukM, and LukS-PV) and an F subunit (HlgB, LukD, LukF-I, LukF', and LukS-PV) (20). Identity within the subunit classes is high, ranging from 59-79% and 71-79% for S and F, respectively, whereas the identity between S and F is only approximately 25% (65) (104). Alpha-hemolysin most resembles an F monomer and is the prototypical PFT. Although the sequence identities between PVL and other PFTs are high, PVL is not hemolytic (104) (20).

Recently, the presence of PVL has been linked to *S. aureus* strains isolated from necrotizing pneumonia patients (78) (46). Necrotizing pneumonia is characterized by massive cell infiltration, severe tissue destruction, and hemorrhage in the air space. Etienne and colleagues conducted a study where they discovered that infection by PVL-positive strains were more common among young, immunocompetent patients (46). These strains caused a fast onset of infection with a high lethality rate. The authors also analyzed lung sections from PVL-positive *S. aureus* necrotizing pneumonia patients and showed overwhelming inflammation in the lungs, as well as the presence of PVL (28, 45). However, it is not known whether PVL is the direct cause for the increased severity of symptoms observed in these patients.

Neutrophils are often the first cells to respond at the site of infection (44). They are recruited by chemoattractive factors like chemokines, such as interleukin-8 (IL-8), and other soluble substances, like leukotrienes and platelet activating factor (106) (135). IL-8 is a chemokine produced and secreted by immune and epithelial cells after activation with bacterial determinants or inflammatory cytokines; after secretion, it may last for several days. Increased levels of IL-8 have been shown in bronchial lavages of pneumonia patients (106) (107). In addition to its pore-forming activity, PVL exposure causes leukocytes to secrete inflammatory mediators (69). After PVL treatment, leukocytes have been shown to release IL-8, hexosaminidase, lysozyme,  $\beta$ -glucuronidase, IL-8, Leukotriene B<sub>4</sub>, and histamine (70) (20) (137) (68) (58).

The significance of PVL in CA-MRSA and necrotizing pneumonia *S. aureus* strains was addressed in this study. We sought to determine whether PVL plays a pivotal role in the inflammation observed in necrotizing pneumonia. Specifically, we tested the ability of PVL to cause inflammation in lung epithelial cells *in vitro* and to cause necrotizing pneumonia in a mouse model.

## **Materials and Methods**

*Generation and purification of PVL subunits-* In order to generate highly active PVL, each subunit was expressed separately, under the control of the native PVL promoter. The plasmids (kindly donated by Francois Vandenesch) were transformed into *S. aureus* 8325-4 that was engineered with deletions of *hla*, *hly*, and *hlg* (kindly donated by Timothy Foster) in order to decrease the chance of contamination by other PFTs. The secreted PVL subunits were purified as previously described (104) using cation-exchange chromatography.

*Rabbit hemolysis assay-* Rabbit erythrocytes (kindly provided by Steven Norris) were washed and resuspended in PBS. A 1% solution of rabbit erythrocytes was incubated with increasing concentrations (1-100 nM) of LukS-PV, LukF-PV, or PVL for 60 minutes at 37°C. The samples were subjected to centrifugation and the absorbance of the supernatant was measured at 525 nm.

*Assessment of protein activity-* LukS-PV binding to isolated human neutrophils was performed using flow cytometry. A three-color assay was developed that allowed us to verify that the neutrophils were pure and that LukS-PV was binding to this population of cells. Neutrophils were incubated with LukS-PV followed by incubation with anti-LukS-PV monoclonal antibody conjugated to PE-Cy5.5 (Nabi). In order to detect the neutrophil population, the cells were stained with anti-CD11b-PE and anti-CD15-FITC (R&D Systems). Furthermore, we tested the purified subunits for leukotoxic activity. Briefly, neutrophils were incubated with increasing concentrations (0.1-30 nM) of PVL, followed by incubation with 2-(4-iodophenyl)-3-(4-nitrophenyl)-5-(2,4-disulfophenyl)-2H-tetrazolium (WST-1) (Roche), a tetrazolium salt used for viability determination (124). The absorbance was measured with a Thermo Max plate reader at 650 nm with reference subtraction at 450 nm.

*IL-8 production by PVL treated epithelial cells-* IL-8 induction from PVL-treated epithelial cells was measured. Briefly, A549 cells were seeded overnight, washed, and incubated with PBS, PVL (1 nM) , or LPS (100 ng/ml) for 24 hours. The cells were washed, RNA was extracted and reverse transcriptase PCR was performed to detect expression of IL-8. The primers used were 5'-AGCTCTGTGTGAAGGTGCAG-3' and 5'-ATTCTGTGTTGGCGCAGT-3' for IL-8 and 5'-CCAGGTCTCCTCTGACT-3' and 5'-TGCTGTAGCCAAATTCGTTG-3' for GAPDH, as a control. Furthermore, secreted IL-8 was measured from cell-conditioned media using the eBioscience IL-8 sandwich ELISA kit. Briefly, A549 cells were seeded overnight, washed, and incubated with PBS, LPS (100 ng/ml), or increasing concentrations of PVL (10 nM – 10  $\mu$ M) for 4 hours. The cell-conditioned medium was pipetted and debris was pelleted by centrifugation. All incubations were conducted as recommended by the manufacturer.

*Pro-inflammatory protein array screen-* In order to determine if PVL could induce secretion of many pro-inflammatory cytokines, a Panomics protein array was incubated with cell-conditioned media from PVL-treated lung epithelial cells. Briefly, A549 cells were seeded overnight, washed, and incubated with 30 nM PVL for 24 hours. The cell-conditioned medium was pipetted, and debris was pelleted by centrifugation. All incubations were performed according to manufacturer's instructions.

## **Results**

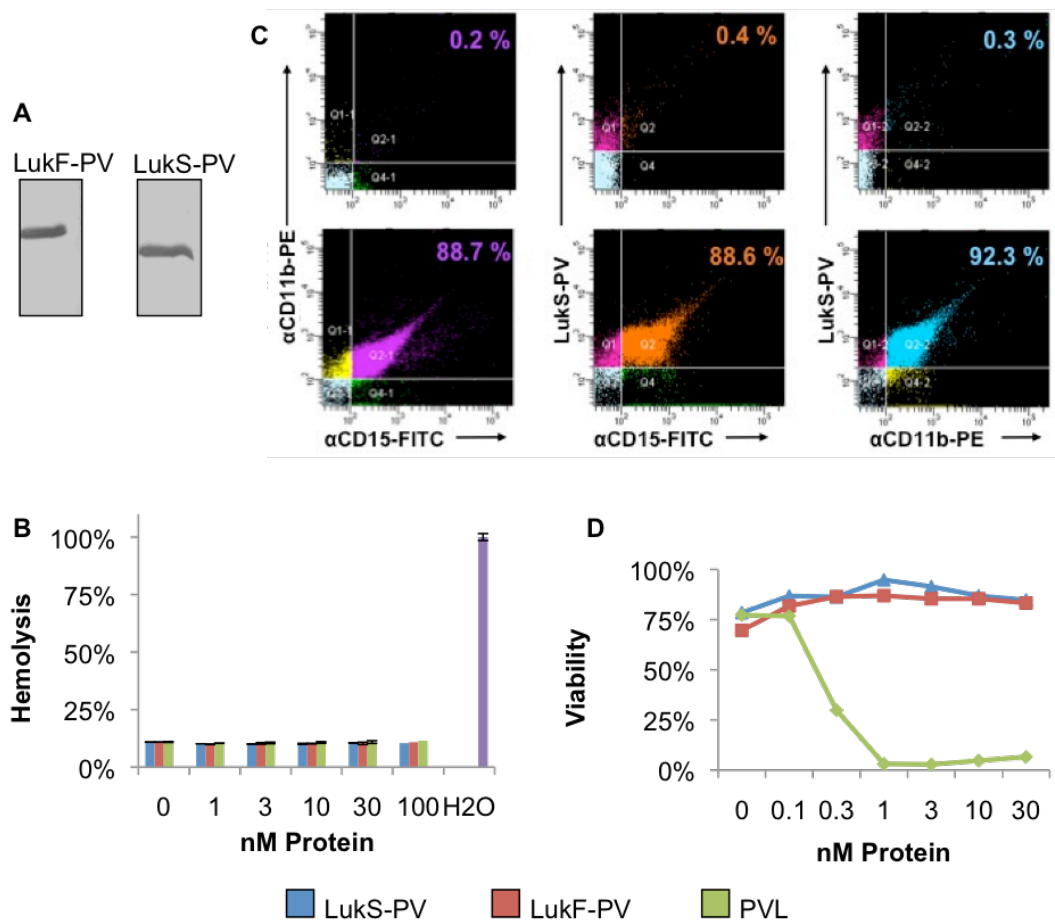
### **Active PVL subunits were produced.**

The purity of PVL subunits was confirmed by SDS-PAGE, and Western blotting (Figure 2-1a). Rabbit erythrocytes were incubated with increasing concentrations of purified LukS-PV, Luk-PV, or PVL to assess whether the toxin preparation was contaminated with other PFTs (Figure 2-1b). The results confirmed the purity of the PVL preparation. Next, the toxin's activity on isolated human neutrophils was examined. Flow cytometry binding experiments confirmed that the LukS-PV subunit bound to CD15 and CD11b double positive cells (Figure 2-1c). Furthermore, PVL readily lysed human neutrophils, with an LD<sub>50</sub> of 250 pM (Figure 2-1d).

### **PVL-induced inflammation from lung epithelial cells**

To determine if PVL production by pneumonia-causing *S. aureus* strains triggered inflammatory responses from lung epithelial cells, experiments were performed using *in vitro* cultured A549 cells. The ability of PVL to stimulate IL-8 production in A549 cells was examined. The cells were incubated with PVL or LPS, as a positive control, followed by detection of IL-8 expression using RT-PCR (Figure 2-2a). The PVL-treated epithelial cells produced approximately the same amount of IL-8 as the LPS-treated cells, and untreated cells did not produce IL-8, indicating that PVL induced expression of the proinflammatory cytokine. Next, the ability of PVL to induce secretion of IL-8 by A549 cells was examined. The cells were incubated with PBS, LPS, or increasing concentrations of PVL (10 nM- 10  $\mu$ M), and the cell-conditioned media was harvested. The concentration of secreted IL-8 was measured using a sandwich ELISA. Results showed that PVL-treated A549 cells secreted similar amounts of IL-8 as that secreted by LPS-stimulated cells (Figure 2-2b). Together, these data indicate that PVL-stimulated A549 cells express and secrete IL-8.

Figure 2-1. The purified Pantone-Valentine Leukocidin subunits are active. (A) Western blots: The LukF-PV (left) and LukS-PV (right) proteins were separated by SDS-PAGE and immunoblotted with protein-specific monoclonal antibodies followed by goat-anti-mouse IgG. (B) Hemolysis assay: Rabbit erythrocytes were suspended in PBS and incubated with increasing concentrations (1-100 nM) of LukS-PV, LukF-PV, or both subunits for 30 minutes. Erythrocytes treated with water served as a positive control, and for normalization. (C) Flow cytometry: Isolated human neutrophils were incubated with 0.5 nM LukS-PV followed by anti-LukS-PV conjugated to Pe-Cy5.5, anti-CD15-FITC, and anti-CD11b-PE. Top panels are controls of the bottom panels. (D) Neutrophil viability assay: Isolated human neutrophils were incubated with increasing concentrations (1-100 nM) of LukS-PV, LukF-PV, or both subunits prior to the addition of WST-1 for viability determination.



**A**

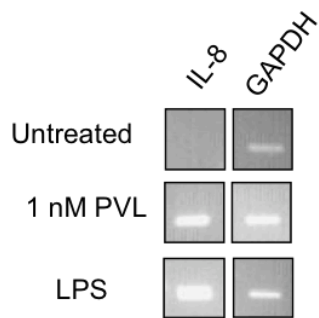
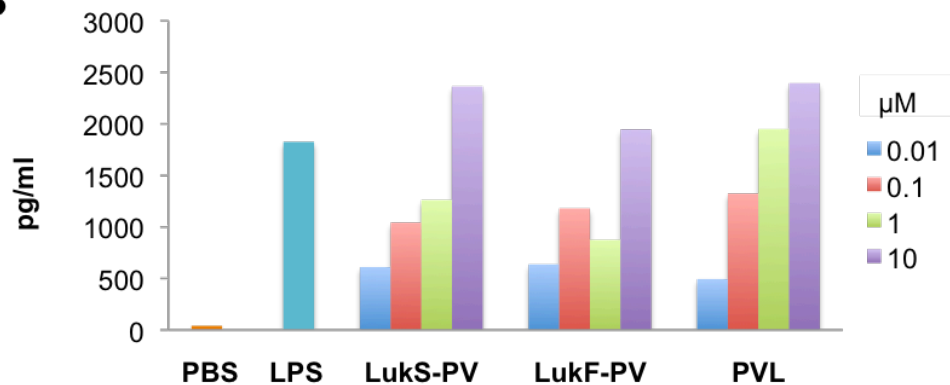
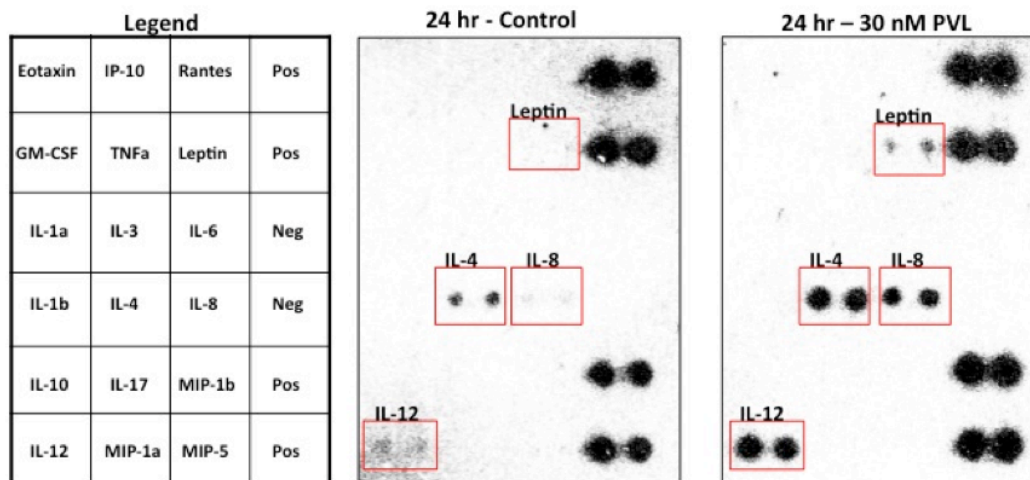


Figure 2-2. PVL-induced inflammatory cytokine secretion from alveolar epithelial cells. (A) Induction of IL-8 expression measured by Reverse-transcriptase PCR: Lung epithelial cells were incubated with PVL, LPS, or untreated followed by RNA extraction and RT-PCR with primers for IL-8 or GAPDH. (B) Induction of IL-8 secretion by lung epithelial cells. Cells were incubated with PBS, LPS, or increasing concentrations (10 nM -10  $\mu$ M) of LukS-PV, LukF-PV, or both subunits. The IL-8 concentrations of cell-conditioned medium were determined by sandwich ELISA. (C) Panomics inflammatory cytokine protein array: Induction of inflammatory cytokine secretion from PVL-treated lung epithelial cells was determined by incubating the array membranes with cell-conditioned medium.

**B**



**C**



To determine if PVL induced the secretion of additional pro-inflammatory mediators, a Panomics protein array was used. A549 cells were treated with PVL and cell-conditioned media were collected and used for protein array incubation (Figure 2-2c). The secretion profiles of PVL and control cells were compared. PVL-treated epithelial cells secreted IL-8, the Th2-promoting cytokine IL-4, and the Th1-promoting cytokines IL-12 and Leptin (in lesser quantity). However, PVL failed to induce secretion of eotaxin, IP-10, Rantes, granulocyte-monocyte colony stimulating factor, tumor necrosis factor- $\alpha$ , IL-1, IL-3, IL-6, IL-10, IL-17, MIP-1, and MIP-5. These results confirmed the secretion of IL-8, and identified the ability of PVL to induce secretion of additional cytokines from A549 cells.

### **PVL-induced necrotizing pneumonia and active immunization in a murine pneumonia model**

An acute mouse model of pneumonia was developed and used to determine if instillation with PVL causes pneumonia. In this model, LukS-PV by itself did not cause pneumonia, presumably because both of the toxin subunits are required for its pore-forming activity. However, instilling both PVL components resulted in pathology that was comparable to that observed in PVL-positive *S. aureus* infected animals, and PVL-negative *S. aureus* caused minor inflammation (71) (Figure 2-3). The PVL-instilled mice had severe inflammation, vascular leakage, and disrupted alveolar structure. Additionally, 70% of mice instilled with 10  $\mu$ g of protein died within 24 hours. These results indicate that both PVL subunits are required to cause necrotizing pneumonia. PVL by itself is sufficient to cause lethality in mice and both subunits are required for the toxicity.

Further studies evaluated the PVL subunits as vaccinogens. Mice were immunized with either PVL subunit and subsequently challenged with a lethal dose of the virulent *S. aureus* USA300 strain (Figure 2-4) (13). Active immunization with LukS-PV resulted in survival of 75% of the mice challenged; whereas 50% of mice immunized with LukF-PV or



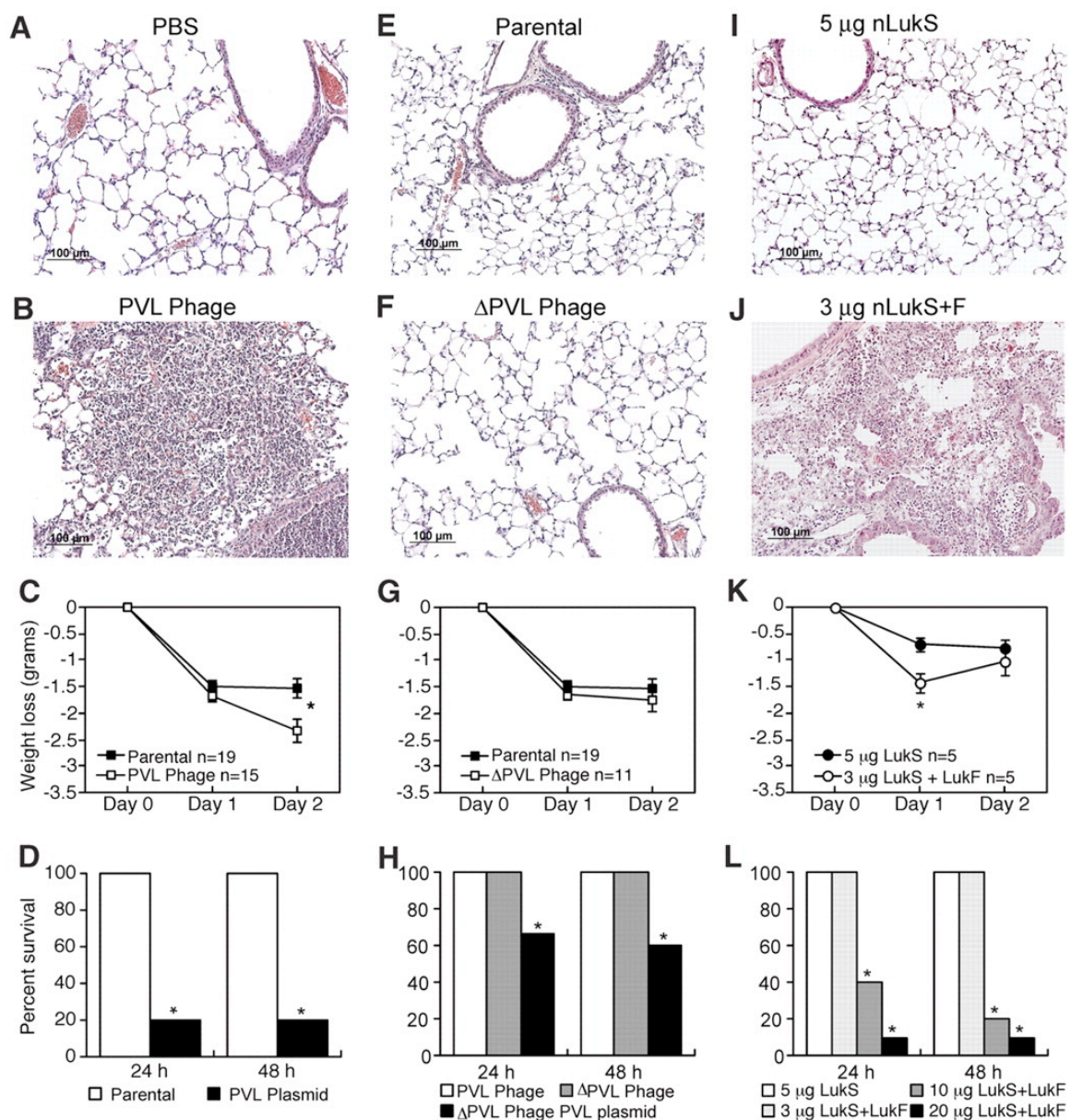


Figure 2-3. PVL expression enhances the virulence of isogenic *S. aureus* strains. (**A**, **B**, **E**, **F**, **I**, and **J**) Lung histology of mice infected with PVL-positive and PVL-negative strains or inoculated with PVL toxin. The sections are representative of at least three separate experiments. Scale bar, 100  $\mu$ m. (**C**, **G**, and **K**) Line graphs indicate weight loss in grams. (**C**) Parental versus PVL phage;  $*P < 0.001$ . (**G**) Parental versus PVL phage; no statistical difference observed. (**K**) Animals inoculated with 3  $\mu$ g of LukS+F-PV versus 5  $\mu$ g LukS-PV;  $*P < 0.01$  on day 1. (**D**, **H**, and **L**) Mouse survival. (**D**) Parental and PVL plasmid; (**H**) PVL phage, PVL phage, and PVL phage PVL plasmid; (**L**) 20  $\mu$ g or 10  $\mu$ g of LukS+LukF-PV versus 3  $\mu$ g LukS+LukF-PV or 5  $\mu$ g LukS-PV,  $*P < 0.0001$ . Reprinted from Science 315 (5815), The Staphylococcus aureus Pantone-Valentine Leukocidin Causes Necrotizing Pneumonia, M Labandeira-Rey, FCouzon, S Boisset, EL. Brown, M Bes, Y Benito, EM Barbu, V Vazquez, M Hook, J Etienne, F Vandenesch, MG Bowden, 2007, with permission from the American Association for the Advancement of Science (71).

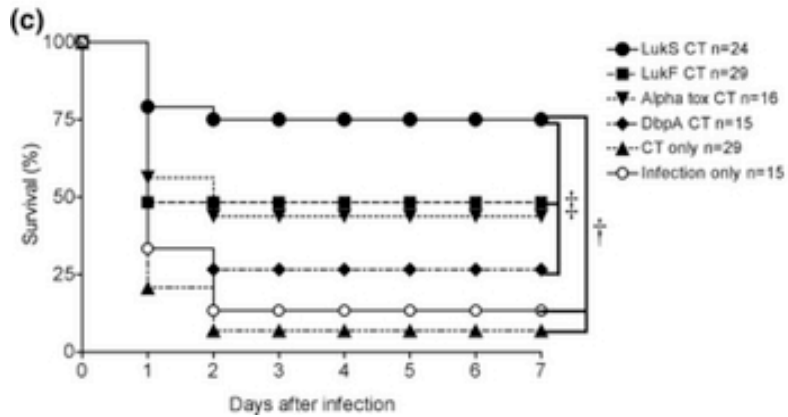


Figure 2-4. Percent survival following intranasal inoculation with *Staphylococcus aureus* USA300. Balb/c mice (total numbers used/group indicated in parentheses) were vaccinated subcutaneously with recombinant LukF, LukS, control proteins or adjuvant alone prior to infection with  $5 \times 10^7$  CFUs of *S. aureus* in a volume of 20  $\mu$ L. Mouse survival was monitored for up to 7 days post-infection. Reprinted from Clinical Microbiology and Infection 15(2), 156-164, EL Brown, O Dumitrescu, D Thomas, C Badiou, EM Koers, P Choudhury, V Vazquez, J Etienne, G Lina, F Vandenesch, and MG Bowden, The Panton-Valentine leukocidin vaccine protects mice against lung and skin infections caused by *Staphylococcus aureus* USA300, 2008 with permission from John Wiley and Sons (13).

$\alpha$ -HL survived the infection. These results indicate that the PVL subunits can generate a protective response against lethal challenge by PVL-producing *S. aureus* in a pneumonia model.

## **Discussion**

Due to the increased numbers of MRSA cases, many epidemiological studies have been conducted to identify correlations between the presence of potential virulence factors with *S. aureus*-caused diseases. The *pvl* genes have been detected in strains that cause severe necrotizing pneumonia. Therefore, we sought to determine whether we could experimentally link the presence of PVL in these strains to the severity of disease.

In order to study the toxin, recombinant subunits LukS-PV and LukF-PV were generated in a *S. aureus* strain deficient in the expression of  $\alpha$ -,  $\beta$ -, and  $\gamma$ -hemolysins. The toxin preparation was pure, devoid of other toxins and cell-wall components, and was fully active towards human neutrophils. Prior to conducting mouse experiments, *in vitro* experiments with lung epithelial cells were performed, and I detected IL-8 secretion from toxin-treated A549 cells. Results from the mouse model have clearly implicated PVL as a cause of necrotizing pneumonia. An acute model of pneumonia was used to compare the virulence of PVL-positive versus PVL-negative strains and PVL protein instillation into the mice. Indeed, the PVL-positive infected mice developed severe pneumonia; whereas, the PVL-negative strains caused mild inflammation. Surprisingly, instilling mice with PVL protein alone was sufficient to cause necrotizing pneumonia (71).

Furthermore, a vaccine study performed with the PVL subunits showed that mucosal vaccination with LukS-PV protein was a successful active immunization strategy, as immunized mice showed higher percentage of survival after challenge with a clinical isolate than control mice (13).

Results from experiments performed with the recombinant PVL toxin combined its correlation with strains that cause necrotizing pneumonia. Necrotizing pneumonia causes lung tissue destruction, vascular leakage, and overwhelming inflammation. *In vitro* experiments conducted with epithelial cells treated with each subunit or both resulted in the release of IL-8 from epithelial cells.

However, the overwhelming inflammation seen during necrotizing pneumonia cannot be solely attributed to PVL-induced IL-8 secretion from airway epithelial cells. Instead, the PVL-induced pneumonia was only observed in mice instilled with both PVL subunits, suggesting that the toxin's ability to cause pneumonia may be related to its ability to lyse leukocytes. Therefore, the pneumonia is likely due to the toxin's high activity on infiltrating neutrophils and resident alveolar macrophages, and its ability to cause epithelial cell inflammation is less of a factor. To test the contribution of leukocyte inflammation, the experiments described herein could be performed on leukocyte-depleted animals. Previous efforts to conduct these experiments resulted in morbidity and mortality of all animals, whether infected with PVL-negative or PVL-positive *S. aureus*, because the leukopenia rendered them more susceptible to staphylococcal disease.

In conclusion, virulence factors that are correlated epidemiologically with specific disease can be studied *in vitro* and *in vivo* to link the presence of genes with disease causation.

## **CHAPTER III**

### **The MSCRAMM Bbp targets the Fibrinogen A $\alpha$ chain**

## CHAPTER III

### The MSCRAMM Bbp targets the Fibrinogen A $\alpha$ chain

#### Introduction

*S. aureus* possesses cell-surface adhesins to aid in the attachment, colonization, and invasion of host tissues. The bacteria may also use adhesins or Microbial Surface Components Recognizing Adhesive Matrix Molecules (MSCRAMMs) to evade host immune responses. MSCRAMMs can target both extracellular matrix and blood plasma molecules and several MSCRAMMs have more than one ligand (Table 3-1).

The domain organization and predicted structures of the Sdr subset of the MSCRAMMs are similar, although sequence identity among the Sdr proteins may be low. One difference among the Sdr proteins is the B-repeat content. The clumping factors do not contain B-repeats, while SdrC has two, SdrD has five, and SdrE and Bbp have three. Also, SdrE and Bbp have been described as allelic variants with higher identity between these two than among any of the other Sdr proteins. Many studies have correlated the presence of the Sdr proteins in *S. aureus* isolated from healthy or sick individuals. Analysis of isolates from carriage strains and strains that cause invasive disease revealed that the *clfA*, *clfB*, and *sdrC* genes were present in almost all of the isolates, regardless of the source. However, only 38-56% of isolates contained the genes *sdrD*, *SdrE*, and *bbp* (100). Interestingly the authors found *sdrE* in 40% of the carriage isolates and in 56% of the strains causing invasive disease; this led to the conclusion that *sdrE* is preferentially associated with invasive strains (100).

A second study examined the genes encoding for SdrC, SdrD, and SdrE/Bbp in carriage and invasive isolates (111). The primers used for this study do not differentiate *sdrE* from *bbp*. *sdrC* was found in all strains; *sdrD* was associated with MRSA. *sdrE/bbp* was present at similar levels in MSSA and MRSA. Furthermore, the authors concluded that

Table 3-1. *Staphylococcus aureus* MSCRAMMs with multiple ligands.

MSCRAMM	Ligands
Protein A	IgG, von Willebrand Factor, TNF $\alpha$ receptor (TNFR), epidermal growth factor receptor (EGFR)
FnbpA	fibronectin, fibrinogen (Fg), elastin
FnbpB	fibronectin, fibrinogen
ClfA	fibrinogen, complement regulator factor I
ClfB	fibrinogen, cytokeratin 10



both *SdrD* and *SdrE/bbp* may be important in osteomyelitis. Lastly, when Tristan and colleagues evaluated carriage, endocarditis, and hematogeneous osteomyelitis/arthritis isolates, they detected *bbp* (*sdrE* was not tested) in 21%, 11%, and 38% of the respective isolates (127). These studies indicate that *sdrE* and *bbp* may be present in *S. aureus* isolated from carriers and from patients with invasive disease.

Together, these epidemiological data suggest that the disease with which *bbp* preferentially associates is osteomyelitis. However, the fact that the isolates in the study by Tristan and colleagues evaluated hematogeneous osteomyelitis isolates may indicate a role for Bbp in the blood. Moreover, patients suffering from diabetic osteomyelitis had higher titers to Bbp than patients with soft-tissue infections (101). Furthermore, Bbp studies have revealed bone-sialoprotein (BSP), a major constituent of bone, as a ligand for Bbp binding. Therefore, it is a potential staphylococcal virulence factor. Because several MSCRAMMs have multiple ligands, I hypothesized that Bbp may recognize other host proteins.

Fibrinogen (Fg) is a blood glycoprotein involved in the clotting cascade and cell signaling. It is targeted by many MSCRAMMs (Figure 3-1). It is a dimeric protein composed of two  $A\alpha$ ,  $B\beta$ , and  $\gamma$  chains that are held together by intra- and inter-chain disulfide bonds. Additionally, its overall structure has been solved by crystallography; however, the structure of the carboxy-terminus of the  $A\alpha$  chain has only been partially elucidated (67) (17). In order to form fibrin, the fibrinopeptides A and B must be cleaved from the amino-terminus of the  $A\alpha$  and  $B\beta$  chains, respectively, to expose sites that are important for the lateral aggregation of protofibrils. Additionally, the transglutaminase Factor XIIIa catalyzes the formation of covalent bonds that crosslink the fibrin fibrils.

The remarkable domain organization similarity among Bbp and other staphylococcal Fg-binding MSCRAMMs prompted further study to determine if a second ligand for Bbp exists. A ligand screen revealed that Bbp<sub>N2N3</sub> recognizes human Fg. Therefore, I

conducted a series of experiments that localized the binding to residues on Fg A $\alpha$  that are not targeted by other MSCRAMMs. Bbp on the surface of bacterial cells mediated attachment to the mapped residues in Fg A $\alpha$ . Furthermore, pretreatment of Fg with Bbp<sub>N2N3</sub> inhibited the formation of fibrin.

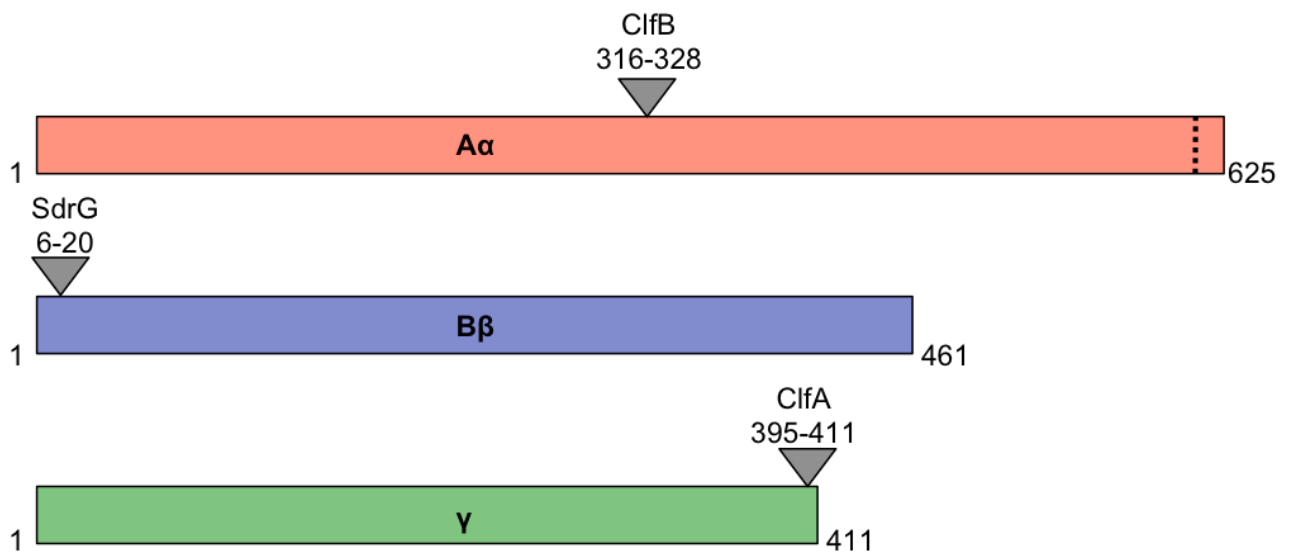


Figure 3-1. MSCRAMMs target different sites in the fibrinogen chains. Cartoon of the separate chains indicating the residues targeted by ClfA ( $\gamma$  395-411), SdrG ( $B\beta$  6-20), and ClfB ( $A\alpha$  316-328).

## **Materials and Methods**

*Commercial reagents-* Plasminogen, von Willebrand Factor, and fibronectin depleted human fibrinogen was from Enzyme Research, human fibronectin was from Chemicon, collagen I from rat tail tendons was from Cultrex R&D, recombinant human collagen III was from FibroGen. Bovine serum albumin fraction V (BSA) was from Serological Proteins, Inc. Restriction enzymes and T4 ligase were from New England Biolabs. Isopropyl-beta-D-thiogalactopyranoside (IPTG) was from Gold BioTechnology, Inc. Chromatography media and anti-His monoclonal antibody were purchased from GE Healthcare unless otherwise noted. Nitrocellulose membrane, goat-anti-mouse-alkaline phosphatase, goat-anti-rabbit-alkaline phosphatase, and goat-anti-rabbit-horseradish peroxidase were purchased from Bio-Rad. Donkey-anti-goat-horseradish peroxidase was from Applied Biological Materials Inc. Superblock, used to block solid-phase assay wells, and NBT/BCIP, for developing western blots were from ThermoFisher. Lysostaphin, Luria broth, SigmaFast OPD, used to develop solid phase assays, laminin from Engelbreth-Holm-Swarm murine sarcoma basement membrane, collagen IV from fibroblast and epithelial cell co-culture, goat-anti-human-Fg, bovine neck ligament elastin, and bovine nasal septum collagen II, and thrombin were from Sigma. Brain-heart-infusion broth (BHIB) was from Remel. M17 media was purchased from Oxoid. Oligonucleotides were purchased from IDT.

*Media and growth conditions-* *Escherichia coli* strain TOP 10 (Invitrogen) was used for subcloning Fg truncation mutants, and strains XL-1 Blue and XL-10 Gold (Stratagene) were used for expression of recombinant proteins. *E. coli* was cultured at 37°C with shaking (250 rpm) in Luria broth supplemented with kanamycin (50 µg/ml) for TOP 10 or ampicillin (100 µg/ml) for XL-1 Blue and XL-10 Gold. *Lactococcus lactis* was cultured in M17 supplemented with glucose (0.5%) and erythromycin (5 µg/ml) at 30°C. *Staphylococcus*

Table 3-2. Oligonucleotides used in this study.

Primer name	Oligonucleotide sequence
pQE30-BbpF	CCC <u>GATCC</u> GTTGCTTCAAACAATGTTAATGAT
pQE30-BbpR	CCC <u>AAGCTT</u> TTTATTTCAGGTTTAACAGTACCGTCACC
pQE30-FgAα1F	CGG <u>GATCC</u> GCAGATAGTGGTGAAGGT
pQE30-FgAα1-575R	CGA <u>AAGCTT</u> TTTAGGAGTCTCCTCTGTTGTAAGT
pQE30-FgAα1-560R	CGA <u>AAGCTT</u> TTTAGTAACTTGAAGATTACCACG
pCU1-BbpPrF	CGG <u>GATCC</u> GATATAACATACATCAACAT
pCU1-BbpTrR	CGT <u>CTAGA</u> AATATTATCGCCTCATATAAG

*aureus* strains MRSA 252 and Newman derivatives were cultured at 37°C with shaking (250 rpm) in Brain-heart-infusion broth (BHIB) supplemented with erythromycin (5 µg/ml), tetracycline (2 µg/ml), and/or chloramphenicol (10 µg/ml) as needed.

*Recombinant Bbp<sub>N2N3</sub>* - The N2N3 region of Bbp was cloned according to previously described methods (129). Briefly, *S. aureus* 024 (kindly donated by C. Ryden) genomic DNA was used to amplify the N2N3 sequence using the primers listed in Table 3-2 corresponding to the N2N3 subdomains of Bbp for digestion with BamHI and HindIII and ligation into pQE30. The plasmid was transformed into XL-1 Blue and sequenced to verify its integrity. This construct was generated by Jenny K. Horndahl in our laboratory. *E. coli*-Bbp<sub>N2N3</sub> was cultured to exponential phase, induced with 200 µM IPTG, and grown for an additional 3 hours. The cells were pelleted, lysed, and purification of Bbp<sub>N2N3</sub> was accomplished using Ni<sup>2+</sup> affinity chromatography as previously described (22) on a HiTrap Chelating column. Fractions were analyzed by SDS-PAGE, pooled, and dialyzed for anion exchange-purification using a Q HP Sepharose. To assess the purity of Bbp<sub>N2N3</sub>, the protein was run on 10% SDS-PAGE and stained with Coomassie blue or electrotransferred to nitrocellulose. The membrane was blocked with TBS containing 0.1% Tween-20 (TBST) and 1% BSA, and was probed with anti-His monoclonal, followed by anti-mouse-AP. Bbp<sub>N2N3</sub> was further analyzed by mass spectrometry (not shown).

*Anti-N1 monoclonal antibody*- Mouse monoclonal antibody 8B7 recognizing the N1 subdomain of the A domain of Bbp was kindly donated by Pietro Speziale.

*Rabbit-anti-BbpN2N3 antibodies*- Polyclonal antisera to Bbp<sub>N2N3</sub> were generated in two rabbits at Rockland Immunochemicals under the Fast Production Protocol. IgG was purified using protein A-sepharose (ThermoFisher) affinity chromatography. Next, the IgG

was cleared for crossreactive binding to Sdr proteins before positive affinity purification on Bbp<sub>N2N3</sub> coupled to EZlink beads (ThermoFisher).

*Bbp expression from clinical strains-* *S. aureus* clinical isolate MRSA 252 from blood was obtained from Network on Antimicrobial Resistance in *Staphylococcus aureus* (NARSA). *S. aureus* TCH 60 and TCH 959 skin and abscess isolates, respectively, were kindly donated by Kristina Hulten. To examine the *in vitro* expression of Bbp in the strains, overnight cultures were diluted 1:100 into fresh BHIB. Exponential phase cultures were harvested at an OD<sub>600</sub> of 0.55, 0.6, 0.7, 0.8, and 0.9. The cell-wall proteins were harvested by lysostaphin extraction as previously described (21). Subsequently, the proteins were separated on SDS-PAGE and electrotransferred to nitrocellulose membrane for Western blotting with monoclonal-anti-N1 and polyclonal anti-Bbp<sub>N2N3</sub> antibodies.

*Protein modeling-* The predicted structure of Bbp<sub>N2N3</sub> was modeled based on the solved structure of previously crystallized MSCRAMMs (102) (43) using the Ribbons program. Structural modeling was performed by Dr. Vannakambadi Ganesh in our laboratory.

*Bbp<sub>N2N3</sub> ligand screen-* Binding of Bbp<sub>N2N3</sub> to various extracellular matrix and plasma proteins was determined using an ELISA-type solid-phase assay. BSA, Fg, fibronectin, collagen type I-IV, and elastin were coated on microtiter wells at 1 µg per well, and laminin was coated at 10 µg per well overnight at 4°C in bicarbonate buffer pH 8.3. The next day, the wells were washed with TBST, blocked and incubated with ten-fold dilutions of Bbp<sub>N2N3</sub> (0.1-10 µM), followed by rabbit anti-Bbp<sub>N2N3</sub> and goat-anti-rabbit HRP for detection of bound Bbp<sub>N2N3</sub>. The wells were developed with SigmaFast OPD, and the absorbance was measured at 450 nm with a Thermo Max plate reader (Molecular Devices).

*Fg binding assay* – To detect binding of Fg to Bbp, a solid-phase assay was performed. Microtiter wells were coated with increasing amounts of Bbp<sub>N2N3</sub> (0.25-2.5 µg) overnight in bicarbonate buffer pH 8.3. The next day, wells were washed, blocked, probed with soluble Fg (1 µM) and detected with anti-human Fg followed by anti-goat-HRP. The wells were developed, and the absorbance was measured at 450 nm.

*Fg species screen* – Human, mouse (Enzyme Research), cat, dog, cow, sheep, and pig (Sigma) Fg, were coated on microtiter wells at 10 µg/ml overnight in bicarbonate buffer pH 8.3. The next day, the wells were washed, blocked, and probed with 500 nM Bbp<sub>N2N3</sub> and ClfA<sub>N2N3</sub> followed by mouse anti-His-HRP. The wells were developed and the absorbance was measured at 450 nm.

*Surface Plasmon Resonance (SPR)* – SPR was performed at 25°C on a BIAcore 3000 system (GE Healthcare). Twelve microliters of Fg in 10 mM sodium acetate pH 5.5 (10 µg/ml) was injected onto an activated CM5 chip surface at a flow rate of 5 µl/min. Approximately 1600 Response Units (RU) of Fg were immobilized via amine coupling. A second uncoupled flow cell was activated and deactivated to serve as a reference cell for binding experiments. Increasing concentrations of Bbp<sub>N2N3</sub> (40 nM-2.56 µM in TBS-0.005% Tween 20) were injected to determine the kinetics of the interaction between Fg and Bbp<sub>N2N3</sub>. The reference cell sensorgrams were subtracted from the experimental cell sensorgram. BIAevaluation software was used to determine kinetic constants. Xiaowen Liang performed these experiments.

*SDS-PAGE and Far Western of Reduced Fg*- Laemmli sample buffer containing 10 mM dithiothreitol was added to Fg for SDS-PAGE separation. The gels were either stained with Coomassie blue or electrotransferred to nitrocellulose for blotting. Briefly, the membranes



were blocked with TBST containing 1% BSA followed by probing with Bbp<sub>N2N3</sub> (15 µg/ml), ClfA<sub>N2N3</sub> (15 µg/ml), or SdrG<sub>N2N3</sub> (5 µg/ml). The bound proteins were detected with anti-His monoclonal antibody followed by anti-mouse-AP.

*E. coli Fg constructs and C-terminal truncation mutants* - *E. coli* expressing full-length recombinant His-tagged Fg chains A $\alpha$ , B $\beta$ , and  $\gamma$  have been previously described (81) (8, 9). Plasmid containing the Fg A $\alpha$  sequence was used as template to amplify the DNA corresponding to mature A $\alpha$  residues 1-575 and 1-560 using the primers listed in Table 3-2. Selected plasmids were digested, the inserts ligated to pQE30, and the plasmids transformed into XL-1 Blue cells. Sequencing was used to verify the integrity of the plasmids pQE30-A $\alpha$ 1-575 and pQE30-A $\alpha$ 1-560. The proteins were expressed and induced with 200 µM IPTG as described above for Bbp<sub>N2N3</sub>, purified using Ni<sup>2+</sup> affinity chromatography in the presence of 8M urea (Sigma), and separated on 10% SDS-PAGE or used for binding assays.

*E. coli Fg construct solid-phase assays*- Fg, recombinant Fg chains, and A $\alpha$  truncation mutants were coated on microtiter wells in bicarbonate buffer overnight. The wells were washed, blocked, probed with Bbp<sub>N2N3</sub> (15.6-500 nM) and detected with anti-Bbp<sub>N2N3</sub> and anti-rabbit-HRP. The wells were developed and the absorbance was measured at 450 nm.

*E. coli Fg construct Far Westerns*- Laemmli sample buffer containing 10 mM dithiothreitol was added to recombinant Fg constructs and truncation mutants for SDS-PAGE separation followed by staining with Coomassie blue or transferring to nitrocellulose. The membranes were blocked with 1% BSA and probed with Bbp<sub>N2N3</sub> (15 µg/ml) followed by detection with anti-Bbp<sub>N2N3</sub> and anti-rabbit-AP.

Table 3-3. Constructs used in this study.

<u>CONSTRUCT</u>	<u>VECTOR</u>	<u>RESIDUES</u>	<u>SOURCE</u>
<i>E. coli</i> Bbp <sub>N2N3</sub>	pQE30	270-599	This study
<i>E. coli</i> SdrG <sub>N2N3</sub>	pQE30	273-597	(102)
<i>E. coli</i> ClfA <sub>N2N3</sub>	pQE30	229-545	(43)
<i>E. coli</i> Fg A $\alpha$	pQE30	Full length mature A $\alpha$	(81)
<i>E. coli</i> Fg A $\alpha$ 1-575	pQE30	1-575 of mature A $\alpha$	This study
<i>E. coli</i> Fg A $\alpha$ 1-560	pQE30	1-560 of mature A $\alpha$	This study
<i>E. coli</i> Fg B $\beta$	pQE30	Full length mature B $\beta$	(8)
<i>E. coli</i> Fg $\gamma$	pQE30	Full length mature $\gamma$	(9)
<i>L. lactis</i> -vector	pKS80	Empty vector	(21)
<i>L. lactis</i> -Bbp	pKS80	Full length Bbp	This study
<i>S. aureus</i> Newman bald-vector	pCU1	Empty vector	(21)
<i>S. aureus</i> Newman bald-Bbp	pCU1	Full length Bbp (with promoter and terminator)	This study

*Lactococcus lactis*-Bbp1615- The entire *bbp* coding region from strain *S. aureus* B504 (kindly donated by Ed Feil) was ligated into the pKS80 plasmid for constitutive expression. The plasmid was transformed into *Lactococcus lactis* MG1363. This complemented strain expresses Bbp on the surface of *L. lactis* under a constitutive promoter and was kindly provided by Timothy Foster.

*S. aureus* Newman bald-Bbp – The strain *S. aureus* DU6023 *clfA5 isdA clfB::Em<sup>r</sup> ΔsdrCDE::Tc<sup>r</sup>* (21) will be referred to as Newman bald and was used for expression of full-length Bbp on the surface of the bacteria under the control of its native promoter as previously described for other MSCRAMMs (21). Briefly, the DNA was amplified from *S. aureus* MRSA252 (kindly provided by NARSA) using the primers listed in Table 3-2, and subcloned into TOPO-Zero Blunt (Invitrogen) for transformation into *E. coli* TOP 10 cells. The plasmid was digested with BamHI and XbaI; the insert was ligated to the shuttle vector pCU1, and the plasmid was transformed into XL-10 Gold cells (Stratagene). Sequencing was used to verify the integrity of the plasmid pCU1-Bbp. The plasmid was purified and transformed into electrocompetent *S. aureus* 8325-4 and plated on BHIB with chloramphenicol. Subsequently, pCU1-Bbp was electroporated into electrocompetent Newman bald cells.

*Bacterial adherence assays:* Binding of *L. lactis*-Bbp or Newman bald-Bbp to the Fg A $\alpha$  truncation mutants was tested in crystal violet adherence assays. Microtiter wells were coated with A $\alpha$ 1-575 and A $\alpha$ 1-560 in bicarbonate buffer overnight. The next day, the wells were washed with phosphate-buffered saline (PBS), blocked with PBS-1%BSA, and washed with PBS supplemented with 0.5 mM magnesium chloride and 0.1 mM calcium chloride (PBS-Ca<sup>2+</sup>-Mg<sup>2+</sup>). *L. lactis*-Bbp and *L. lactis*-vector were grown overnight, washed in PBS-Ca<sup>2+</sup>-Mg<sup>2+</sup>, and resuspended in PBS-Ca<sup>2+</sup>-Mg<sup>2+</sup> at an OD<sub>600</sub> of 1.0. Newman bald-

Bbp and Newman-bald vector were grown overnight, diluted 1:50, and grown to an OD<sub>600</sub> of 0.6. The cells were washed and resuspended to an OD<sub>600</sub> of 2.0 in PBS-Ca<sup>2+</sup>-Mg<sup>2+</sup>. The blocked and washed wells were incubated with 0.1 ml of bacterial suspension for 1.5 hours at 30°C for *L. lactis* or 37°C for Newman bald strains. The wells were washed with PBS-Ca<sup>2+</sup>-Mg<sup>2+</sup>, then fixed with paraformaldehyde (4%) for 30 minutes. After washing with PBS-Ca<sup>2+</sup>-Mg<sup>2+</sup>, the wells were incubated with crystal violet (0.5%) for 3 minutes. The wells were washed and the crystal violet was dissolved in acetic acid (5%). The absorbance of the wells was measured at 590 nm.

*Synthetic peptides*- Fg A $\alpha$  peptides (Table 3-4) corresponding to the human sequences 551-575, 561-565, 556-570, 551-565, and a scrambled 51-575 were synthesized by Biomatik.

*Isothermal titration calorimetry (59)*- The interaction between Bbp<sub>N2N3</sub> protein and soluble Fg A $\alpha$  15mer or 25mer peptides (Table 3-4) was analyzed using a VP-ITC microcalorimeter (MicroCal) at 30°C. The cell contained 15  $\mu$ M Bbp<sub>N2N3</sub> and the syringe contained 225  $\mu$ M peptide in TBS. All samples were degassed for 5 min. The titration was performed with a stirring speed of 300 rpm. The initial injection was 5  $\mu$ l followed by 29 injections of 10  $\mu$ l with an injection speed of 0.5  $\mu$ l/second. Data were fitted to a single binding site model and analyzed using Origin version 5 (MicroCal) software.

*Inhibition assay*- Bbp<sub>N2N3</sub> (150 nM) was incubated with increasing concentrations of Fg A $\alpha$  peptides (0.1 to 30  $\mu$ M) for 30 minutes before incubation in Fg coated wells. The wells were incubated with rabbit-anti-Bbp<sub>N2N3</sub> and goat-anti-rabbit-HRP. The wells were developed with SigmaFast OPD (Sigma), and the absorbance was measured at 450 nm with a Thermo Max plate reader (Molecular Devices).

Table 3-4. Peptides synthesized for this study

Peptide name	Peptide sequence
Fg Aα 551-575	FPSRGKSSSYSKQFTSSTSYNRGDS
Fg Aα Scrambled	GSSQTSKTSDFPRRYFSSKSYGNSS
Fg Aα 551-565	FPSRGKSSSYSKQFT
Fg Aα 556-570	KSSSYSKQFTSSTSY
Fg Aα 561-575	SKQFTSSTSYNRGDS

*Fibrin inhibition assay-* Using the previously described methods (22), thrombin-catalyzed fibrin formation was studied. Briefly, Fg coated wells were incubated with increasing concentrations of Bbp<sub>N2N3</sub>, SdrG<sub>N2N3</sub>, or BSA for 30 minutes prior to the addition of 1.0 NIH unit of thrombin per milliliter. The turbidity of the wells was measured at 405 nm.

## **RESULTS**

### **Bbp is expressed in clinical isolates.**

The presence of *bbp* has been correlated with both carriage and invasive *S. aureus* isolates. In order to study the expression of Bbp from a clinical isolate, I obtained MRSA 252, which is a blood *S. aureus* isolate. The cell-wall proteins were harvested from exponentially growing cultures using lysostaphin digestion. Western blotting the extract with anti-N1 monoclonal antibody revealed the presence of an approximately 175 kDa protein, corresponding to full-length Bbp (Figure 3-2). The Western blot also shows another band of approximately 50 kDa which is the detection of Protein A in the cell-wall extract. Next, I probed the cell-wall extraction with an anti-Bbp<sub>N2N3</sub> affinity-purified polyclonal. Western blotting with the N2N3 polyclonal antibody identified two bands of approximately 100 kDa and 175 kDa in all of the samples (Figure 3-2). In other Sdr proteins, cleavage of the N1 domain by a metalloprotease has been documented (87). Therefore, the higher band is the full-length Bbp, and the lower band is likely to be a form of the protein that is missing the N1 domain. Also, Western blots with the N2N3 polyclonal showed a faint band of lower molecular weight (approximately, 80 kDa) in early time points only (OD<sub>600</sub> of 0.55 and 0.6). These results indicate that Bbp can be detected *in vitro* in a blood isolate.

### **Bbp<sub>N2N3</sub> binds to human fibrinogen.**

To test the binding of Bbp to putative ligands, a construct that contains the putative binding sites, the N2N3 domains, was designed (Figure 3-3). This construct was expressed as a His-fusion protein and purified with affinity and ion-exchange chromatography (Figure 3-4).

An initial screen was performed to examine the binding of recombinant His-tagged Bbp<sub>N2N3</sub> (Figure 3-5a) in a solid-phase assay. Soluble Bbp<sub>N2N3</sub> (0.01 to 10.0 µM) was used

Figure 3-2. *In vitro* expression of Bbp. *S. aureus* MRSA 252 cells were harvested at OD600 = 0.55, 0.60, 0.70, 0.80, and 0.90 and the cell-wall proteins were extracted with lysostaphin digestion. The extract was separated by SDS-PAGE, transferred to nitrocellulose and blotted with anti-N1 domain monoclonal antibody (A) or anti-Bbp<sub>N2N3</sub> affinity purified polyclonal antibody (B).

## MRSA 252 cell wall extraction

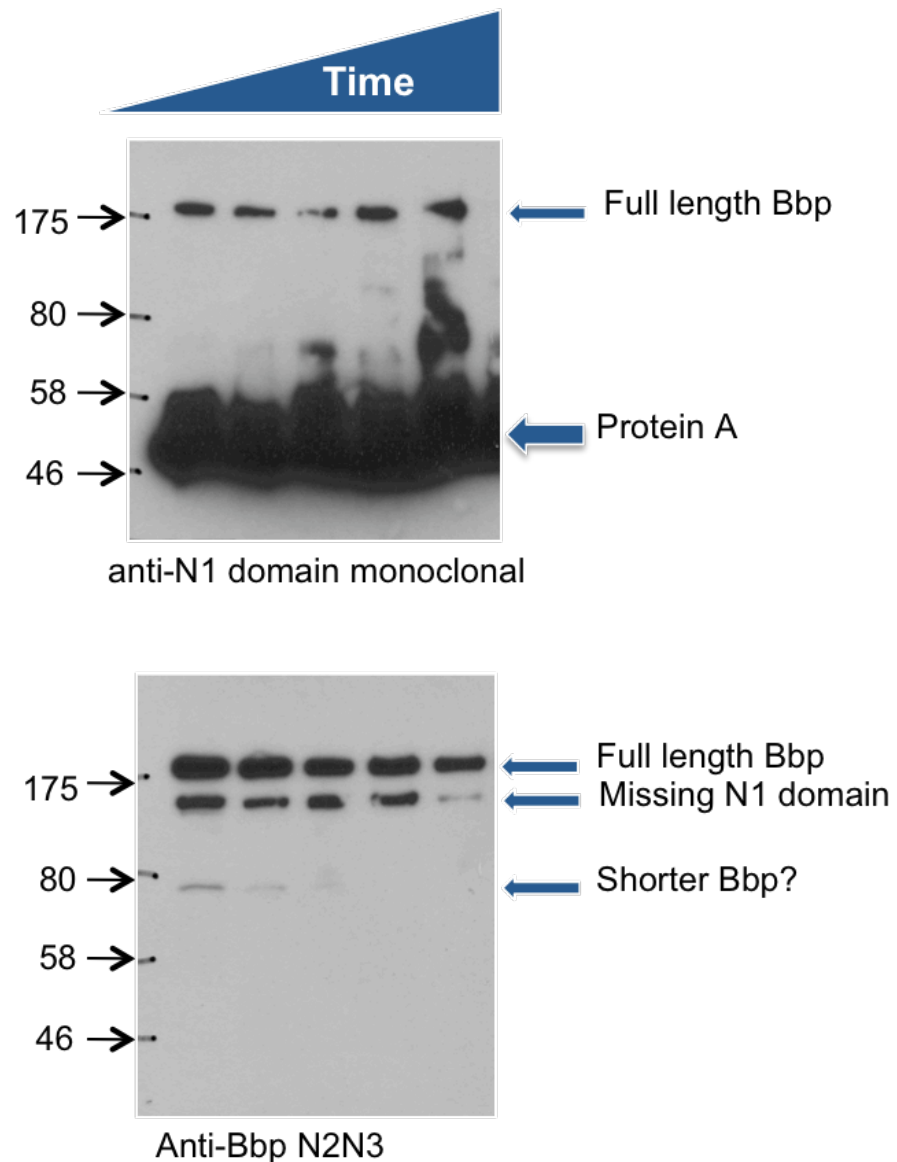
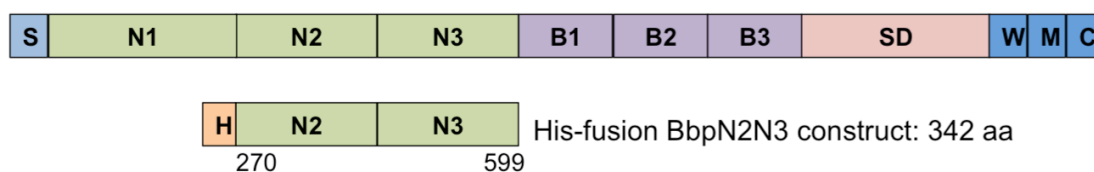




Figure 3-3. Bbp<sub>N2N3</sub> construct. (A) Domain organization of full length Bbp (top) and Bbp<sub>N2N3</sub> (bottom) showing the (S) signal sequence, (N1, N2, N3) amino terminal subdomains of A region, (B1, B2, B3) B-repeats, (SD) Serine-Aspartate repeat region, (W) wall domain, (M) membrane domain, (C) carboxy-terminus. In Bbp<sub>N2N3</sub>, (H) Hexahistidine tag. (B) Structural model of the N2N3 subdomains of Bbp based on the structure of other MSCRAMMs. Beta-sheets are depicted in yellow. The N2 domain is at the bottom of the image, and the N3 domain is at the top.

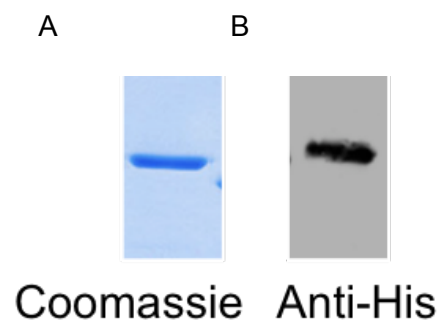
A



B



Figure 3-4. Purified Bbp<sub>N2N3</sub>. (A) Coomassie stained recombinant Bbp<sub>N2N3</sub> (1 µg/lane). (B) Anti-His monoclonal immunoblot of purified Bbp<sub>N2N3</sub>.



to probe microtiter wells coated with extracellular matrix and plasma proteins, followed by detection with polyclonal anti-Bbp<sub>N2N3</sub> and HRP conjugated anti-rabbit polyclonal. In this assay, Bbp<sub>N2N3</sub> recognized Fg in a concentration-dependent, saturable manner but failed to bind to Elastin, Collagen type I – IV, Laminin, Fibronectin, and BSA. To determine if soluble Fg could bind to immobilized Bbp<sub>N2N3</sub> I performed the reverse assay. Wells coated with increasing amounts of Bbp<sub>N2N3</sub> (0.25-2.5 µg) supported Fg binding (Figure 3-5b). These results provide evidence for dose-dependent saturable binding between Bbp<sub>N2N3</sub> and Fg.

Next, I studied the specificity and affinity of the Bbp<sub>N2N3</sub>-Fg interaction. First, the species tropism of Bbp was examined using solid-phase assays. Wells coated with Fg purified from human, cat, dog, cow, sheep, mouse, and pig were probed with Bbp<sub>N2N3</sub>. Our results indicate that Bbp<sub>N2N3</sub> only binds to Fg isolated from human plasma (Figure 3-6). This is in contrast to the Fg-binding activity of ClfA<sub>N2N3</sub>, which exhibits a wider host tropism. These results suggest that Bbp does not recognize a motif present in Fg from different species but one that is specific to human Fg.

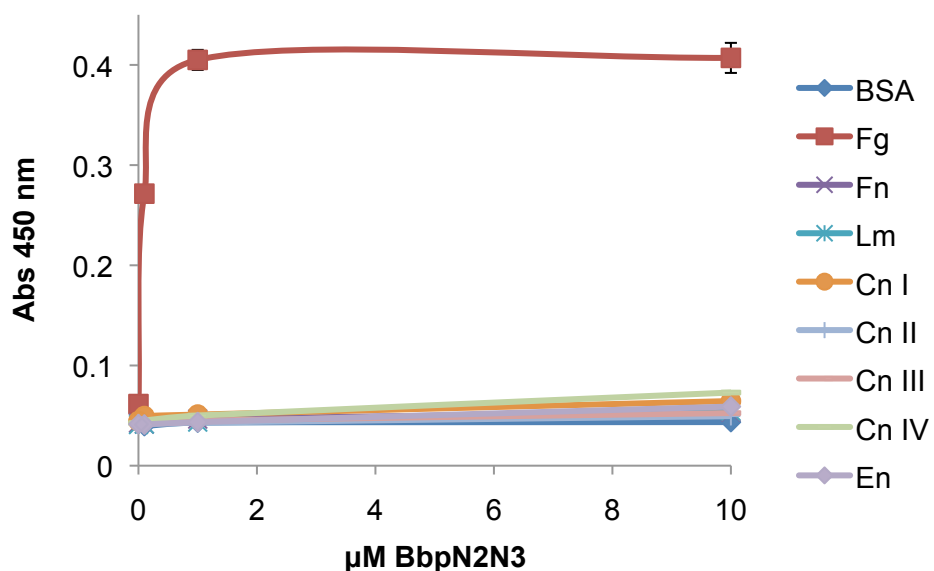
The dissociation constant of Bbp<sub>N2N3</sub> for Fg was examined using SPR. Binding of Bbp<sub>N2N3</sub> (40 nM-2.56 µM) to Fg immobilized on a sensor chip was analyzed using a BIAcore 3000 (Figure 3-7a). The equilibrium analysis revealed a  $K_D$  of 540 +/- 7 nM of Bbp<sub>N2N3</sub> to Fg (Figure 3-7b). Together, these data suggest that human Fg is a second ligand for Bbp<sub>N2N3</sub>.

### **Bbp<sub>N2N3</sub> recognizes the A $\alpha$ chain of fibrinogen.**

In order to determine whether Bbp targets one or multiple Fg chains, I used Far Western analysis. Fg was reduced in sample buffer containing  $\beta$ -mercaptoethanol to dissociate the disulfide bonds that hold the two sets of three polypeptide chains together and separated on SDS-PAGE (Figure 3-8a) followed by transferring to nitrocellulose membrane for Far Western probing. In this assay, Bbp<sub>N2N3</sub> bound to the A $\alpha$  chain of Fg,

Figure 3-5. Bbp<sub>N2N3</sub> binding to Fg. (A) Ligand screen . Putative ligands were coated on microtiter wells and probed with increasing concentrations (0.1-10  $\mu$ M) of Bbp<sub>N2N3</sub> followed by rabbit-anti-Bbp<sub>N2N3</sub> and goat-anti-rabbit-HRP. (B) Increasing amounts of Bbp<sub>N2N3</sub> (0.25 to 2.5  $\mu$ g) were coated on microtiter wells and probed with 1  $\mu$ M Fg followed by goat-anti-human Fg and donkey-anti-goat-HRP.

A



B

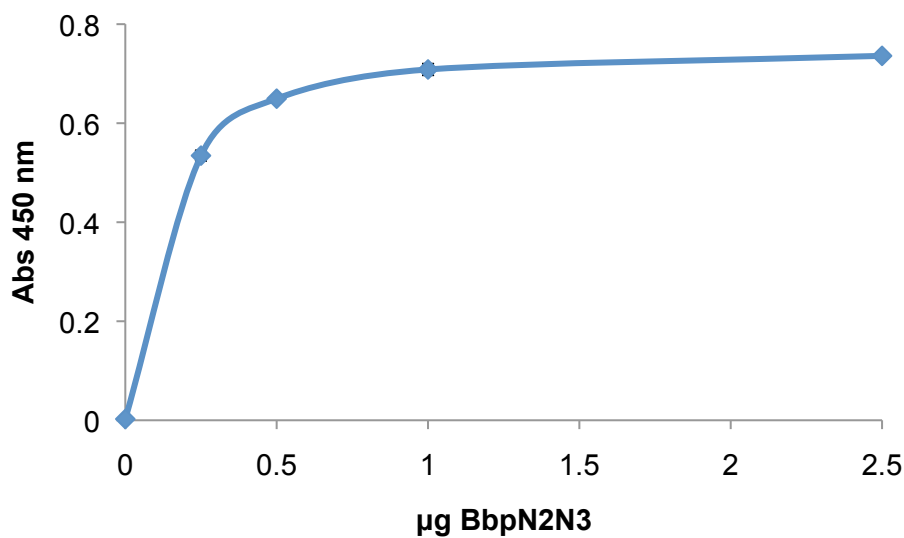


Figure 3-6. Fg species screen. Microtiter wells were coated with 1  $\mu$ g of human, canine, feline, bovine, ovine, murine, or porcine Fg, or BSA in bicarbonate buffer overnight. The wells were probed with 500 nM Bbp<sub>N2N3</sub> or ClfA<sub>N2N3</sub>, followed by protein specific rabbit polyclonal antibodies and goat-anti-rabbit-HRP.

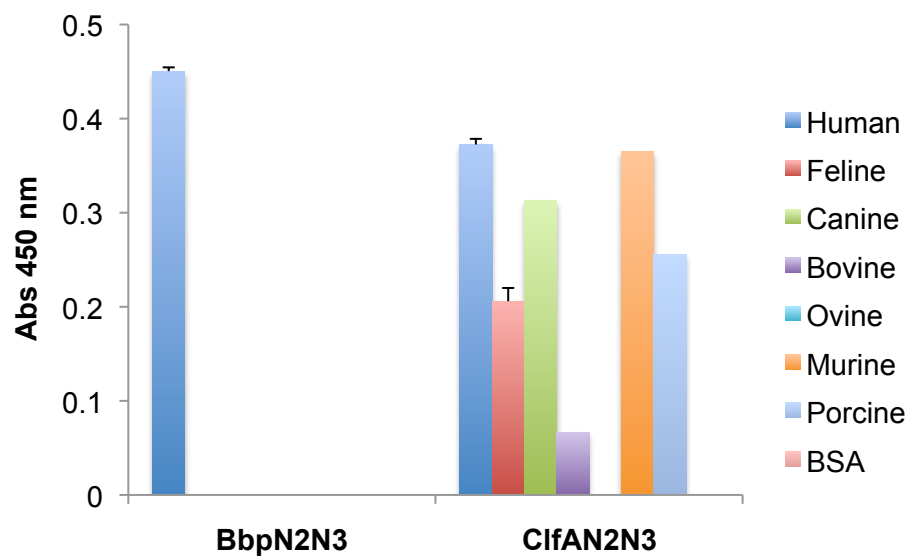
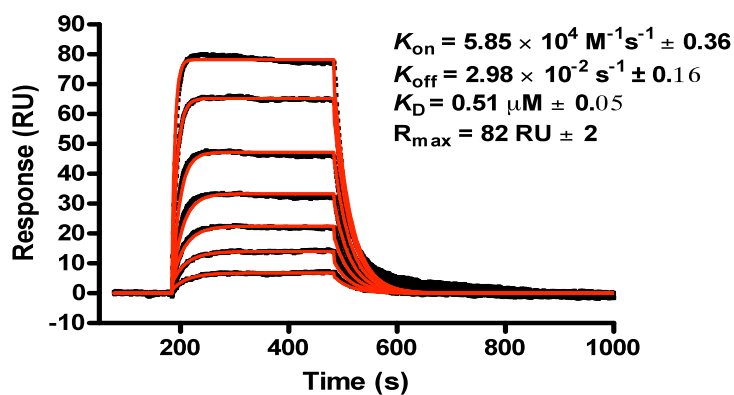
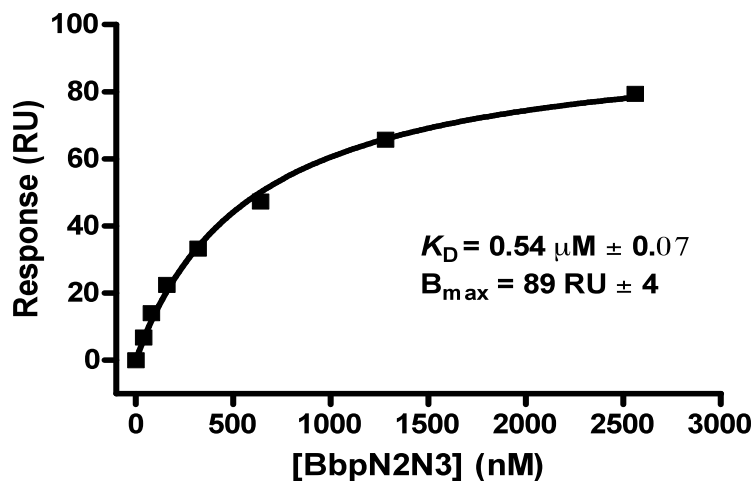


Figure 3-7. Bbp<sub>N2N3</sub> Surface Plasmon Resonance. Two-fold linear dilutions (2.56 to 0.04  $\mu\text{M}$ ) of Bbp<sub>N2N3</sub> were injected over the Fg immobilized on a Biacore sensor chip. (A) Response curves for each injection of Bbp<sub>N2N3</sub> (Black) are overlaid with the global fitting to a 1:1 binding model (Red). Kinetic parameters were obtained from the fitting. (B) Equilibrium analysis: Responses at equilibrium of the SPR curves were fit to a one-site binding isotherm to obtain the affinity and binding maximum. Experiment performed by Xiaowen Liang.

A



B



while the previously characterized MSCRAMMs SdrG<sub>N2N3</sub> and ClfA<sub>N2N3</sub> bound to the B $\beta$  and  $\gamma$  chains, respectively (Figure 3-8b).

In order to verify our Far Western results obtained with reduced Fg, I tested binding of Bbp<sub>N2N3</sub> to the individual Fg chains. Recombinant full-length A $\alpha$ , B $\beta$ , and  $\gamma$  were expressed as His-tagged constructs and purified (Figure 3-9a). Individual chains were immobilized on microtiter plates and probed for Bbp<sub>N2N3</sub> (15.6-500 nM) binding using a solid-phase assay (Figure 3-9b). The B $\beta$  and  $\gamma$  chains did not support binding, whereas Bbp<sub>N2N3</sub> bound saturably in a concentration-dependent manner to plasma Fg and A $\alpha$ . Together, these results indicate that Bbp<sub>N2N3</sub> binds to a site localized to the human Fg A $\alpha$  chain.

#### **The binding site of Bbp lies within residues 561-575 of the Fg A $\alpha$ chain.**

To map the Bbp<sub>N2N3</sub> binding site, I used a systematic approach and constructed C-terminal truncates of the A $\alpha$  chain (Figure 3-10a). The recombinant Fg A $\alpha$ 1-575 and Fg A $\alpha$ 1-560 were purified (Figure 3-10b lanes 3 and 4, respectively) and examined for binding activity. Far western blots revealed that A $\alpha$ 1-575 retained the Bbp<sub>N2N3</sub> binding site; however no binding was detected to A $\alpha$ 1-560 (Figure 3-10b), suggesting that no residues N-terminal to 561 are necessary for binding. To further confirm our results, a solid phase assay comparing the binding of Bbp<sub>N2N3</sub> to A $\alpha$ 1-560 and A $\alpha$ 1-575 revealed that only A $\alpha$ 1-575 could support saturable, concentration-dependent binding (Figure 3-11a). These results indicate that the residues that mediate binding of Bbp<sub>N2N3</sub> to Fg lie in the A $\alpha$  chain between 561 and 575.

Figure 3-8. Reduced Fg Far Western. Fg was reduced and separated on SDS-PAGE followed by Coomassie staining (A) to reveal the three chains A $\alpha$  (top band), B $\beta$  (middle band) and  $\gamma$  (bottom band) or electrotransferred for Far Western blotting (B). Membranes were probed with Bbp<sub>N2N3</sub> (left), SdrG<sub>N2N3</sub> (middle), and ClfA<sub>N2N3</sub> (right). Followed by incubation with protein-specific rabbit polyclonals and goat-anti-rabbit-AP.

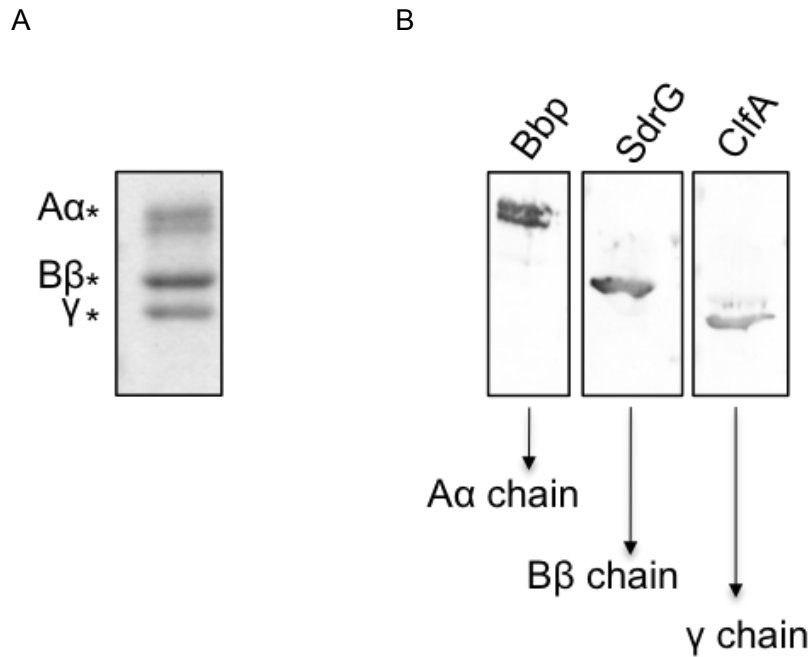




Figure 3-9. Purified individual Fg chains. (A) Coomassie stained gel showing the individually expressed and purified His-tagged Fg chain constructs compared with reduced human Fg (left). (B) Fg, and recombinant individual A $\alpha$ , B $\beta$ , and  $\gamma$  chains were coated on microtiter wells overnight in bicarbonate buffer. They were probed with Bbp<sub>N2N3</sub> followed by anti-Bbp<sub>N2N3</sub> and goat-anti-rabbit-HRP.

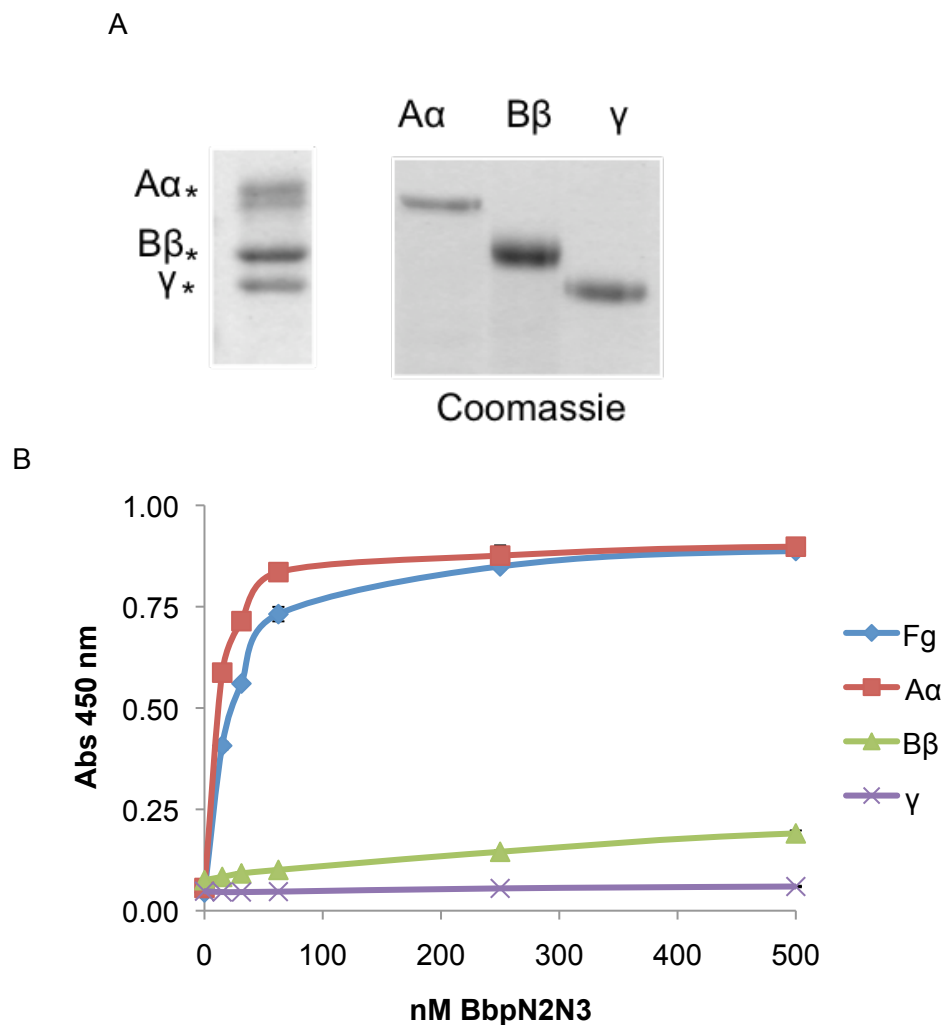
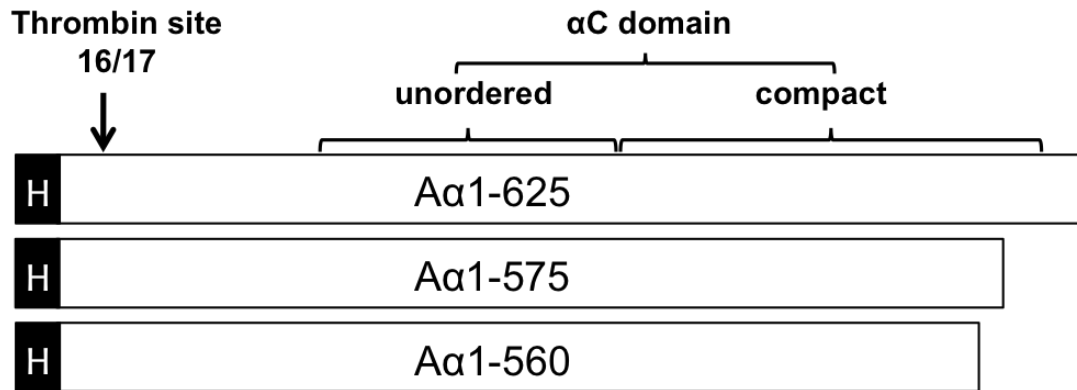
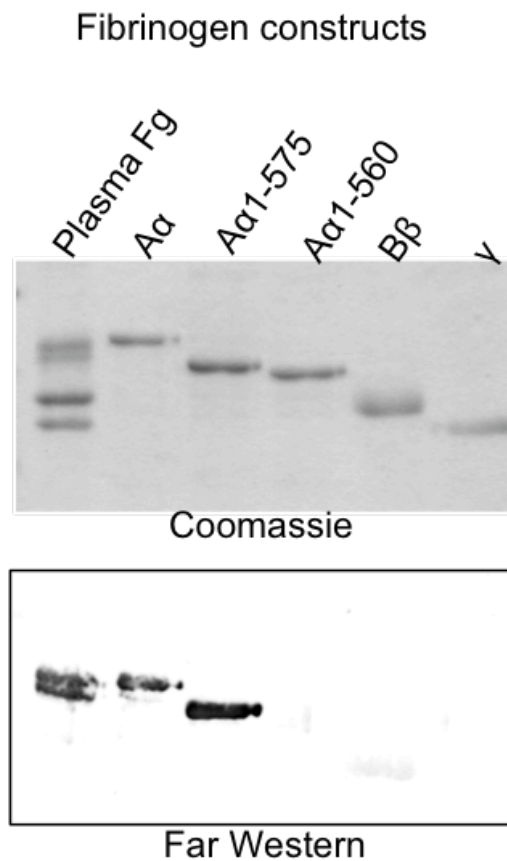


Figure 3-10. A $\alpha$  truncation mutants. Cartoon schematic of the full-length and truncated A $\alpha$  chain constructs. (B) Coomassie stained gel of Fg, recombinant A $\alpha$ , A $\alpha$  1-575 and A $\alpha$  1-560, B $\beta$ , and  $\gamma$  (top) and Bbp<sub>N2N3</sub> Far Western (bottom).

A



B



### **Full-length Bbp binds to Fg A $\alpha$ chain residues 561-575.**

The apathogenic bacterium *Lactococcus lactis* has been successfully used as a heterologous host for full-length MSCRAMM cell surface display (21). Therefore, I employed this method to determine whether Bbp expressed on the surface of a cell could recognize the mapped residues. Using a bacterial adherence assay, I determined that *L. lactis*-Bbp bound to plates coated with A $\alpha$ 1-575; whereas the empty-vector construct *L. lactis*-pKS80 did not bind to A $\alpha$ 1-560 or A $\alpha$ 1-560 coated wells (Figure 3-11b). This result indicates that full-length Bbp exhibits binding to the mapped residues.

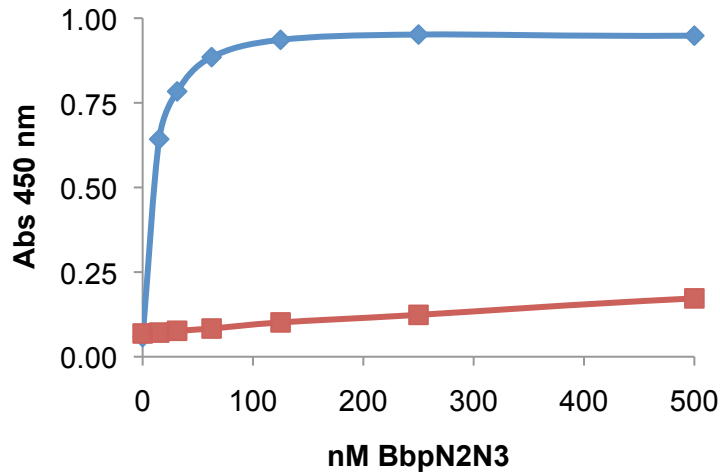
The *S. aureus* Newman bald strain lacks surface expression of the MSCRAMMs ClfA, ClfB, IsdA, IsdB, SdrC, SdrD, and SdrE (21). Therefore, this strain was used to introduce full-length *bbp* under the control of its native promoter. The strains Newman bald-pCU1 and Newman bald-Bbp were assessed for binding to A $\alpha$ 1-575 and A $\alpha$ 1-560 in an adherence assay. Newman bald-Bbp only adhered to wells coated with A $\alpha$ 1-575 in contrast to the empty vector control, which did not recognize either A $\alpha$  construct (Figure 3-11c). The data gathered with *L. lactis*-Bbp and Newman-bald-Bbp mimic the binding profile exhibited by recombinant Bbp<sub>N2N3</sub>. These data indicate that Bbp on the surface of staphylococcal bacteria can mediate binding to human Fg.

### **Characterization of the interaction between Bbp and peptides from Fg A $\alpha$ .**

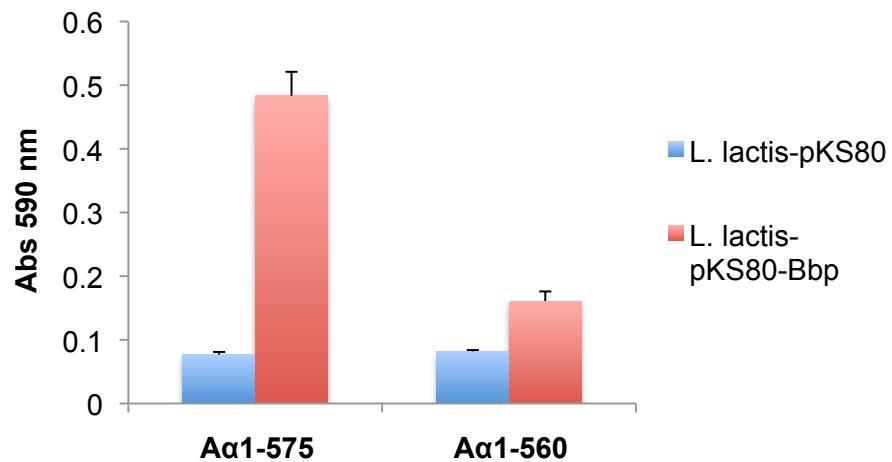
In order to determine the affinity of the interaction between Bbp<sub>N2N3</sub> and Fg A $\alpha$  peptides, ITC was performed. Peptides (225  $\mu$ M) in TBS were titrated into a cell containing 15  $\mu$ M Bbp<sub>N2N3</sub> that had been dialyzed into TBS (Figure 3-12). The one binding site fit model was used to analyze the data, which is summarized in Table 3-5. ITC analysis showed that the peptides A $\alpha$ 551-575 and A $\alpha$ 561-575 bind to Bbp<sub>N2N3</sub> with a  $K_D$  below 1  $\mu$ M, indicating high-affinity binding. Furthermore, no binding was detected from the peptide

Figure 3-11. Full-length and Bbp<sub>N2N3</sub> binding to A $\alpha$  truncation mutants. (A) A $\alpha$  1-575 and A $\alpha$  1-560 coated wells were probed with increasing concentrations (15-500 nM) of Bbp<sub>N2N3</sub>, followed by anti-Bbp<sub>N2N3</sub> antibody and anti-rabbit-HRP; (B) stationary-phase *L. lactis*-pKS80 and *L. lactis*-pKS80-Bbp, and (C) exponential-phase *S. aureus* Newman bald-pCU1 and *S. aureus* Newman bald-pCU1-Bbp.

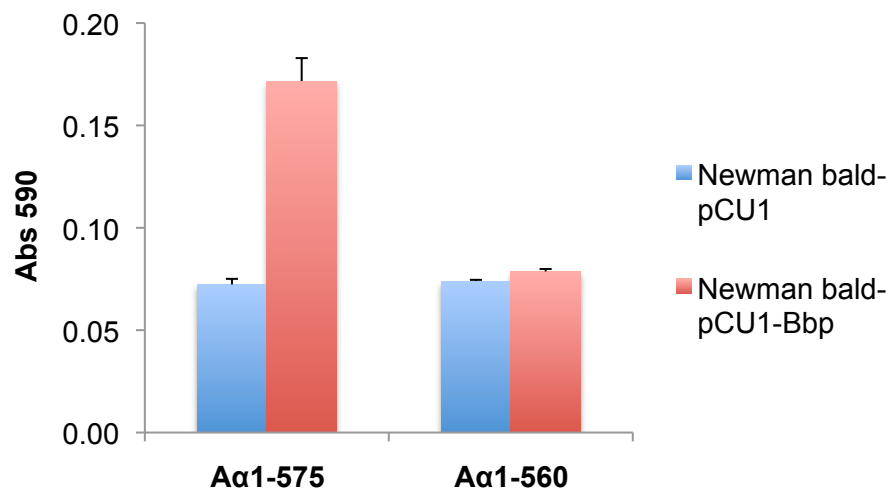
A



B



C



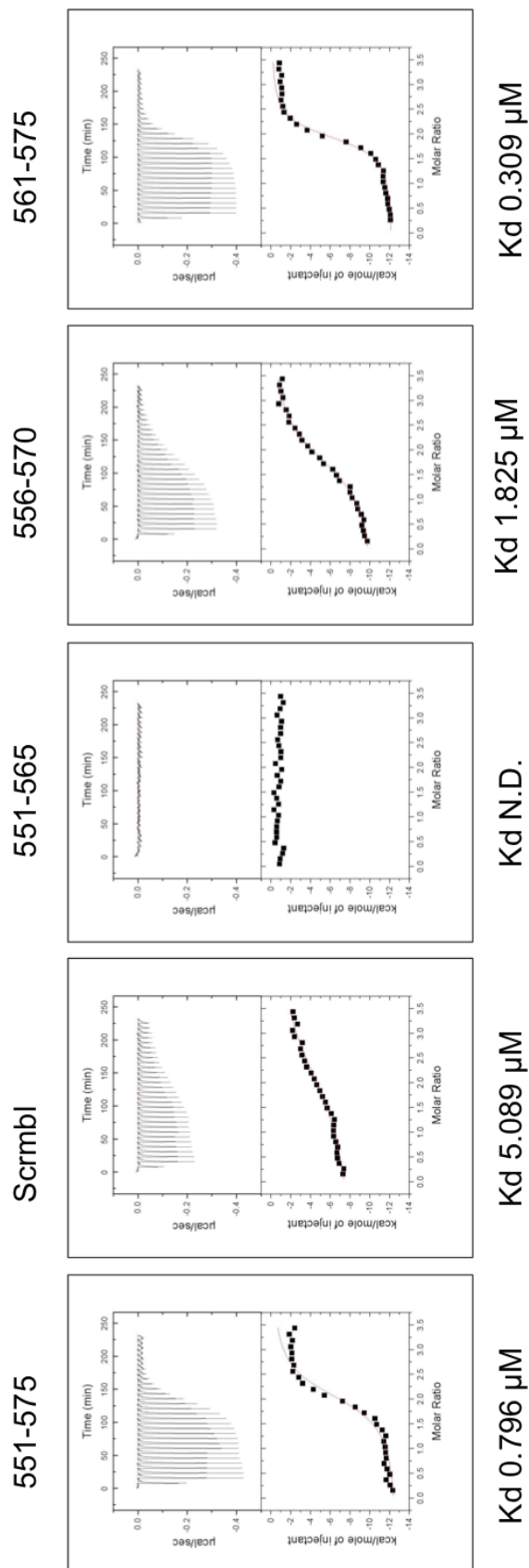


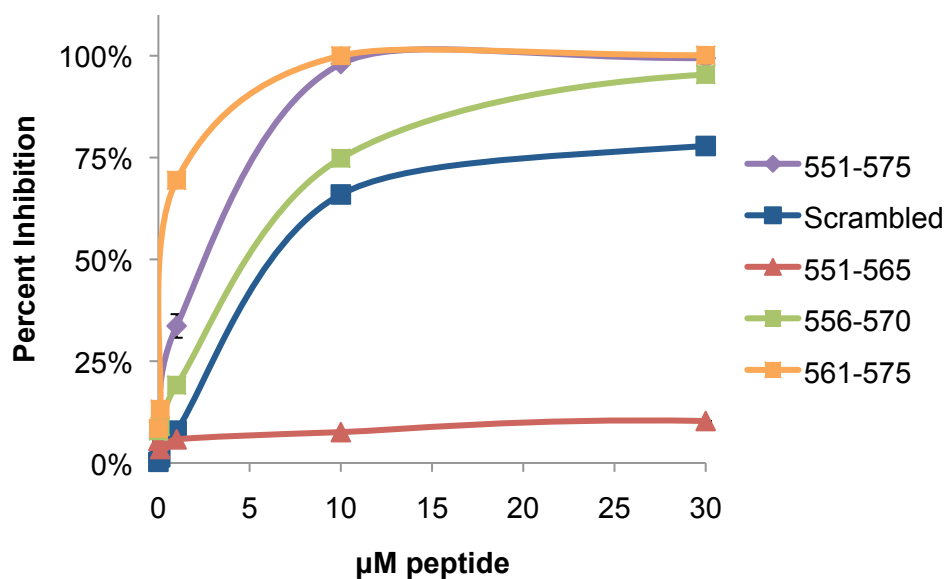
Figure 3-12. Isothermal titration calorimetry of Fg A $\alpha$  peptides and Bbp<sub>N2N3</sub>. Binding of 225  $\mu$ M peptides to 15  $\mu$ M protein was measured with a VP-ITC. The samples were degassed for 5 minutes and 10  $\mu$ l of the peptides were titrated at 0.5  $\mu$ l/sec into the cell containing Bbp<sub>N2N3</sub>. All experiments were conducted in TBS at 30°C with a stirring speed of 300 rpm.

Table 3-5. Isothermal Titration Calorimetry data

	<b>N</b>	<b>K</b>	<b><math>\Delta H</math></b> <b>(kcal/mol)</b>	<b><math>\Delta S</math></b> <b>(kcal/mol)</b>	<b><i>K<sub>d</sub> (calc)</i></b>
<b>551-575</b>	2.074	1.256E6	-1.269E4	-13.95	<i>0.796 <math>\mu M</math></i>
<b>Scrm</b>	2.633	1.965E5	-8.296E3	-3.149	<i>5.089 <math>\mu M</math></i>
<b>551-565</b>	N.D.	N.D.	N.D.	N.D.	<i>N.D.</i>
<b>556-570</b>	1.894	5.477E5	-1.039E4	-8.030	<i>1.825 <math>\mu M</math></i>
<b>561-575</b>	1.902	3.227E6	-1.222E4	-10.51	<i>0.309 <math>\mu M</math></i>

Figure 3-13. Peptide inhibition. (A) Bbp<sub>N2N3</sub> (150 nM) was preincubated with increasing concentrations (0.1 – 30  $\mu$ M) of peptides prior to incubation in Fg-coated wells. (B) Chart showing the peptide sequences and relative inhibition scores.

A



B

Inhibition		551	561	571
++	551-575	FPSRG	KSSSY SKQFT	SSTSY <u>NRGDS</u>
-/+	Scrambled	GSSQT	SKTSD	FPRRY FSSKS YGNSS
-	551-565	FPSRG	KSSSY SKQFT	
+	556-570		KSSSY SKQFT	SSTSY
+++	561-575		SKQFT	SSTSY <u>NRGDS</u>

Figure 3-14. Alignment of sequences from several species corresponding to human A $\alpha$  561-575.

Human	SKQF-TSSTSYNRGDS
Dog	SKQFVTSSTTYNRGDS
Cat	SKQLVATSKTYNRGDS
Pig	SKQIT--KTINREGR
Cow	SKQFVSSSTTVNRGGS
Rat	RKQVT-----
Mouse	KKQVT-----



A $\alpha$ 551-565, suggesting that these residues are not important for binding, and further strengthening our data with the truncated Fg A $\alpha$  chain mutants. The peptide A $\alpha$  556-571 exhibited binding with a  $K_D$  of 1.8  $\mu$ M. Therefore residues contained in this peptide can mediate binding to Bbp<sub>N2N3</sub> albeit with less affinity. Truncation analysis experiments together with ITC indicate that Bbp<sub>N2N3</sub> binds specifically to A $\alpha$  residues 561-575.

To further characterize the binding specificity of Bbp<sub>N2N3</sub> to Fg, I performed inhibition experiments with the synthetic Fg A $\alpha$  peptides. Bbp<sub>N2N3</sub> was preincubated with increasing concentrations of peptides (0.1-30  $\mu$ M) before addition to Fg coated wells in a solid-phase assay (3-13a). The A $\alpha$ 551-575, A $\alpha$ 561-575, and A $\alpha$ 556-570 peptides fully abolished binding of Bbp<sub>N2N3</sub> to Fg. The scrambled peptide showed partial inhibition of binding, which did not reach 100% inhibition. Additionally, the A $\alpha$ 551-565 peptide could not inhibit the interaction. The results obtained from the inhibition assays are in direct accordance with the data gathered in ITC experiments, meaning that the inhibitory activity imparted by the peptides is directly related to their ability to bind to Bbp<sub>N2N3</sub> (Figure 3-13b).

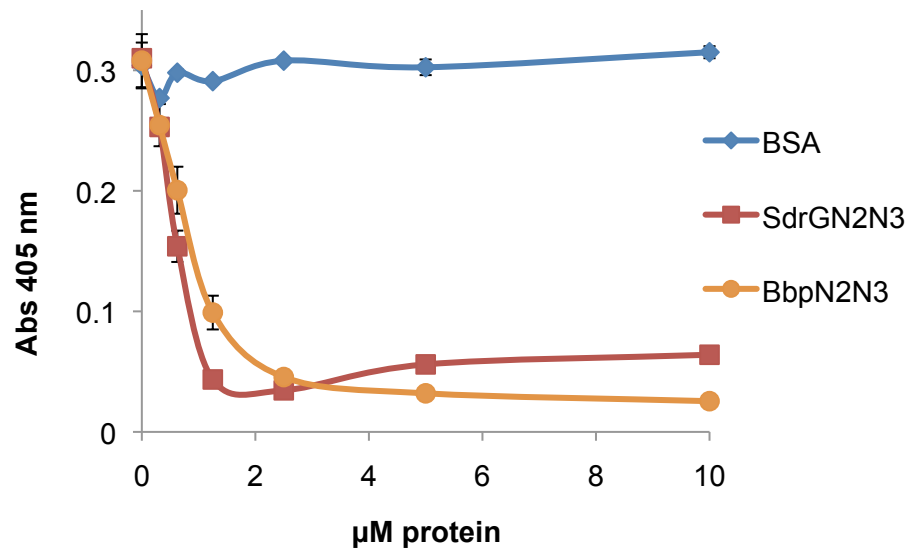
A Clustal alignment of the Fg A $\alpha$  561-575 of Fg from many species was performed (Figure 3-14). The results indicate that the sequence of human, canine, and feline fibrinogen are related. All three contain the second A $\alpha$  RGD site; whereas only part of the residues are present in porcine or bovine Fg. Furthermore, I observed that the rat and murine sequences are distant from the human. These species do not contain the RGD site, nor a stretch of polar, uncharged residues. The alignment data indicate that the feline and canine Fg are the closest to human. The canine and human sequences only differ by two residues, yet canine Fg does not support binding of Bbp.

### **Bbp inhibits fibrin formation**

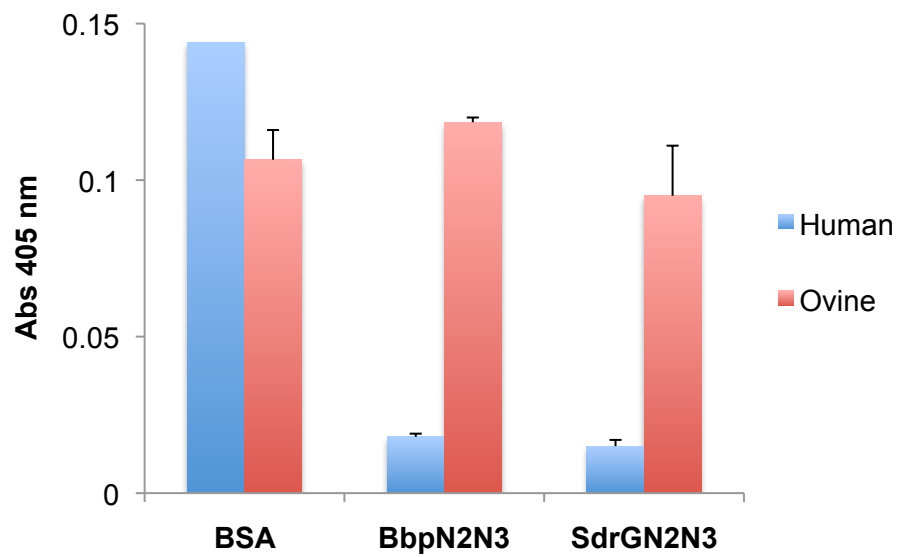
In order to examine the consequences of Bbp binding to Fg, I studied its effect on fibrin formation. Fg-coated wells were pretreated with increasing concentrations of Bbp<sub>N2N3</sub>, SdrG<sub>N2N3</sub>, a Fg-binding MSCRAMM of *S. epidermidis*, as a positive control, or BSA as a negative control prior to addition of thrombin. Bbp<sub>N2N3</sub> inhibited the formation of fibrin in a concentration-dependent manner, and similarly to SdrG<sub>N2N3</sub> (Figure 3-15a). Human thrombin is capable of cleaving the Fg of other species. Therefore, I examined whether the effect on fibrin formation exerted by Bbp was species specific. The data show that Bbp<sub>N2N3</sub> cannot inhibit thrombin-catalyzed fibrin formation from ovine Fg (Figure 3-15b). Our results indicate that pre-treatment of Fg with Bbp inhibits thrombin-catalyzed fibrin formation.

Figure 3-15. Inhibition of fibrin formation. Increasing concentrations (0.03 – 10  $\mu\text{M}$ ) (A) or 1  $\mu\text{M}$  (B) of BSA, SdrG<sub>N2N3</sub>, or BbpN<sub>2N3</sub> were preincubated in human Fg-coated (A and B) or ovine Fg-coated (B) wells prior to the addition of  $\alpha$ -thrombin.

A



B



## **Discussion**

*S. aureus* uses a multitude of virulence factors to cause a wide range of diseases. The MSCRAMMs can mediate binding of *S. aureus* to host proteins, thereby facilitating colonization. MSCRAMMs, including the Sdr family of proteins, are capable of recognizing many ligands. Here, the identification of human Fg A $\alpha$  as a second ligand for Bbp is reported.

The data indicate that a strong interaction occurs between the two proteins. I observed that Bbp<sub>N2N3</sub> was capable of binding to immobilized as well as reduced Fg, and recombinant, denatured Fg A $\alpha$  chain, which is typical of Fg-binding MSCRAMMs (Figure 3-5a, 8b, 10b, 11). These data indicate that the MSCRAMM binds to a linear sequence in the ligand. Furthermore, Biacore experiments with immobilized Fg resulted in a  $K_D$  of 540 nM, (Figure 3-7) and the  $K_D$  generated from ITC with peptide A $\alpha$ 561-575 was 309 nM (Figure 3-12). The affinities gathered with the two methods have similar values. It is possible that the affinity was lower in Biacore experiments due to the immobilization of Fg, as this may have hidden or obscured the available binding site for Bbp<sub>N2N3</sub>. Additionally, ITC was performed with both the peptide and the protein in solution, with stirring, and in a 5°C warmer atmosphere. Therefore, the experimental conditions in ITC may have been more conducive to the binding events between Bbp<sub>N2N3</sub> and the A $\alpha$  peptides.

Also speaking to the specificity of the interaction is that Bbp only targets human Fg (Figure 3-6). Alignment of the sequences corresponding to the human Fg A $\alpha$ 561-575 revealed small differences among the residues present in human, feline, and canine Fg (Figure 3-14). Specifically, the canine sequence contains an extra hydrophobic residue at position 565. This offsets the stretch of polar, uncharged residues found between 565 and 571 by one position. Also, Ser<sup>569</sup> in humans is a Thr in the canine sequence. Although

these are the only two differences between the human and canine sequences, they are enough to abrogate Bbp<sub>N2N3</sub> binding to canine Fg.

The results obtained with recombinant Bbp<sub>N2N3</sub> were confirmed using constructs that express the full-length protein on the surface of two heterologous hosts. *L. lactis* and *S. aureus* Newman bald provided a platform to study the binding contribution from a single MSCRAMM in prior studies (21). In this study, Bbp on the surface of both bacteria mediated attachment to immobilized A $\alpha$ 1-575 but not to A $\alpha$ 1-560 (Figure 3-11b, c). These data indicate that the full-length protein under the control of its native promoter can lead to Fg adherence.

The binding site of Bbp<sub>N2N3</sub> was mapped to A $\alpha$ 561-575, which ends with the second RGD site of the A $\alpha$  chain. Reports have suggested a role for the second A $\alpha$  RGD in binding to the integrins  $\alpha_5\beta_1$  and  $\alpha_V\beta_3$  (120) (119). Although further studies are required in order to determine what downstream effects occur upon Bbp binding to Fg, one possible effect could be the abrogation of the Fg A $\alpha$ -integrin interaction.

The effects of the Bbp-Fg interaction on clotting were examined. We detected an abrogation of fibrin formation when Fg was preincubated with Bbp. The residues A $\alpha$ 561-575 to which we have mapped Bbp binding lie in the  $\alpha$ C domain of Fg. This domain may mediate binding between fibrils to form fibrin. Also the residues are adjacent to a proposed transglutaminase target (116). Further experiments will determine the effects of Bbp binding on lateral association of fibrin monomers into crosslinked fibrin.

BSP was previously described as a ligand of Bbp, and this interaction may play a specific role in facilitating *S. aureus* osteomyelitis. Osteomyelitis is an infection of the bone, which may be accompanied or caused by hematogeneous spread. It is possible that Bbp may function in two capacities: as an important factor in osteomyelitis and as a contributing factor in *S. aureus* hematologic diseases, such as sepsis. Future studies regarding the

expression profile of Bbp in certain disease settings or disease-specific models may aid in elucidating the contribution of Bbp to *S. aureus* pathogenesis.

Fg was identified as a novel ligand for the MSCRAMM Bbp. The binding site was mapped to the residues 561-575, which represents a novel MSCRAMM target in Fg. Also, the interaction of Bbp with Fg inhibits the formation of fibrin. Future studies will further define the consequences of Bbp binding to Fg.

## **CHAPTER IV**

### **Binding mechanism of Bbp to fibrinogen**

## CHAPTER IV

### Binding mechanism of Bbp to fibrinogen

#### Introduction

The binding that occurs between MSCRAMMs and their ligands has been shown to be a dynamic event that can result in conformational changes. This is the case for the fibronectin-binding MSCRAMMs of *Borrelia burgdorferi*, *Streptococcus pyogenes* and *S. aureus* (105) (113). The Fnbps from these bacteria form a tandem-beta zipper upon ligand-binding. Also, the collagen adhesins, Cna and Ace from *S. aureus* and *Enterococcus faecalis*, respectively, bind to their ligand through the collagen hug model (142) (80). The *S. epidermidis* fibrinogen-binding protein, SdrG binds via the dock, lock, and latch (DLL) model (102). Furthermore, ClfA binds to Fg via a variant of the DLL mechanism (43). Evidence gathered from alanine scanning, truncation analysis, peptide studies, and crystallization has permitted the elucidation of the binding mechanisms of MSCRAMMs.

The A region of SdrG, ClfA, Cna, and Ace is subdivided into immunoglobulin-like N subdomains and contains the ligand-binding domains. The collagen-binding MSCRAMMs have a ligand-binding pocket between the N1 and N2 subdomains; whereas, the ligand-binding site of fibrinogen-binding MSCRAMMs is located between the N2 and N3 subdomains.

The dock, lock, and latch mechanism of SdrG binding to the Fg B $\beta$  was elucidated using biochemical and structural assays. In the unbound, apo-SdrG<sub>N2N3</sub> structure the MSCRAMM is in an open conformation with an unoccupied ligand-binding trench. A co-crystal of the complex formed by SdrG<sub>N2N3</sub> with the B $\beta$ 6-20 peptide showed that the MSCRAMM is in a closed conformation after ligand binding (102). In the latter structure, the N3 extension, or latch, is inserted into the N2 domain and forms a complemented  $\beta$ -



sheet (102). Additionally, the co-crystal provides information about the interacting residues in both the MSCRAMM and the peptide.

To provide more evidence for the DLL, experiments were performed with truncation mutants. The SdrG<sub>N2N3</sub> was truncated to determine that the latching event was necessary for ligand binding. Furthermore, the open and closed conformations were covalently engineered by the insertion of cysteine residues into SdrG<sub>N2N3</sub> (10). Because the Sdr proteins are similar in domain organization and folding, the dock, lock, and latch mechanism of binding has been proposed for this family of MSCRAMMs.

The collagen hug model of Cna and Ace (from *Enterococcus faecalis*) is similar to DLL. One striking difference is that the N1 and N2 domains have a longer linker region that accommodates the collagen triple helix. Upon ligand binding, Cna and Ace wrap around or “hug” the collagen peptide. The N1, linker, and N2 ultimately form a tunnel where the collagen peptide is bound (142). Similar studies to those performed for SdrG<sub>N2N3</sub> with constructs that are permanently open or closed, or that have mutations in the C-terminal extension or “latch” were used in experiments to support the collagen hug binding mechanism (Figure 4-3) (80).

Bbp is an MSCRAMM implicated in *S. aureus* osteomyelitis. It has been demonstrated that Bbp binds to bone-sialoprotein, a component of bone and dentin. Because targeting multiple ligands is a common trait among previously characterized MSCRAMMs, I determined whether Bbp followed this trend. In previous studies I identified the binding site of Bbp on human Fg A $\alpha$ . Importantly, Fg binding from full-length Bbp expressed on the surface of heterologous hosts was detected (Figure 3-11). The binding residues on the Fg A $\alpha$  chain include an RGD site, which suggests that the binding of Bbp may inhibit normal fibrinogen signaling (Figure 3-14). Furthermore, I determined that Bbp inhibits fibrin formation (Figure 3-15). MSCRAMMs use dynamic mechanisms to bind to their ligands. Sequence similarity and structural modeling suggest that of Bbp<sub>N2N3</sub> may bind

to fibrinogen in the same fashion as other MSCRAMMs. I sought to decipher the binding mechanism between Bbp and fibrinogen.

## **Materials and Methods**

*Commercial reagents:* The reagents used for this chapter are described in Chapter II.

*Design of Bbp<sub>N2N3</sub> mutants by MSCRAMM comparison* - Clustal sequence alignment was performed on the amino acid sequences corresponding to the N2N3 domains of Bbp, SdrG and ClfA, and the structure of Bbp<sub>N2N3</sub> was modeled based on solved MSCRAMM structures using Ribbons (Chapter III, Figure 3-3). The Bbp lock truncation is at Ile<sup>583</sup> and the Bbp latch residues begin at Ser<sup>589</sup>. A disulfide bond mutant was constructed with the substitutions E376C and P598C.

*Bbp<sub>N2N3</sub> mutants-* *S. aureus* MRSA 252 genomic DNA was used as template to amplify the DNA corresponding to Bbp 270-582 ( $\Delta$ Lock and latch) and 270-588 ( $\Delta$ Latch), and 270-599 E376C / P598C sequences using the primers listed in Table 4-1. The products were subcloned into TOPO Zero Blunt vector and transformed into TOP3 cells. After sequence verification, the plasmids were digested and inserts were ligated into pQE30 for transformation into XL1 Blue cells. *E. coli*-Bbp<sub>N2N3</sub> $\Delta$ Lock, *E. coli*-Bbp<sub>N2N3</sub> $\Delta$ Latch, and *E. coli*-Bbp<sub>N2N3</sub>E376C/P598C (BbpCys-Cys) were cultured to exponential phase, induced with 200  $\mu$ M IPTG, and grown for an additional 3 hours. The cells were pelleted, lysed, and purification of mutants was accomplished using Ni<sup>2+</sup> affinity chromatography as previously described (22) on a HiTrap Chelating column. Fractions were analyzed by SDS-PAGE, pooled, and dialyzed for anion exchange-purification using a Q HP Sepharose. To assess purity, the proteins were run on 10% SDS-PAGE and stained with Coomassie blue. The BbpCys-Cys construct was run under both nonreducing and reducing conditions to verify the formation of a disulfide bond. The nonreduced sample appeared smaller than the reduced sample.

Table 4-1. Oligonucleotides used in this study

Primer name	Oligonucleotide sequence
pQE30N2N3For	CGGGATCCGTTGCTTCAAACAATGTTAAT
pQE30LockRev	CGAAGCTTTTAAGTATTAGTGTAACCTGCATA
pQE30LatchRev	CGAAGCTTTTAGTCAGTAGTTGATAAAATAGT
Bbp376CRev	GACATTCTCACATCTATCAAC
Bbp376CFor	GTTGATAGATGTGAGAATGTC
Bbp598CRev	CCCAAGCTTTTATTCAGGTTTACAAGATACCGCAC

*Solid-phase binding assays-* Fg was coated on microtiter wells overnight in bicarbonate buffer at 10 µg/ml. The wells were blocked with Superblock and probed with increasing concentrations (0.1 – 10 µM) of Bbp<sub>N2N3</sub>, Bbp<sub>N2N3</sub>ΔLock, and Bbp<sub>N2N3</sub>ΔLatch and detected with anti-Bbp<sub>N2N3</sub> and anti-rabbit-HRP. The wells were developed and the absorbance was measured at 450 nm. To assess the binding of the BbpCys-Cys, Fg-coated wells were incubated with the Bbp<sub>N2N3</sub> or BbpCys-Cys in the presence or absence of 5 mM dithiothreitol (DTT).

*BbpCys-Cys Far Western-* Laemmli sample buffer containing 10 mM DTT was added to Fg for SDS-PAGE separation followed by transferring to nitrocellulose. The membranes were blocked with 1% BSA and probed with BbpCys-Cys (15 µg/ml) in the presence or absence of 5 mM DTT in TBST, followed by detection with anti-Bbp<sub>N2N3</sub> and anti-rabbit-AP.

## **RESULTS**

### **Bbp<sub>N2N3</sub> mutants were designed by MSCRAMM comparison.**

To reveal the locking and latching sequences and closed disulfide bond locations in Bbp, two approaches were taken. First, the amino acid sequences corresponding to the N2N3 domains of Bbp, SdrG and ClfA were aligned using Clustal (Figure 4-1). Second, the structure of Bbp<sub>N2N3</sub> was modeled based on solved MSCRAMM structures using Ribbons (Figure 3-3). The analyses revealed that the lock and latch truncations are at Ile<sup>583</sup> and Ser<sup>589</sup>, respectively. Furthermore, structural analysis predicted that the residues Glu<sup>376</sup> and Pro<sup>598</sup> are positioned in a way that if substituted to Cys, they can form a disulfide bond. Therefore, Bbp<sub>N2N3</sub> containing the substitutions E376C and P598C was constructed.

### **The lock and latch are necessary for Bbp<sub>N2N3</sub> binding.**

In order to assess whether the binding of Bbp<sub>N2N3</sub> to Fg is dependent upon the locking and latching residues, a solid-phase ELISA-type assay was conducted. Increasing concentrations of soluble Bbp<sub>N2N3</sub>, Bbp<sub>N2N3</sub>ΔLock, and Bbp<sub>N2N3</sub>ΔLatch (0.01 to 10.0 μM) were used to probe microtiter wells coated with Fg, followed by detection with polyclonal anti-Bbp<sub>N2N3</sub> and HRP conjugated anti-rabbit polyclonal. In this assay, Bbp<sub>N2N3</sub> recognized Fg in a concentration-dependent, saturable manner but Bbp<sub>N2N3</sub>ΔLock and Bbp<sub>N2N3</sub>ΔLatch failed to bind to Fg (Figure 4-2b). This indicates that the binding of Bbp to Fg requires the carboxy-terminal residues in the lock and latch sequences.

### **An open conformation is required for Bbp<sub>N2N3</sub> binding to Fg.**

I determined whether an engineered disulfide bond could force the protein into a closed conformation. SDS-PAGE in the absence or presence of reducing agent indicated that the reduced protein was larger in size. This suggests that the reduction of disulfide

Figure 4-1. Alignment of the N2N3 domains of SdrG, ClfA, and Bbp. Red - conserved motif; green – lock; yellow – latch; blue – cysteine mutations.

```

SdrG_273-597    AEQGSNVNHLIKVTDQSITEGYDDSDGIKAHDAENLIYDVTFEVDKVKSGDTMTVNID
Bbp_270-599    -VASNNVNDLITVTKQMITEGIKD-DGVIQAHGGEHIIYTSDFKIDNAVKAGDTMTVKYD
ClfA_229-545    ---GTDITNQLTNVTVGIDS-----GTTVYPHQAGYVKLNYGFSVPNSAVKGDFTFKITVP
                .:.:. . . * . . : .*: . : *.: . . ***:..

SdrG_273-597    KNTVPSDLTDSFAIPKIKDNSGEIIATGTYDNTNKQITYTFTDYVDKYENIKAHLKLTSY
Bbp_270-599    KHTIPSDITDDFTPVDITDPSGEVIAKGTFDLNTKTITYKFTDYVDRYENVNAKLELNSY
ClfA_229-545    KELNLNGVTSTAKVPPIMAG-DQVLANGVID-SDGNVLYTFTDYVNTKDDVKATLTMPAY
                *. .:*. * .:.*.*. * . : *.*****: :*: * : :*

SdrG_273-597    IDKSKVPNNNTKLDVEYKTALSSVNKTITVEYQKPENRTANLQSMFTNIDTKNHTVEQT
Bbp_270-599    IDKKEVPN-ETNLNLTFFATADKETSKNVKVEYQKPIVKDESNIQSIFSHLDTTKHEVEQT
ClfA_229-545    IDPENVKK-TGNVTLATGIGSTTANKTVLVDYEKYGKFYNLSIKGTIDQIDKTNNTRYQT
                ** .:* : : : . . .*.*: ***** .:.. : :*:..: .**

SdrG_273-597    IYINPLRYSAKETNVNISG-----NGD----EGSTIIDDSIIKVYKVGDNQNLPSNR
Bbp_270-599    IYVNPLKLNKNTNVTIKSGGVADNGDYTTGDGSTIIDSNTIHKVYKVASGQQLPQSNKI
ClfA_229-545    IYVNPSPGDNVIAP--VLTG-----NLKPNTDSNALIDQQNTSIKVYKVDNAADLSES-YF
                **:.* . . :.. * . .: * :..* ***** . :*:.* :

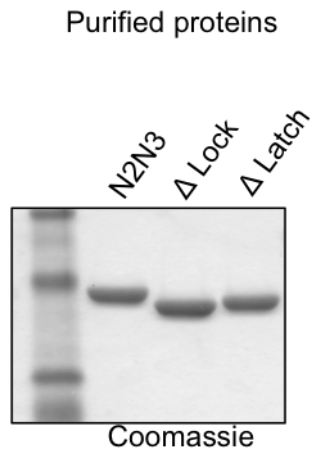
SdrG_273-597    YDYSEYEDVTNDDYAQLGN-NNDVNINFG---NIDSPYIIKVISKYDPNKDDYTTIQQT
Bbp_270-599    YDYSQYEDVTNSVTINKNYGTNMANINFG---DIDSAYIVKVVSKYTPGAEDDLAVQQG
ClfA_229-545    VNPENFEDVTNSVNITFPN-PNQYKVEFNTPDQITTPYIVVNGHIDPNSKGDALRST
                : .:*****. * :*: . :* :*: * .: * . . :*:..

SdrG_273-597    VTMQTTINEYTGFEFRTASYDNTIAFSTSSGQGQGDLPPE--
Bbp_270-599    VRMTTNTKKNYSSY--AGYTNTILSTTDSGGGDGTVPPE--
ClfA_229-545    LYGYNSN----IIWRMSWDNEVAFNNGSSGGDGIDKPVVP
                . . . . * . . ** *.* *

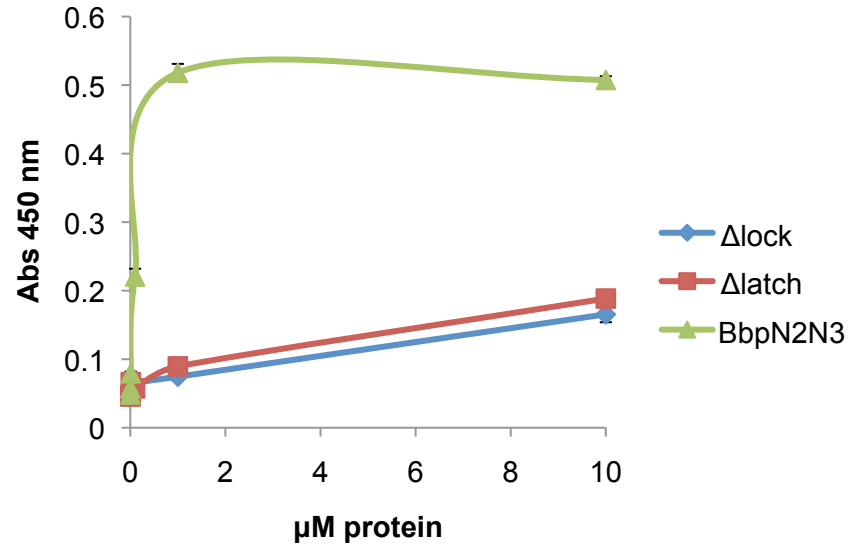
```

Figure 4-2. Delta lock and latch Bbp<sub>N2N3</sub> mutants. (A) Coomassie stained SDS-PAGE of Bbp<sub>N2N3</sub>, Bbp<sub>N2N3</sub>ΔLock, and Bbp<sub>N2N3</sub>ΔLatch. (B) Fg-coated wells were incubated with increasing concentrations of Bbp<sub>N2N3</sub>, Bbp<sub>N2N3</sub>ΔLock, and Bbp<sub>N2N3</sub>ΔLatch (0.01 to 10.0 μM) followed by anti-Bbp<sub>N2N3</sub> and anti-rabbit-HRP.

A



B





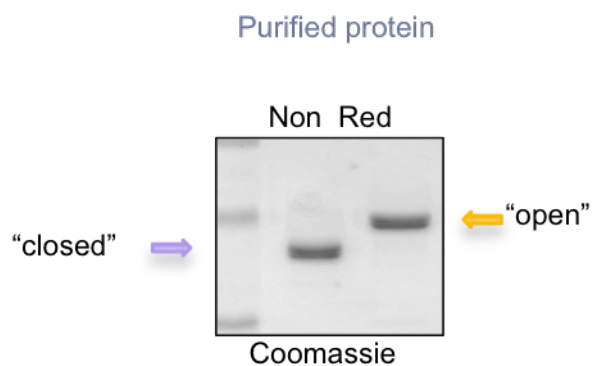
bonds in the sample slows the migration, presumably due to the larger, open conformation of the protein (Figure 4-3a).

The binding to Fg by a double cysteine mutant that formed a disulfide bond between the N2 and N3 domains rendering the molecule in a closed form was examined. Fg-coated wells were probed with increasing concentrations (15 – 1000 nM) of Bbp<sub>N2N3</sub> or BbpCys-Cys. Results indicate that the closed form of Bbp<sub>N2N3</sub> does not bind to Fg (Figure 4-3b).

In order to verify that the abrogation of binding was caused by the closing of the binding site, experiments were performed to rescue the binding of BbpCys-Cys. Far Western blotting was used to compare binding of reduced and nonreduced BbpCys-Cys (Figure 4-4a). A Fg blot probed with BbpCys-Cys in the absence of DTT did not result in signal detection. However, probing with BbpCys-Cys in the presence of DTT resulted in binding. Furthermore, I performed a similar analysis using a solid-phase binding assay. Fg-coated wells were incubated with Bbp<sub>N2N3</sub> and BbpCysCys in the presence of 5 mM DTT (Figure 4-4b). The results indicate that re-opening the closed form of Bbp by disulfide reduction restores the binding of BbpCys-Cys to similar levels as those of Bbp<sub>N2N3</sub>.

Figure 4-3. BbpCys-Cys. (A) BbpCys-Cys was separated on SDS-PAGE in nonreducing and reducing buffer. (B). Fg-coated wells were incubated with increasing concentrations (15 – 1000 nM) of Bbp<sub>N2N3</sub> or BbpCys-Cys followed by anti-Bbp<sub>N2N3</sub> polyclonal antibody and anti-rabbit-HRP.

A



B

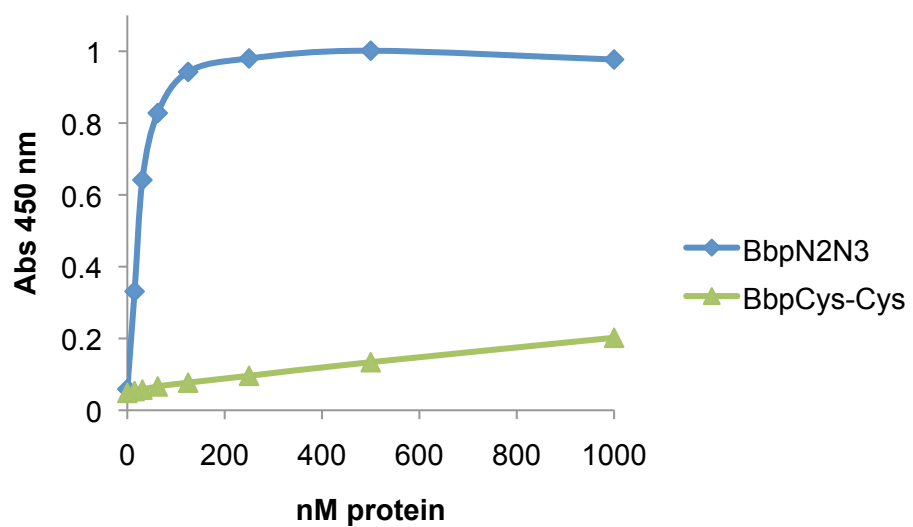
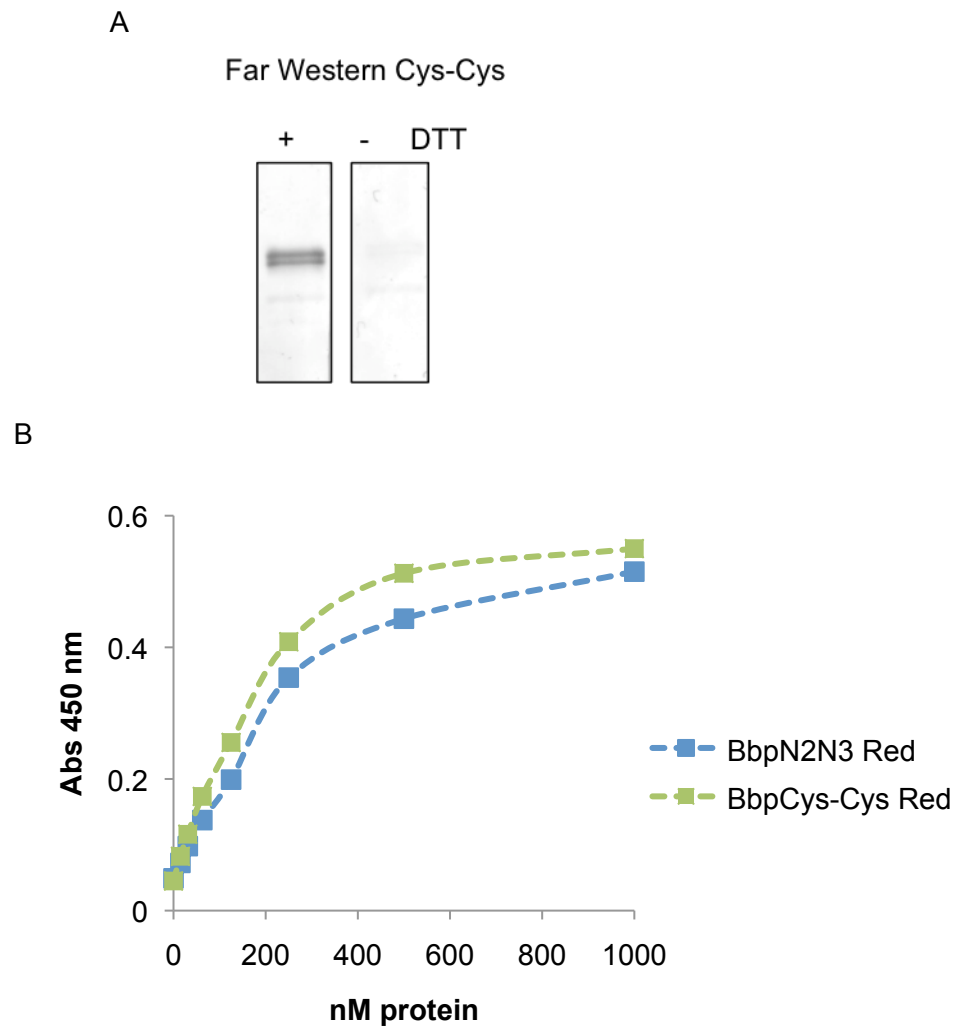


Figure 4-4. Rescue of BbpCys-Cys binding. (A) Reduced Fg was separated on SDS-PAGE and transferred to nitrocellulose membrane for Far Western analysis with BbpCys-Cys (15  $\mu$ g/ml) in the presence (left) or absence (right) of 5 mM DTT followed by rabbit-anti Bbp<sub>N2N3</sub> polyclonal antibody and goat-anti-rabbit-AP. (B) Fg-coated wells were incubated with increasing concentrations of Bbp<sub>N2N3</sub> or BbpCys-Cys in the presence of 5 mM DTT followed by anti-Bbp<sub>N2N3</sub> and anti-rabbit-HRP.



## **DISCUSSION**

The dock, lock, and latch, or variant thereof, has been proposed as the binding mechanism for MSCRAMMs. In this study, Bbp<sub>N2N3</sub> mutants were constructed to examine the effects on binding imparted by the presence of the residues in the carboxy-terminus of the N3 domain known as the lock and latch residues.

In the *S. epidermidis* MSCRAMM SdrG, ligand binding induces conformational changes that include a redirection of the locking residues followed by  $\beta$ -strand complementation that morphs the protein into a closed form with the ligand inside of the binding trench. Therefore, appropriate Bbp<sub>N2N3</sub> constructs were designed by the aid of computer modeling and sequence alignment. These constructs were used to evaluate the regions required for Bbp to bind to Fg. Results indicate that Bbp<sub>N2N3</sub> requires both the lock and latch for binding. Additionally, a disulfide-bonded closed mutant did not bind to Fg, but the binding was restored by reduction of the disulfide bond, indicating that the protein must be open for Fg binding. Therefore, the evidence strongly suggests that Bbp binds to Fg using the dock, lock, and latch model.

Further studies are required in order to prove our hypothesis. To date, the structure of the ligand binding domains of Bbp either in apo-form or in a complex with the ligand have not been solved. Once the structures of the different forms of Bbp are solved, the residues in the protein that bind to the target can be analyzed. Structural assessment of the two forms of Bbp<sub>N2N3</sub> will support the evidence I have gathered biochemically.

Previous studies identified that Bbp inhibits fibrin binding. Although no data has been gathered to examine this inhibition in more detail, the dynamic dock, lock, and latch mechanism could be playing a role. The latching of the Fg molecule into the ligand-binding trench could render the  $\alpha$ C domain unavailable for lateral aggregation of fibrils and could inhibit Factor XIIIa from covalently crosslinking the chains.

The species tropism of Bbp poses some challenges in designing future experiments. The previous study indicated that Bbp was highly specific for the human Fg sequence. Therefore, it is possible that in order to progress to animal studies utilizing Bbp, partially humanized A $\alpha$  mice will be required. Until such a model is available, conducting biochemical, structural, and *in vitro* experiments will provide further understanding of the interaction between Bbp and Fg. Moreover, the consequences of Bbp binding to fibrinogen can be studied.

## **CHAPTER V**

### **Discussion**

## CHAPTER V

### Discussion

Current staphylococcal therapy involves antibiotic use. However, this is not a preventive approach to halt the spread of staphylococcal infections. Preclinical and clinical vaccine studies have targeted bacterial surface and secreted factors. A combination, or multivalent, vaccine that targets several factors could prove to be successful. In the present studies, I sought to analyze two potential virulence factors.

In the second chapter, the epidemiologically suggested link between the Pantone-Valentine Leukocidin (PVL) and necrotizing pneumonia was analyzed. Using a murine model of pneumonia, the ability of a highly purified PVL toxin preparation to cause pneumonia (71) was discovered. Furthermore, the ability of the toxin subunits to elicit a protective response was examined (13). LukS-PV-vaccinated animals exhibited less morbidity and mortality when challenged with a lethal dose of the *S. aureus* strain USA300, which is a predominant antibiotic resistant clone causing CA-MRSA infections.

While the results were able to attribute necrotizing pneumonia to the PVL toxin, the mechanism for this event has not been fully elucidated. As previously discussed, PVL lyses monocytes, macrophages, and polymorphonuclear cells, and this interaction can lead to leukocyte release of inflammatory mediators. Future experiments are needed to fully decipher the mechanisms by which PVL causes the severe inflammatory response observed in the lungs of mice instilled with purified protein. Specifically, whether the toxin itself can cause necrotizing pneumonia in leukocyte-deficient mice has not been determined because these mice experience high morbidity upon staphylococcal exposure. A different approach to gather valuable information would be to use mutant PVL that cannot oligomerize or cause cell lysis. This method was successful for the closely-related  $\alpha$ -Hemolysin.

In the third and fourth chapters, data from experiments conducted with the cell-surface adhesin, Bbp, are presented. Bbp binds to bone-sialoprotein, indicating a role in osteomyelitis. The ability of MSCRAMMs to bind to multiple ligands has been documented for several proteins, and this work identified a novel ligand for the MSCRAMM Bbp. Also, experiments were performed to decipher the binding mechanism of Bbp to Fg.

Screening a panel of typical MSCRAMM ligands for Bbp binding resulted in the identification of fibrinogen (Fg) as a target for Bbp (Figure 3-5). The binding site was mapped to the  $\alpha$ C region, residues 561-575, and peptide studies confirmed the results (Figures 3-11, 3-12, and 3-13). Furthermore, Bbp exhibits high specificity and affinity for human Fg (Figures 3-6 and 3-7).

I am beginning to examine the consequences of Bbp binding to Fg. Already, I have accumulated data showing that Bbp inhibits fibrin formation (Figure 3-15). However, the mechanism underlying this phenomenon has not been studied. It is likely that binding of Bbp to the  $\alpha$ C domain causes steric hindrance that inhibits the lateral aggregation of protofibrils to form fibrin. Furthermore, the transglutaminase Factor XIIIa covalently links the  $\alpha$  chain to itself and to  $\gamma$  chains. The binding site, and surrounding residues, on  $\alpha$ C contain amino acids that are believed to be involved in crosslinking of fibrin (116). Therefore, this is a possible mechanism of inhibition. Studies conducted with  $\alpha$ C mutants may aid in deciphering the mechanism by which Bbp inhibits fibrin formation.

The binding site of Bbp on Fg contains an RGD motif. This specific RGD has been shown to bind to integrins present on endothelial cells, platelets, and fibroblasts. No experiments have been performed to examine the effects of Bbp on Fg-integrin binding. Presumably, binding of Bbp to  $\alpha$ C would occupy the integrin-binding site, or, at the very least, the residues immediately amino-terminal to the integrin binding RGD. Therefore, I



expect that pretreatment of  $\alpha$ C with Bbp would directly inhibit or sterically hinder the integrin-Fg interaction.

The mechanism of Bbp binding to Fg was studied. The data gathered indicate that this interaction occurs via the dock, lock, and latch (DLL) model. Currently, our laboratory is working to obtain a co-crystal structure of Bbp with a Fg peptide. A solved structure would provide the evidence necessary to identify the residues in Bbp that interact with the amino acids in human Fg. These data could pave the way for the design of inhibitors to abrogate the interaction. Because the Bbp binding site includes an RGD site, care must be taken not to inhibit important interactions between Fg and integrins necessary for normal biological functions. For example, our laboratory recently reported the identification of peptides that inhibit the interaction between ClfA and Fg but have no effect on the interaction between Fg and the platelet integrin (43).

Evidence suggests that MSCRAMMs can serve as protective targets for a staphylococcal vaccine. Therefore, our laboratory has worked to identify the molecular interactions between the surface adhesins and the human host. Interestingly, Bbp has been previously termed as an allelic variant of SdrE. I have begun to study SdrE in comparison to Bbp. The two variants have been subjected to sequence alignment for comparison (Figure 5-1). Interestingly, this analysis revealed that the N2N3 domains have the highest sequence variation (approximately 60% identity), but the N1, B repeats, and SD regions have identities above 90%. Furthermore, a crystal structure of the SdrE<sub>N2N3</sub> domains has been solved (Unpublished data by Dr. Vannakambadi Ganesh). A model of Bbp<sub>N2N3</sub> based on the SdrE<sub>N2N3</sub> structure indicates that the structure of Bbp<sub>N2N3</sub> is more rigid in nature (Figure 5-2). Specifically, the  $\beta$ -strands that compose the  $\beta$ -sandwiches are longer in Bbp<sub>N2N3</sub>; whereas in SdrE<sub>N2N3</sub>, the  $\beta$ -sheets are shorter, requiring more inter-strand linker regions.

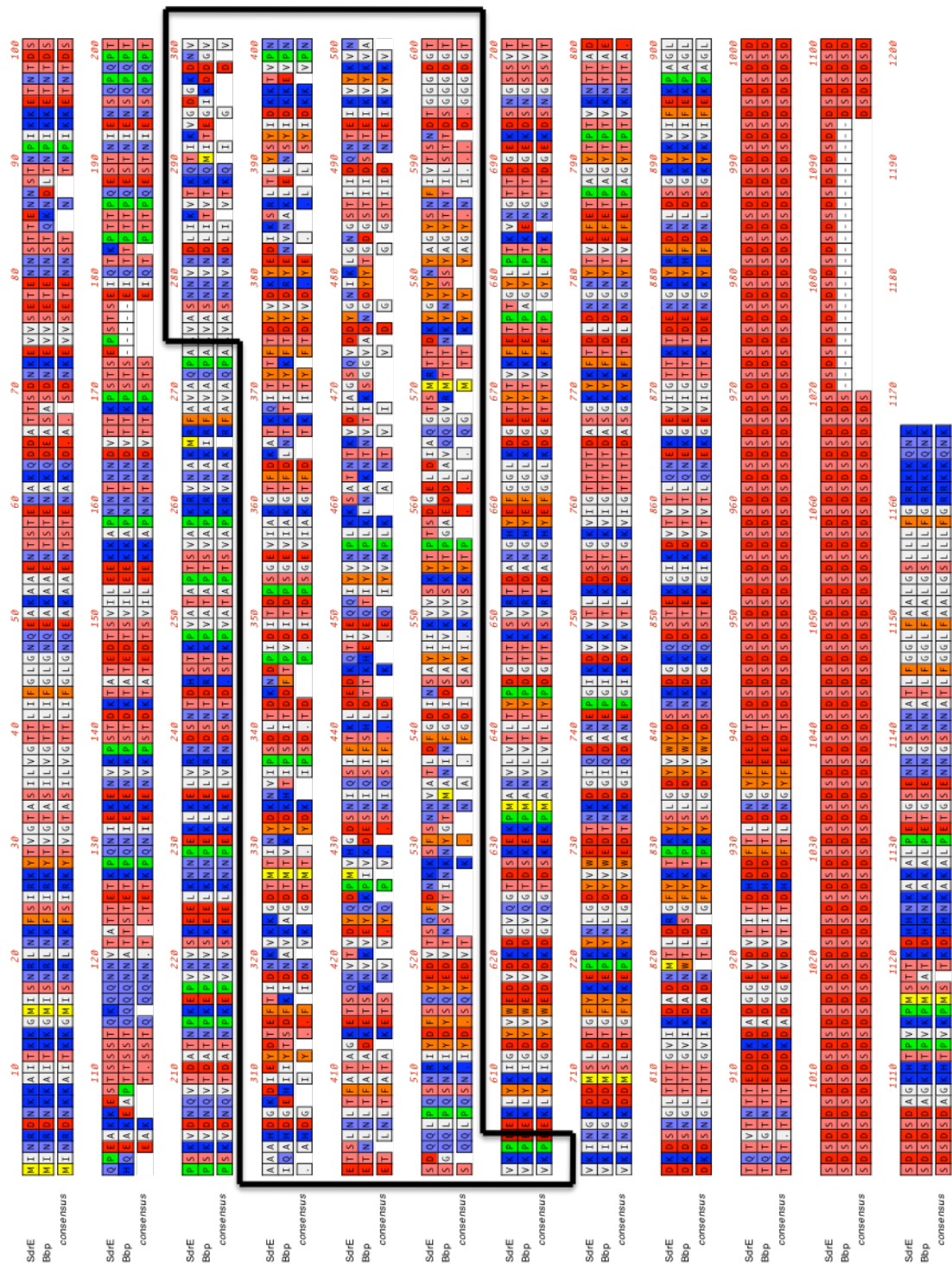
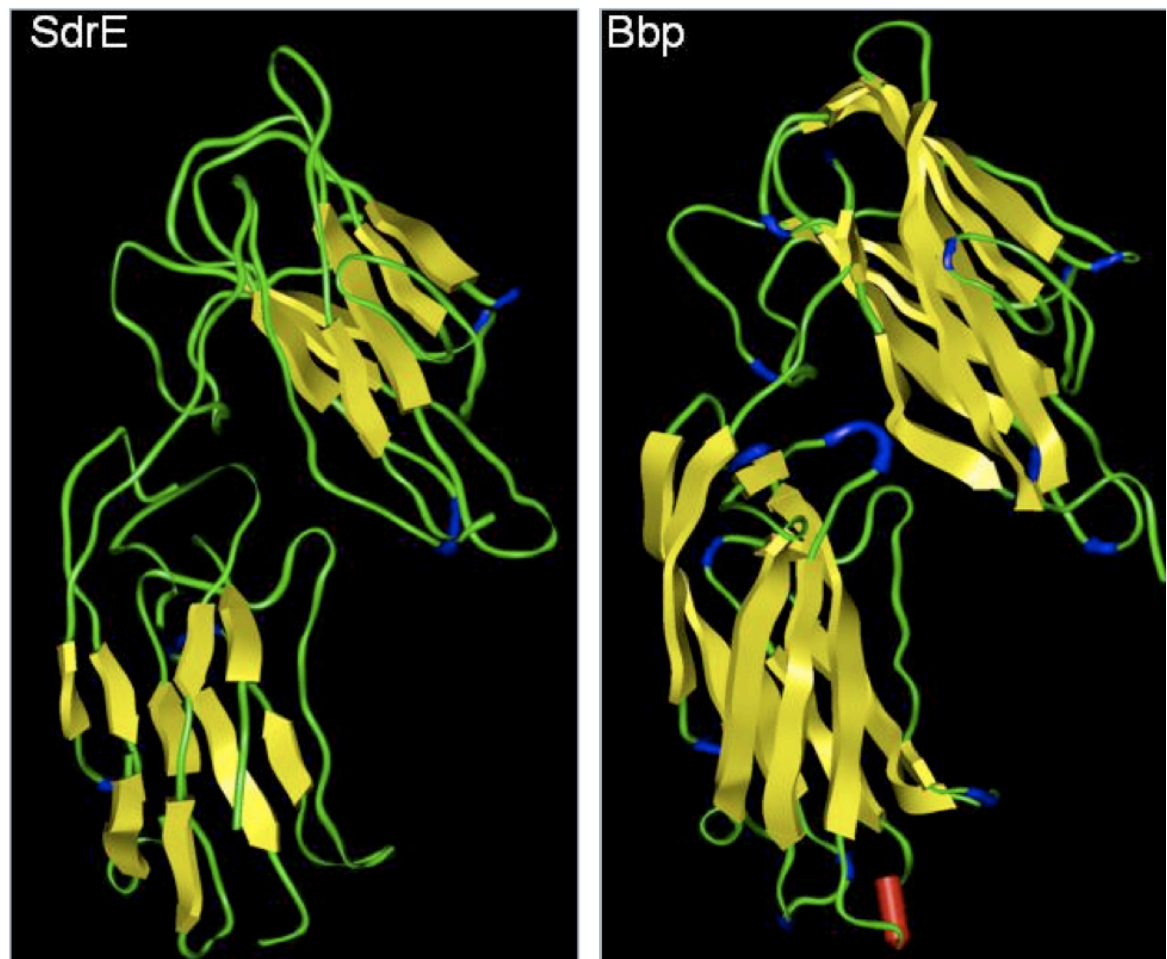


Figure 5-1. Alignment of full-length SdrE (top row) and Bbp (middle row) showing the consensus sequence (bottom row). The boxed area corresponds to the N2N3 domain of both proteins. Alignment performed using MacVector software.

Figure 5-2. Structural comparison of SdrE and Bbp. The N2 domains are at the bottom and the N3 domains are at the top of the images.

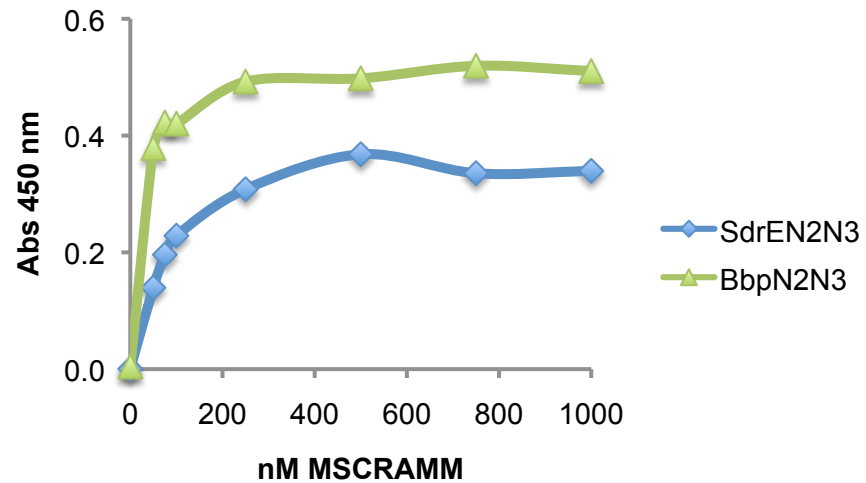


The added flexibility of the SdrE<sub>N2N3</sub> domains was predicted to correlate with activity. Preliminary experiments examining the differences in binding abilities and specificity were performed with the two variants. First, the ability of SdrE<sub>N2N3</sub> to bind to Fg was examined (Figure 5-3a). The results indicate that SdrE<sub>N2N3</sub> binds to Fg in a concentration-dependent, saturable manner. Furthermore, a species screen revealed that SdrE<sub>N2N3</sub> exhibits a wider species tropism for Fg than Bbp<sub>N2N3</sub> (Figure 5-3b). Human, feline, canine, bovine, ovine, rat, and porcine Fg all supported binding to SdrE<sub>N2N3</sub>, albeit at different levels. Next, I determined if the increased flexibility and tropism of SdrE affected its activity towards human Fg. A fibrin inhibition assay revealed that SdrE<sub>N2N3</sub> was capable of inhibiting thrombin-catalyzed fibrin formation to similar levels as Bbp<sub>N2N3</sub> (Figure 5-3c). However, a higher concentration of SdrE<sub>N2N3</sub> is required to reach maximum inhibition. These preliminary data indicate differences in the structure and activities of the ligand binding domains of SdrE and Bbp. Future experiments to biochemically define the differences between the two proteins could be performed with the same reagents that were used to study the interaction between Bbp and Fg. Although the data with SdrE and Fg are preliminary, I have identified the only known ligand of SdrE.

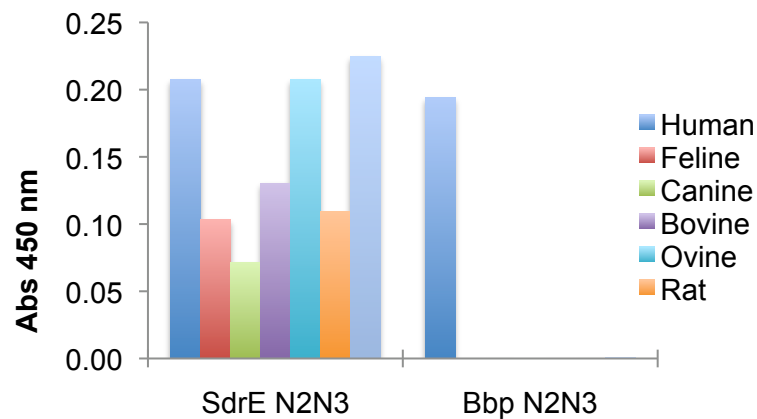
The MSCRAMMs IsdA, IsdB, SdrD, and SdrE were identified as protective targets in an intravenous infection model (118). Vaccination with SdrE led to high antibody titers and a reduction of bacteria in the kidneys. Considering the data generated with SdrE and Bbp, it is possible that Bbp could also serve as a protective immunogen. However, Bbp was not examined in that study. It is also important to note that animal studies with Bbp may not be fully translational to human disease because it only targets human Fg. Therefore, future experiments examining the *in vivo* role of Bbp may require the utilization of mice with partially humanized Fg.

Figure 5-3. Comparison of SdrE<sub>N2N3</sub> and Bbp<sub>N2N3</sub> activities. Human (A) or other species (B) Fg-coated wells were incubated with increasing concentrations (50-1000 nM) (A) or 500 nM SdrEN2N3 and BbpN2N3 followed by protein-specific antibodies and goat-anti rabbit-HRP. (C) Human Fg coated wells were preincubated with 0.03-10  $\mu$ M proteins prior to  $\alpha$ -thrombin addition.

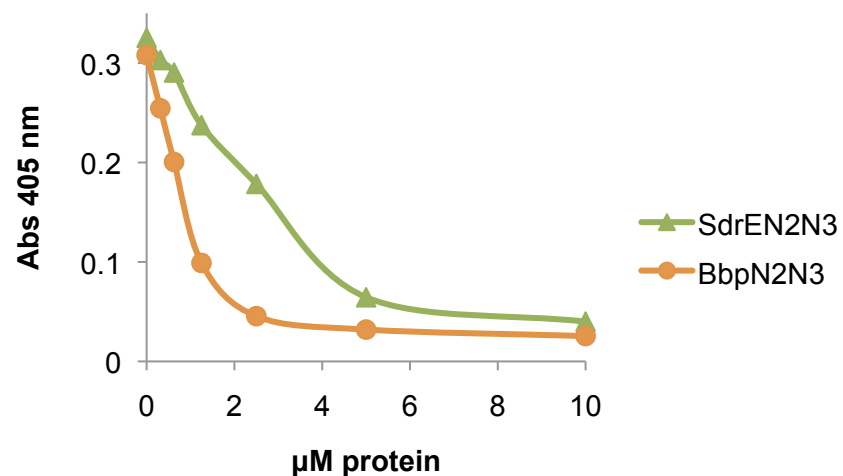
A



B



C



The studies encompassing this dissertation provide new functional data regarding putative staphylococcal virulence factors. Studying putative virulence factors in animal models of disease can provide urgent information necessary for the understanding of complicated disease states. Furthermore, identification of novel ligands for bacterial proteins can lead to the discovery of virulence mechanisms.

## BIBLIOGRAPHY

1. 1929. Editorial Comments: The death of Sir Alexander Ogston. Canadian Medical Association Journal **20**:412.
2. **Alshammary, A., M. Hervas-Malo, and J. L. Robinson.** 2008. Pediatric infective endocarditis: Has Staphylococcus aureus overtaken viridans group streptococci as the predominant etiological agent? The Canadian journal of infectious diseases & medical microbiology = Journal canadien des maladies infectieuses et de la microbiologie médicale / AMMI Canada **19**:63-8.
3. **Andrieux, A., G. Hudry-Clergeon, J. J. Ryckewaert, A. Chapel, M. H. Ginsberg, E. F. Plow, and G. Marguerie.** 1989. Amino acid sequences in fibrinogen mediating its interaction with its platelet receptor, GPIIb/IIIa. J Biol Chem **264**:9258-65.
4. **Athanassa, Z., I. I. Siempos, and M. E. Falagas.** 2008. Impact of methicillin resistance on mortality in Staphylococcus aureus VAP: a systematic review. The European respiratory journal : official journal of the European Society for Clinical Respiratory Physiology **31**:625-32.
5. **Bach, T. L., C. Barsigian, C. H. Yaen, and J. Martinez.** 1998. Endothelial cell VE-cadherin functions as a receptor for the beta15-42 sequence of fibrin. J Biol Chem **273**:30719-28.
6. **Baddour, L. M., C. Lowrance, A. Albus, J. H. Lowrance, S. K. Anderson, and J. C. Lee.** 1992. Staphylococcus aureus microcapsule expression attenuates bacterial virulence in a rat model of experimental endocarditis. J Infect Dis **165**:749-53.
7. **Balaban, N., and A. Rasooly.** 2000. Staphylococcal enterotoxins. Int. J. Food Microbiol **61**:1-10.

8. **Bolyard, M., and S. Lord.** 1989. Expression in *Escherichia coli* of the human fibrinogen B beta chain and its cleavage by thrombin. *Journal of Biological Chemistry*:1202-1206.
9. **Bolyard, M. G., and S. T. Lord.** 1988. High-level expression of a functional human fibrinogen gamma chain in *Escherichia coli*. *Gene* **66**:183-92.
10. **Bowden, M. G., A. P. Heuck, K. Ponnuraj, E. Kolosova, D. Choe, S. Gurusiddappa, S. V. Narayana, A. E. Johnson, and M. Hook.** 2008. Evidence for the "dock, lock, and latch" ligand binding mechanism of the staphylococcal microbial surface component recognizing adhesive matrix molecules (MSCRAMM) SdrG. *J Biol Chem* **283**:638-47.
11. **Bramley, A. J., A. H. Patel, M. O'Reilly, R. Foster, and T. J. Foster.** 1989. Roles of alpha-toxin and beta-toxin in virulence of *Staphylococcus aureus* for the mouse mammary gland. *Infect Immun* **57**:2489-94.
12. **Brooks, G. F., J. S. Butel, and S. A. Morse.** 1998. Jawetz, Melnick, and Adelberg's *Medical Microbiology*, 21 ed. Appleton & Lange, Stamford, Connecticut.
13. **Brown, E. L., O. Dumitrescu, D. Thomas, C. Badiou, E. M. Koers, V. Vazquez, J. Etienne, G. Lina, and F. Vandenesch.** 2009. The Panton-Valentine leukocidin vaccine protects mice against lung and skin infections caused by *Staphylococcus aureus* USA300. *Clinical Microbiology and Infections* **15**:156-164.
14. **Bubeck Wardenburg, J., T. Bae, M. Otto, F. R. Deleo, and O. Schneewind.** 2007. Poring over pores: alpha-hemolysin and Panton-Valentine leukocidin in *Staphylococcus aureus* pneumonia. *Nature medicine* **13**:1405-6.
15. **Bubeck Wardenburg, J., and O. Schneewind.** 2008. Vaccine protection against *Staphylococcus aureus* pneumonia. *The Journal of experimental medicine* **205**:287-94.



16. **Bubeck-Wardenburg, J., T. Bae, M. Otto, F. R. Deleo, and O. Schneewind.** 2007. Poring over pores: alpha-hemolysin and Panton-Valentine leukocidin in *Staphylococcus aureus* pneumonia. *Nature medicine* **13**:1405-6.
17. **Burton, R. A., G. Tsurupa, R. R. Hantgan, N. Tjandra, and L. Medved.** 2007. NMR solution structure, stability, and interaction of the recombinant bovine fibrinogen alphaC-domain fragment. *Biochemistry* **46**:8550-60.
18. **Chambers, H. F., and F. R. Deleo.** 2009. Waves of resistance: *Staphylococcus aureus* in the antibiotic era. *Nature reviews. Microbiology* **7**:629-641.
19. **Chavakis, T., M. Hussain, S. M. Kanse, G. Peters, R. G. Bretzel, J. I. Flock, M. Herrmann, and K. T. Preissner.** 2002. *Staphylococcus aureus* extracellular adherence protein serves as anti-inflammatory factor by inhibiting the recruitment of host leukocytes. *Nat Med* **8**:687-93.
20. **Colin, D. A., I. Mazurier, S. Sire, and V. Finck-Barbancon.** 1994. Interaction of the two components of leukocidin from *Staphylococcus aureus* with human polymorphonuclear leukocyte membranes: sequential binding and subsequent activation. *Infect Immun* **62**:3184-8.
21. **Corrigan, R. M., H. Miajlovik, and T. J. Foster.** 2009. Surface proteins that promote adherence of *Staphylococcus aureus* to human desquamated nasal epithelial cells. *BMC Microbiology* **9**.
22. **Davis, S. L., S. Gurusiddappa, K. W. Mccrea, and S. Perkins.** 2001. SdrG , a Fibrinogen-binding Bacterial Adhesin of the Microbial Surface Components Recognizing Adhesive Matrix Molecules Subfamily from *Staphylococcus epidermidis* , Targets the Thrombin Cleavage Site in the Bbeta Chain. *Journal of Biological Chemistry* **276**:27799 -27805.
23. **Defres, S., C. Marwick, and D. Nathwani.** 2009. MRSA as a cause of lung infection including airway infection, community-acquired pneumonia and hospital-

- acquired pneumonia. The European respiratory journal : official journal of the European Society for Clinical Respiratory Physiology **34**:1470-6.
24. **Deisenhofer, J.** 1981. Crystallographic refinement and atomic models of a human Fc fragment and its complex with fragment B of protein A from *Staphylococcus aureus* at 2.9- and 2.8-A resolution. *Biochemistry* **20**:2361-70.
  25. **Deivanayagam, C. C., S. Perkins, S. Danthuluri, R. T. Owens, T. Bice, T. Nanavathy, T. J. Foster, M. Hook, and S. V. Narayana.** 1999. Crystallization of ClfA and ClfB fragments: the fibrinogen-binding surface proteins of *Staphylococcus aureus*. *Acta Crystallogr D Biol Crystallogr* **55**:554-6.
  26. **DeJonge, M., D. Burchfield, B. Bloom, M. Duenas, W. Walker, M. Polak, E. Jung, D. Millard, R. Schelonka, F. Eyal, A. Morris, B. Kapik, D. Roberson, K. Kesler, J. Patti, and S. Hetherington.** 2007. Clinical trial of safety and efficacy of INH-A21 for the prevention of nosocomial staphylococcal bloodstream infection in premature infants. *J Pediatr* **151**:260-5, 265 e1.
  27. **Dinges, M. M., P. M. Orwin, and P. atrick Schlievert.** 2000. Exotoxins of *Staphylococcus aureus*. *Clin. Microbiol. Rev* **13**:16-34.
  28. **Elasri, M. O., J. R. Thomas, R. A. Skinner, J. S. Blevins, K. E. Beenken, C. L. Nelson, and M. S. Smeltzer.** 2002. *Staphylococcus aureus* collagen adhesin contributes to the pathogenesis of osteomyelitis. *Bone* **30**:275-80.
  29. **Enright, M. C., D. A. Robinson, G. Randle, E. J. Feil, H. Grundmann, and B. G. Spratt.** 2002. The evolutionary history of methicillin-resistant *Staphylococcus aureus* (MRSA). *Proc Natl Acad Sci U S A* **99**:7687-92.
  30. **Entenza, J. M., P. Moreillon, M. M. Senn, J. Kormanec, P. M. Dunman, B. Berger-Bachi, S. Projan, and M. Bischoff.** 2005. Role of sigmaB in the expression of *Staphylococcus aureus* cell wall adhesins ClfA and FnbA and contribution to infectivity in a rat model of experimental endocarditis. *Infect Immun* **73**:990-8.

31. **Farley, J. E.** 2008. Epidemiology, clinical manifestations, and treatment options for skin and soft tissue infection caused by community-acquired methicillin-resistant *Staphylococcus aureus*. *Journal of the American Academy of Nurse Practitioners* **20**:85-92.
32. **Fey, P. D., B. Said-Salim, M. E. Rupp, S. H. Hinrichs, D. J. Boxrud, C. C. Davis, B. N. Kreiswirth, and P. M. Schlievert.** 2003. Comparative molecular analysis of community- or hospital-acquired methicillin-resistant *Staphylococcus aureus*. *Antimicrob Agents Chemother* **47**:196-203.
33. **Fitton, J. E., A. Dell, and W. V. Shaw.** 1980. The amino acid sequence of the delta haemolysin of *Staphylococcus aureus*. *FEBS Lett* **115**:209-12.
34. **Fitzgerald, J. R., T. J. Foster, and D. Cox.** 2006. The interaction of bacterial pathogens with platelets. *Nat Rev Microbiol* **4**:445-57.
35. **Fitzgerald, J. R., A. Loughman, F. Keane, M. Brennan, M. Knobel, J. Higgins, L. Visai, P. Speziale, D. Cox, and T. J. Foster.** 2006. Fibronectin-binding proteins of *Staphylococcus aureus* mediate activation of human platelets via fibrinogen and fibronectin bridges to integrin GPIIb/IIIa and IgG binding to the FcγRIIIa receptor. *Molecular microbiology* **59**:212-30.
36. **Flick, M. J., X. Du, D. P. Witte, M. Jirouskova, D. A. Soloviev, S. J. Busuttil, E. F. Plow, and J. L. Degen.** 2004. Leukocyte engagement of fibrin(ogen) via the integrin receptor α<sub>IIb</sub>β<sub>3</sub>/Mac-1 is critical for host inflammatory response in vivo. *J Clin Invest* **113**:1596-606.
37. **Forrest, G. N., and K. Tamura.** 2010. Rifampin combination therapy for nonmycobacterial infections. *Clinical microbiology reviews* **23**:14-34.
38. **Forsgren, A., and J. Sjoquist.** 1966. "Protein A" from *S. aureus*. I. Pseudo-immune reaction with human gamma-globulin. *J Immunol* **97**:822-7.

39. **Foster, T. J., and M. Höök.** 1998. Surface protein adhesins of *Staphylococcus aureus*. *Trends Microbiol* **6**:484-488.
40. **Fowler, T., E. R. Wann, D. Joh, S. Johansson, T. J. Foster, and M. Hook.** 2000. Cellular invasion by *Staphylococcus aureus* involves a fibronectin bridge between the bacterial fibronectin-binding MSCRAMMs and host cell beta1 integrins. *Eur J Cell Biol* **79**:672-9.
41. **Fowler, V. G., Jr., H. W. Boucher, G. R. Corey, E. Abrutyn, A. W. Karchmer, M. E. Rupp, D. P. Levine, H. F. Chambers, F. P. Tally, G. A. Vigliani, C. H. Cabell, A. S. Link, I. DeMeyer, S. G. Filler, M. Zervos, P. Cook, J. Parsonnet, J. M. Bernstein, C. S. Price, G. N. Forrest, G. Fatkenheuer, M. Gareca, S. J. Rehm, H. R. Brodt, A. Tice, and S. E. Cosgrove.** 2006. Daptomycin versus standard therapy for bacteremia and endocarditis caused by *Staphylococcus aureus*. *N Engl J Med* **355**:653-65.
42. **Gailit, J., C. Clarke, D. Newman, M. G. Tonnesen, M. W. Mosesson, and R. A. Clark.** 1997. Human fibroblasts bind directly to fibrinogen at RGD sites through integrin alpha(v)beta3. *Exp Cell Res* **232**:118-26.
43. **Ganesh, V. K., J. J. Rivera, E. Smeds, Y.-P. Ko, M. G. Bowden, E. R. Wann, S. Gurusiddappa, J. R. Fitzgerald, and M. Höök.** 2008. A structural model of the *Staphylococcus aureus* ClfA-fibrinogen interaction opens new avenues for the design of anti-staphylococcal therapeutics. *PLoS pathogens* **4**:1-10.
44. **Gautam, N., A. M. Olofsson, H. Herwald, L. F. Iversen, E. Lundgren-Akerlund, P. Hedqvist, K. E. Arfors, H. Flodgaard, and L. Lindbom.** 2001. Heparin-binding protein (HBP/CAP37): a missing link in neutrophil-evoked alteration of vascular permeability. *Nature medicine* **7**:1123-7.
45. **Genestier, A., M. Michallet, G. Prevost, G. Bellot, L. Chalabreysse, S. Peyrol, F. Thivolet, J. Etienne, G. Lina, F. M. Vallette, F. Vandenesch, and L. Genestier.**

2005. *Staphylococcus aureus* Pantón-Valentine leukocidin directly targets mitochondria and induces Bax-independent apoptosis of human neutrophils. Journal of Clinical Investigation, In Press.
46. **Gillet, Y., B. Issartel, P. Vanhems, J. C. Fournet, G. Lina, M. Bes, F. Vandenesch, Y. Piemont, N. Brousse, D. Floret, and J. Etienne.** 2002. Association between *Staphylococcus aureus* strains carrying gene for Pantón-Valentine leukocidin and highly lethal necrotising pneumonia in young immunocompetent patients. *Lancet* **359**:753-9.
  47. **Gomez, M. I., A. Lee, B. Reddy, A. Muir, G. Soong, A. Pitt, A. Cheung, and A. Prince.** 2004. *Staphylococcus aureus* protein A induces airway epithelial inflammatory responses by activating TNFR1. *Nat Med* **10**:842-8.
  48. **Gómez, M. I., M. O'Seaghdha, M. Magargee, T. J. Foster, and A. S. Prince.** 2006. *Staphylococcus aureus* protein A activates TNFR1 signaling through conserved IgG binding domains. *The Journal of biological chemistry* **281**:20190-6.
  49. **Gonzalez, B. E., G. Martinez-Aguilar, K. G. Hulten, W. A. Hammerman, J. Coss-Bu, A. Avalos-Mishaan, E. O. Mason, Jr., and S. L. Kaplan.** 2005. Severe *Staphylococcal* sepsis in adolescents in the era of community-acquired methicillin-resistant *Staphylococcus aureus*. *Pediatrics* **115**:642-8.
  50. **Goodyear, C. S., and G. J. Silverman.** 2003. Death by a B cell superantigen: In vivo VH-targeted apoptotic supraclonal B cell deletion by a *Staphylococcal* Toxin. *J Exp Med* **197**:1125-39.
  51. **Gorak, E. J., S. M. Yamada, and J. D. Brown.** 1999. Community-acquired methicillin-resistant *Staphylococcus aureus* in hospitalized adults and children without known risk factors. *Clin Infect Dis* **29**:797-800.
  52. **Gould, F. K., R. Brindle, P. R. Chadwick, A. P. Fraise, S. Hill, D. Nathwani, G. L. Ridgway, M. J. Spry, and R. E. Warren.** 2009. Guidelines (2008) for the

- prophylaxis and treatment of methicillin-resistant *Staphylococcus aureus* (MRSA) infections in the United Kingdom. *The Journal of antimicrobial chemotherapy* **63**:849-861.
53. **Guidet, B., P. Aegerter, R. Gauzit, P. Meshaka, and D. Dreyfuss.** 2005. Incidence and impact of organ dysfunctions associated with sepsis. *Chest* **127**:942-51.
54. **Hair, P. S., C. G. Echague, A. M. Sholl, J. A. Watkins, J. A. Geoghegan, T. J. Foster, and K. M. Cunnion.** 2010. Clumping factor A interaction with complement factor I increases C3b cleavage on the bacterial surface of *Staphylococcus aureus* and decreases complement-mediated phagocytosis. *Infect Immun* **78**:1717-27.
55. **Handagama, P. J., D. L. Amrani, and M. A. Shuman.** 1995. Endocytosis of fibrinogen into hamster megakaryocyte alpha granules is dependent on a dimeric gamma A configuration. *Blood* **85**:1790-5.
56. **Harrison, P., B. Wilbourn, N. Debili, W. Vainchenker, J. Breton-Gorius, A. S. Lawrie, J. M. Masse, G. F. Savidge, and E. M. Cramer.** 1989. Uptake of plasma fibrinogen into the alpha granules of human megakaryocytes and platelets. *J Clin Invest* **84**:1320-4.
57. **Hartleib, J., N. Köhler, R. B. Dickinson, G. S. Chhatwal, J. J. Sixma, O. M. Hartford, T. J. Foster, G. Peters, B. E. Kehrel, and M. Herrmann.** 2000. Protein A is the von Willebrand factor binding protein on *Staphylococcus aureus*. *Blood* **96**:2149-56.
58. **Hensler, T., B. König, G. Prevost, Y. Piemont, M. Koller, and W. König.** 1994. Leukotriene B4 generation and DNA fragmentation induced by leukocidin from *Staphylococcus aureus*: protective role of granulocyte-macrophage colony-stimulating factor (GM-CSF) and G-CSF for human neutrophils. *Infect Immun* **62**:2529-35.

59. **Herold, B. C., L. C. Immergluck, M. C. Maranan, D. S. Lauderdale, R. E. Gaskin, S. Boyle-Vavra, C. D. Leitch, and R. S. Daum.** 1998. Community-acquired methicillin-resistant *Staphylococcus aureus* in children with no identified predisposing risk. *Jama* **279**:593-8.
60. **Hienz, S. A., T. Schennings, A. Heimdahl, and J. I. Flock.** 1996. Collagen binding of *Staphylococcus aureus* is a virulence factor in experimental endocarditis. *J Infect Dis* **174**:83-8.
61. **Hoiby, N., J. O. Jarlov, M. Kemp, M. Tvede, J. M. Bangsberg, A. Kjerulf, C. Pers, and H. Hansen.** 1997. Excretion of ciprofloxacin in sweat and multiresistant *Staphylococcus epidermidis*. *Lancet* **349**:167-9.
62. **Jardetzky, T. S., J. H. Brown, J. C. Gorga, L. J. Stern, R. G. Urban, Y. I. Chi, C. Stauffacher, J. L. Strominger, and D. C. Wiley.** 1994. Three-dimensional structure of a human class II histocompatibility molecule complexed with superantigen. *Nature* **368**:711-8.
63. **Jett, M., W. Brinkley, R. Neill, P. Gemski, and R. Hunt.** 1990. *Staphylococcus aureus* enterotoxin B challenge of monkeys: correlation of plasma levels of arachidonic acid cascade products with occurrence of illness. *Infect Immun* **58**:3494-9.
64. **Kanafani, Z., H. Boucher, V. Fowler, C. Cabell, B. Hoen, J. Miro, T. Lalani, G. Vigliani, M. Champion, R. Corey, and D. Levine.** 2010. Daptomycin compared to standard therapy for the treatment of native valve endocarditis. *Enfermedades infecciosas y microbiologia clinica* **Feb 24**:1-6.
65. **Kaneko, J., and Y. Kamio.** 2004. Bacterial two-component and hetero-heptameric pore-forming cytolytic toxins: structures, pore-forming mechanism, and organization of the genes. *Biosci Biotechnol Biochem* **68**:981-1003.

66. **Keane, F. M., A. Loughman, V. Valtulina, M. Brennan, P. Speziale, and T. J. Foster.** 2007. Fibrinogen and elastin bind to the same region within the A domain of fibronectin binding protein A, an MSCRAMM of *Staphylococcus aureus*. *Mol Microbiol* **63**:711-23.
67. **Kollman, J. M., L. Pandi, M. R. Sawaya, M. Riley, and R. F. Doolittle.** 2009. Crystal structure of human fibrinogen. *Biochemistry* **48**:3877-86.
68. **Konig, B., M. Koller, G. Prevost, Y. Piemont, J. E. Alouf, A. Schreiner, and W. Konig.** 1994. Activation of human effector cells by different bacterial toxins (leukocidin, alveolysin, and erythrogenic toxin A): generation of interleukin-8. *Infect Immun* **62**:4831-7.
69. **Konig, B., G. Prevost, and W. Konig.** 1997. Composition of staphylococcal bi-component toxins determines pathophysiological reactions. *J Med Microbiol* **46**:479-85.
70. **Konig, B., G. Prevost, Y. Piemont, and W. Konig.** 1995. Effects of *Staphylococcus aureus* leukocidins on inflammatory mediator release from human granulocytes. *J Infect Dis* **171**:607-13.
71. **Labandeira-Rey, M., F. Couzon, S. Boisset, E. L. Brown, M. Bes, Y. Benito, E. M. Barbu, V. Vazquez, M. Hook, J. Etienne, F. Vandenesch, and M. G. Bowden.** 2007. *Staphylococcus aureus* Panton-Valentine leukocidin causes necrotizing pneumonia. *Science* **315**:1130-3.
72. **Ladhani, S., O. S. Konana, S. Mwarumba, and M. C. English.** 2004. Bacteraemia due to *Staphylococcus aureus*. *Arch Dis Child* **89**:568-71.
73. **Le Loir, Y., F. Baron, and M. Gautier.** 2003. *Staphylococcus aureus* and food poisoning. *Genetics and molecular research : GMR* **2**:63-76.



74. **Lee, J. C., J. S. Park, S. E. Shepherd, V. Carey, and A. Fattom.** 1997. Protective efficacy of antibodies to the *Staphylococcus aureus* type 5 capsular polysaccharide in a modified model of endocarditis in rats. *Infect Immun* **65**:4146-51.
75. **Lee, L. Y., X. Liang, M. Hook, and E. L. Brown.** 2004. Identification and characterization of the C3 binding domain of the *Staphylococcus aureus* extracellular fibrinogen-binding protein (Efb). *J Biol Chem* **279**:50710-6.
76. **Lee, S. Y., K. P. Lee, and J. W. Lim.** 1996. Identification and biosynthesis of fibrinogen in human uterine cervix carcinoma cells. *Thromb Haemost* **75**:466-70.
77. **Li, H., A. Llera, D. Tsuchiya, L. Leder, X. Ysern, P. M. Schlievert, K. Karjalainen, and R. A. Mariuzza.** 1998. Three-dimensional structure of the complex between a T cell receptor beta chain and the superantigen staphylococcal enterotoxin B. *Immunity* **9**:807-16.
78. **Lina, G., Y. Piemont, F. Godail-Gamot, M. Bes, M. O. Peter, V. Gauduchon, F. Vandenesch, and J. Etienne.** 1999. Involvement of Panton-Valentine leukocidin-producing *Staphylococcus aureus* in primary skin infections and pneumonia. *Clin Infect Dis* **29**:1128-32.
79. **Liu, C. Z., M. H. Shih, and P. J. Tsai.** 2005. ClfA(221-550), a fibrinogen-binding segment of *Staphylococcus aureus* clumping factor A, disrupts fibrinogen function. *Thromb Haemost* **94**:286-94.
80. **Liu, Q., K. Ponnuraj, Y. Xu, V. K. Ganesh, J. Sillanpaa, B. E. Murray, S. V. Narayana, and M. Hook.** 2007. The *Enterococcus faecalis* MSCRAMM ACE binds its ligand by the Collagen Hug model. *J Biol Chem* **282**:19629-37.
81. **Lord, S. T.** 1985. Expression of a cloned human fibrinogen cDNA in *Escherichia coli*: synthesis of an A alpha polypeptide. *DNA* **4**:33-8.
82. **Lowy, F. D.** 1998. *Staphylococcus aureus* infections. *N Engl J Med* **339**:520-32.

83. **Mack, J., C. Vermeiren, D. E. Heinrichs, and M. J. Stillman.** 2004. In vivo heme scavenging by *Staphylococcus aureus* IsdC and IsdE proteins. *Biochem Biophys Res Commun* **320**:781-8.
84. **Makogonenko, E., G. Tsurupa, K. Ingham, and L. Medved.** 2002. Interaction of fibrin(ogen) with fibronectin: further characterization and localization of the fibronectin-binding site. *Biochemistry* **41**:7907-13.
85. **Maresso, A. W., and O. Schneewind.** 2006. Iron acquisition and transport in *Staphylococcus aureus*. *BioMetals* **19**:193-203.
86. **Mazmanian, S. K., H. Ton-That, K. Su, and O. Schneewind.** 2002. An iron-regulated sortase anchors a class of surface protein during *Staphylococcus aureus* pathogenesis. *Proc Natl Acad Sci U S A* **99**:2293-8.
87. **McAleese, F. M., E. J. Walsh, M. Sieprawaska, J. Potempa, and T. J. Foster.** 2001. Loss of clumping factor B fibrinogen binding activity by *Staphylococcus aureus* involves cessation of transcription, shedding and cleavage by metalloprotease. *The Journal of biological chemistry* **276**:29969-78.
88. **Medved, L., and J. W. Weisel.** 2009. Recommendations for nomenclature on fibrinogen and fibrin. *Journal of thrombosis and haemostasis : JTH* **7**:355-9.
89. **Menzies, B. E., and D. S. Kernodle.** 1994. Site-directed mutagenesis of the alpha-toxin gene of *Staphylococcus aureus*: role of histidines in toxin activity in vitro and in a murine model. *Infect Immun* **62**:1843-7.
90. **Mollick, J. A., R. G. Cook, and R. R. Rich.** 1989. Class II MHC molecules are specific receptors for staphylococcus enterotoxin A. *Science* **244**:817-20.
91. **Mosesson, M. W., K. R. Siebenlist, and D. A. Meh.** 2001. The structure and biological features of fibrinogen and fibrin. *Ann N Y Acad Sci* **936**:11-30.

92. **Napolitano, L. M.** 2009. Severe soft tissue infections. *Infectious disease clinics of North America* **23**:571-591.
93. **Nathwani, D., M. Morgan, R. G. Masterton, M. Dryden, B. D. Cookson, G. French, and D. Lewis.** 2008. Guidelines for UK practice for the diagnosis and management of methicillin-resistant *Staphylococcus aureus* (MRSA) infections presenting in the community. *Journal of Antimicrobial Chemotherapy* **62**:216-216.
94. **Navarre, W. W., and O. Schneewind.** 1999. Surface proteins of gram-positive bacteria and mechanisms of their targeting to the cell wall envelope. *Microbiol Mol Biol Rev* **63**:174-229.
95. **Nilsson, I. M., J. C. Lee, T. Bremell, C. Ryden, and A. Tarkowski.** 1997. The role of staphylococcal polysaccharide microcapsule expression in septicemia and septic arthritis. *Infect Immun* **65**:4216-21.
96. **O'Brien, L., S. W. Kerrigan, G. Kaw, M. Hogan, J. Penadés, D. Litt, D. J. Fitzgerald, T. J. Foster, and D. Cox.** 2002. Multiple mechanisms for the activation of human platelet aggregation by *Staphylococcus aureus*: roles for the clumping factors ClfA and ClfB, the serine aspartate repeat protein SdrE and protein A. *Molecular Microbiology* **44**:1033-1044.
97. **Odrlijin, T. M., C. W. Francis, L. A. Sporn, L. A. Bunce, V. J. Marder, and P. J. Simpson-Haidaris.** 1996. Heparin-binding domain of fibrin mediates its binding to endothelial cells. *Arterioscler Thromb Vasc Biol* **16**:1544-51.
98. **Patel, A. H., P. Nowlan, E. D. Weavers, and T. Foster.** 1987. Virulence of protein A-deficient and alpha-toxin-deficient mutants of *Staphylococcus aureus* isolated by allele replacement. *Infect Immun* **55**:3103-10.
99. **Patti, J. M., B. L. Allen, M. J. McGavin, and M. Hook.** 1994. MSCRAMM-mediated adherence of microorganisms to host tissues. *Annu Rev Microbiol* **48**:585-617.

100. **Peacock, S. J., C. E. Moore, A. Justice, M. Kantzanou, L. Story, K. Mackie, G. O'Neill, and N. P. Day.** 2002. Virulent combinations of adhesin and toxin genes in natural populations of *Staphylococcus aureus*. *Infect. Immun* **70**:4987-4996.
101. **Persson, L., C. Johansson, and C. Ryden.** 2009. Antibodies to *Staphylococcus aureus* bone sialoprotein-binding protein indicate infectious osteomyelitis. *Clin Vaccine Immunol* **16**:949-52.
102. **Ponnuraj, K., M. G. Bowden, S. Davis, S. Gurusiddappa, D. Moore, D. Choe, Y. Xu, M. Hook, and S. V. L. Narayana.** 2003. A "dock, lock, and latch" structural model for a staphylococcal adhesin binding to fibrinogen. *Cell* **115**:217-28.
103. **Postma, B., M. J. Poppelier, J. C. van Galen, E. R. Prossnitz, J. A. van Strijp, C. J. de Haas, and K. P. van Kessel.** 2004. Chemotaxis inhibitory protein of *Staphylococcus aureus* binds specifically to the C5a and formylated peptide receptor. *J Immunol* **172**:6994-7001.
104. **Prevost, G., B. Cribier, P. Couppie, P. Petiau, G. Supersac, V. Finck-Barbancon, H. Monteil, and Y. Piemont.** 1995. Panton-Valentine leucocidin and gamma-hemolysin from *Staphylococcus aureus* ATCC 49775 are encoded by distinct genetic loci and have different biological activities. *Infect Immun* **63**:4121-9.
105. **Raibaud, S., U. Schwarz-Linek, J. H. Kim, H. T. Jenkins, E. R. Baines, S. Gurusiddappa, M. Höök, and J. R. Potts.** 2005. *Borrelia burgdorferi* binds fibronectin through a tandem beta-zipper, a common mechanism of fibronectin binding in staphylococci, streptococci, and spirochetes. *The Journal of Biological Chemistry* **280**:18803-9.
106. **Remick, D. G.** 2005. Interleukin-8. *Critical care medicine* **33**:S466-7.
107. **Rodriguez, J. L., C. G. Miller, L. E. DeForge, L. Kelty, C. J. Shanley, R. H. Bartlett, and D. G. Remick.** 1992. Local production of interleukin-8 is associated with nosocomial pneumonia. *The Journal of trauma* **33**:74-81; discussion 81-2.

108. **Rooijackers, S. H. M., K. P. M. van Kessel, and J. a. G. van Strijp.** 2005. Staphylococcal innate immune evasion. *Trends in microbiology* **13**:596-601.
109. **Rott, O., K. Mignon-Godefroy, B. Fleischer, J. Charreire, and E. Cash.** 1995. Superantigens induce primary T cell responses to soluble autoantigens by a non-V beta-specific mechanism of bystander activation. *Cell Immunol* **161**:158-65.
110. **Ryden, C., A. I. Yacoub, I. Maxe, D. Heinegard, A. Oldberg, A. Franzen, A. Ljungh, and K. Rubin.** 1989. Specific binding of bone sialoprotein to *Staphylococcus aureus* isolated from patients with osteomyelitis. *Eur J Biochem* **184**:331-6.
111. **Sabat, A., D. C. Melles, G. Martirosian, H. Grundmann, A. V. Belkum, and W. Hryniewicz.** 2006. Distribution of the Serine-Aspartate Repeat Protein-Encoding *sdr* Genes among Nasal-Carriage and Invasive *Staphylococcus aureus* Strains. *Society* **44**:1135-1138.
112. **Schaffer, A. C., and J. C. Lee.** 2009. Staphylococcal vaccines and immunotherapies. *Infectious disease clinics of North America* **23**:153-71.
113. **Schwarz-Linek, U., J. M. Werner, A. R. Pickford, S. Gurusiddappa, J. H. Kim, E. S. Pilka, J. A. Briggs, T. S. Gough, M. Hook, I. D. Campbell, and J. R. Potts.** 2003. Pathogenic bacteria attach to human fibronectin through a tandem beta-zipper. *Nature* **423**:177-81.
114. **Shinefield, H., S. Black, A. Fattom, G. Horwith, S. Rasgon, J. Ordonez, H. Yeoh, D. Law, J. B. Robbins, R. Schneerson, L. Muenz, S. Fuller, J. Johnson, B. Fireman, H. Alcorn, and R. Naso.** 2002. Use of a *Staphylococcus aureus* conjugate vaccine in patients receiving hemodialysis. *N Engl J Med* **346**:491-6.
115. **Smeltzer, M. S., and A. F. Gillasp.** 2000. Molecular pathogenesis of staphylococcal osteomyelitis. *Poult Sci* **79**:1042-9.

116. **Sobel, J. H., and M. A. Gawinowicz.** 1996. Identification of the alpha chain lysine donor sites involved in factor XIIIa fibrin cross-linking. *J Biol Chem* **271**:19288-97.
117. **Stott, N. S.** 2001. Review article: Paediatric bone and joint infection. *J Orthop Surg (Hong Kong)* **9**:83-90.
118. **Stranger-Jones, Y. K., T. Bae, and O. Schneewind.** 2006. Vaccine assembly from surface proteins of *Staphylococcus aureus*. *Proc Natl Acad Sci U S A* **103**:16942-7.
119. **Suehiro, K., J. Gailit, and E. F. Plow.** 1997. Fibrinogen is a ligand for integrin alpha5beta1 on endothelial cells. *J Biol Chem* **272**:5360-6.
120. **Suehiro, K., J. Mizuguchi, K. Nishiyama, S. Iwanaga, D. H. Farrell, and S. Ohtaki.** 2000. Fibrinogen binds to integrin alpha(5)beta(1) via the carboxyl-terminal RGD site of the Aalpha-chain. *J Biochem* **128**:705-10.
121. **Supersac, G., Y. Piemont, M. Kubina, G. Prevost, and T. J. Foster.** 1998. Assessment of the role of gamma-toxin in experimental endophthalmitis using a hlg-deficient mutant of *Staphylococcus aureus*. *Microb Pathog* **24**:241-51.
122. **Tacconelli, E.** 2009. Antimicrobial use: risk driver of multidrug resistant microorganisms in healthcare settings. *Current opinion in infectious diseases* **22**:352-358.
123. **Takeda, Y.** 1966. Studies of the metabolism and distribution of fibrinogen in healthy men with autologous 125-I-labeled fibrinogen. *J Clin Invest* **45**:103-11.
124. **Tan, A. S., and M. V. Berridge.** 2000. Superoxide produced by activated neutrophils efficiently reduces the tetrazolium salt, WST-1 to produce a soluble formazan: a simple colorimetric assay for measuring respiratory burst activation and for screening anti-inflammatory agents. *J Immunol Methods* **238**:59-68.
125. **Tenover, F. C., L. K. McDougal, R. V. Goering, G. Killgore, S. J. Projan, J. B. Patel, and P. M. Dunman.** 2006. Characterization of a strain of community-

- associated methicillin-resistant *Staphylococcus aureus* widely disseminated in the United States. *J Clin Microbiol* **44**:108-18.
126. **Thakker, M., J. S. Park, V. Carey, and J. C. Lee.** 1998. *Staphylococcus aureus* serotype 5 capsular polysaccharide is antiphagocytic and enhances bacterial virulence in a murine bacteremia model. *Infect Immun* **66**:5183-9.
  127. **Tristan, A., L. Ying, M. Bes, J. Etienne, F. Vandenesch, and G. Lina.** 2003. Use of Multiplex PCR To Identify *Staphylococcus aureus* Adhesins Involved in Human Hematogenous Infections. *Society* **41**:4465-4467.
  128. **Tsurupa, G., R. R. Hantgan, R. A. Burton, I. Pechik, N. Tjandra, and L. Medved.** 2009. Structure, stability, and interaction of the fibrin(ogen) alphaC-domains. *Biochemistry* **48**:12191-201.
  129. **Tung, H., B. Guss, U. Hellman, L. Persson, K. Rubin, and C. Ryden.** 2000. A bone sialoprotein-binding protein from *Staphylococcus aureus*: a member of the staphylococcal Sdr family. *Biochem J* **345 Pt 3**:611-9.
  130. **Vernachio, J., A. S. Bayer, T. Le, Y. L. Chai, B. Prater, A. Schneider, B. Ames, P. Syribey, J. Robbins, and J. M. Patti.** 2003. Anti-clumping factor A immunoglobulin reduces the duration of methicillin-resistant *Staphylococcus aureus* bacteremia in an experimental model of infective endocarditis. *Antimicrob Agents Chemother* **47**:3400-6.
  131. **Walsh, E. J., H. Miajlovic, O. V. Gorkun, and T. J. Foster.** 2008. Identification of the *Staphylococcus aureus* MSCRAMM clumping factor B ( ClfB ) binding site in the aC-domain of human fibrinogen. *Microbiology*:550-558.
  132. **Walsh, E. J., L. M. O'Brien, X. Liang, M. Hook, and T. J. Foster.** 2004. Clumping factor B, a fibrinogen-binding MSCRAMM (microbial surface components recognizing adhesive matrix molecules) adhesin of *Staphylococcus aureus*, also binds to the tail region of type I cytokeratin 10. *J Biol Chem* **279**:50691-9.

133. **Weisman, L. E.** 2007. Antibody for the prevention of neonatal nosocomial staphylococcal infection: a review of the literature. *Arch Pediatr* **14 Suppl 1**:S31-4.
134. **Wertheim, H. F., E. Walsh, R. Choudhury, D. C. Melles, H. A. Boelens, H. Miajlovic, H. A. Verbrugh, T. Foster, and A. van Belkum.** 2008. Key role for clumping factor B in *Staphylococcus aureus* nasal colonization of humans. *PLoS Med* **5**:e17.
135. **Werz, O., and D. Steinhilber.** 2006. Therapeutic options for 5-lipoxygenase inhibitors. *Pharmacol Ther* **112**:701-18.
136. **Westphal, N., B. Plicht, and C. Naber.** 2009. Infective endocarditis--prophylaxis, diagnostic criteria, and treatment. *Deutsches Ärzteblatt international* **106**:481-490.
137. **Woodin, A. M., J. E. French, and V. T. Marchesi.** 1963. Morphological changes associated with the extrusion of protein induced in the polymorphonuclear leucocyte by staphylococcal leucocidin. *Biochem J* **87**:567-71.
138. **Yacoub, A., P. Lindahl, K. Rubin, M. Wendel, D. Heinegard, and C. Ryden.** 1994. Purification of a bone sialoprotein-binding protein from *Staphylococcus aureus*. *Eur J Biochem* **222**:919-25.
139. **Yang, Z., J. M. Kollman, L. Pandi, and R. F. Doolittle.** 2001. Crystal structure of native chicken fibrinogen at 2.7 Å resolution. *Biochemistry* **40**:12515-23.
140. **Yang, Z., I. Mochalkin, and R. F. Doolittle.** 2000. A model of fibrin formation based on crystal structures of fibrinogen and fibrin fragments complexed with synthetic peptides. *Proc Natl Acad Sci U S A* **97**:14156-61.
141. **Young, A. E., and K. L. Thornton.** 2007. Toxic shock syndrome in burns: diagnosis and management. *Archives of disease in childhood. Education and practice edition* **92**:ep97-100.



142. **Zong, Y., Y. Xu, X. Liang, D. R. Keene, A. Hook, S. Gurusiddappa, M. Hook, and S. V. Narayana.** 2005. A 'Collagen Hug' model for *Staphylococcus aureus* CNA binding to collagen. *EMBO J* **24**:4224-36.

## VITA

Vanessa Vazquez earned the degree Associate of Science in Industrial Laboratory Technology from The Oklahoma State University in 2001. During her undergraduate years, from 1999 to 2003, she held the position of Food and Water Microbiology and Analytical Chemistry Laboratory Technician at OKLABS, Inc in Oklahoma City. In 2003, she graduated *summa cum laude* from the University of Central Oklahoma. There, she earned a Bachelor of Science in Biology with a minor in Chemistry. In August of 2003, she entered The University of Texas Health Science Center at Houston Graduate School of Biomedical Sciences.